United States
Environmental Protection
Agency

EPA/530-SW-84-001
APRIL 1984

C1

Solid Waste

EPA

Procedures for Modeling Flow Through Clay Liners to Determine Required Liner Thickness

Draft

Technical Resource Document For Public Comment

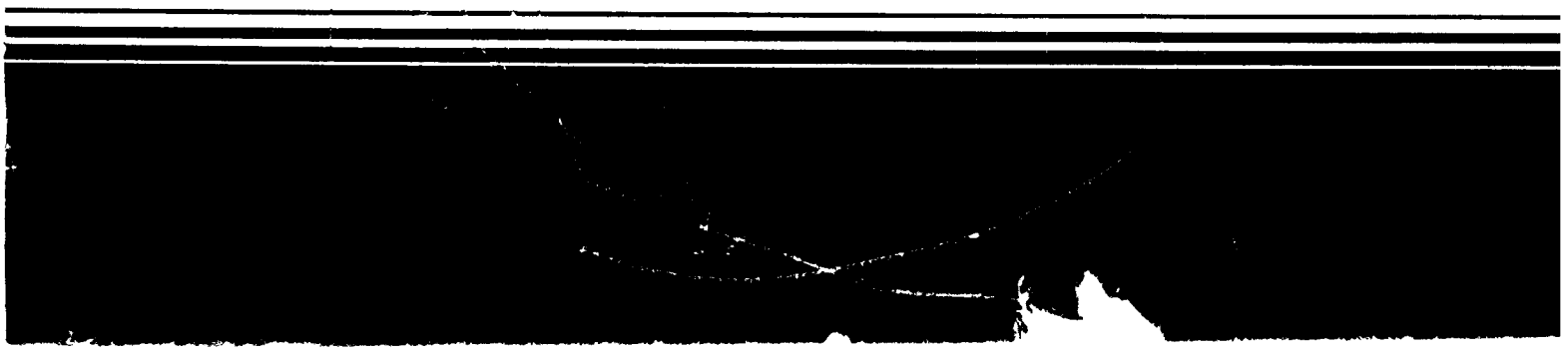

PROCEDURES FOR MODELING FLOW THROUGH CLAY LINERS TO DETERMINE REQUIRED LINER THICKNESS

EPA/530-SW-84-001

This report was prepared for the
Office of Solid Waste
under Contract No. 68-02-3168

U.S. ENVIRONMENTAL PROTECTION AGENCY
1984

DISCLAIMER

This report was prepared by Daniel J. Goode and Patricia A. Smith of GCA Corporation, Technology Division, Bedford, Massachusetts under Contract No. 68-02-3168. This is a draft report that is being released by EPA for public comment on the accuracy and usefulness of the information in it. The report has received extensive technical review but the Agency's peer and administrative review process has not yet been completed. Therefore it does not necessarily reflect the views or policies of the Agency. Mention of trade names or commercial products does not constitute endorsement or recommendation for use.

ACKNOWLEDGMENTS

The authors, Daniel J. Goode and Patricia A. Smith, express their appreciation to Dr. P. Christopher D. Milly who provided guidance and review during this project and who computed verification analytical solutions for model testing. The burden of producing this technical document in a readable form was carried by GCA's fine publications staff, to whom the authors are indebted.

FOREWORD

The Environmental Protection Agency was created because of increasing public and governmental concern about the dangers of pollution to the health and welfare of the American people. Noxious air, foul water, and spoiled land are tragic testimony to the deterioration of our natural environment. The complexity of the environment and the interplay of its components require a concentrated and integrated attack on the problem.

The Office of Solid Waste is responsible for issuing regulations and guidelines on the proper treatment, storage, and disposal of hazardous wastes, in order to protect human health and the environment from the potential harm associated with improper management of these wastes. These regulations are supplemented by guidance manuals and technical guidelines, in order to assist the regulated community and facility designers understand the scope of the regulatory program. Publications like this one provide facility designers with state-of-the-art information on design and performance evaluation techniques.

This document describes technical procedures for determining adequate thicknesses of single soil liners. It includes a performance simulation model that is based on numerical techniques recommended in guidance.

John H. Skinner
Director, Office of Solid Waste
U.S Environmental Protecton Agency

CONTENTS

CONTENTS (continued)

FIGURES

FIGURES (continued)

TABLES

1. INTRODUCTION

The Part 264 Subpart K regulation and associated guidance (47 FR 32274) broadens the legal storage options available to owners and operators of hazardous waste facilities insofar as allowance is made for the use of adequate single soil liners to create surface impoundments for temporary storage of wastes. Upon closure of the impoundment, all wastes and all parts of the liner permeated by wastes are to be removed for treatment, storage, or disposal at a RCRA hazardous waste management facility.

In order to assist the design and engineering of adequate single clay liners, GCA prepared this report which details the procedures for determining adequate thicknesses of single soil liners. An example is presented of a performance simulation model which is based on numerical techniques recommended in draft guidance.

This report includes a conceptual model of vertical unsaturated flow through porous media and the governing differential equations (Section 2); referenced methods for conducting field and laboratory tests to generate the soil property data required for model use and liner design (Section 3); and an example of computer-assisted procedures for modelling flow through natural clay liners. Finite difference and finite element techniques were selected for analysis of the models nonlinear governing equations (Section 4). These numerical procedures have sufficient flexibility to be able to incorporate many different soil types, soils with spatially varying properties, and temporal variations. The utility of the model in design evaluation and the application of a GCA-developed finite difference model are demonstrated through simulation of a hypothetical liner's performance.

2. CONCEPTUAL MODEL OF FLOW THROUGH LINER

2.1 Description of Physical Problem

The flow domain for liner breakthrough (shown in Figure 2-1) consists of the following: a layer of liquid in the impoundment of depth h_1 (L); a natural soil liner of thickness d (L); a layer of underlying site soil, which may or may not be saturated; and a constantly saturated ground water layer of the same site soil. For this study, only vertical processes are considered.

A schematic of the initial liquid pressure distribution is shown in Figure 2-2. Before installation of the liner, the soil moisture at the site can be assumed to be in static equilibrium with the underlying water table and saturated zone. Departures from this condition can occur if there is significant evaporation from or recharge to the water table, and these departures can be easily quantified. The soil liner is installed on top of the site soil and is compacted. The liner is homogeneous and hence has an initially constant moisture content and constant pressure over its entire thickness.

After the impoundment is filled, the flow system is not in equilibrium, and liquid will flow vertically down from the impoundment into the liner, and eventually into the site soil and saturated ground water zone. Our goals are to simulate this flow and to predict the liner thickness required to prevent leachate from reaching ground water during the impoundment's design life.

2.2 Mathematical Statements

2.2.1 Governing Equation of Vertical Unsaturated Flow--

The governing equation for one-dimensional unsaturated flow in the vertical direction can be written [see Bear, 1979, p. 214]:

$$\frac{\partial \psi}{\partial t}\frac{d\theta}{d\psi} - \frac{\partial}{\partial z}\left[K(\psi)\frac{\partial \psi}{\partial z} + K(\psi)\right] = 0 \qquad (2\text{-}1)$$

in which $\psi \approx \phi - z$ [L] is matric potential or capillary pressure head, where ϕ [L] is piezometric head; θ [-] is volumetric moisture content; $K(\psi) = K_r(\psi)\, K_s$ [LT^{-1}] is unsaturated hydraulic conductivity, where $K_r(\psi)$ [-] is relative hydraulic conductivity, and K_s [LT^{-1}] is saturated hydraulic conductivity; z [L] is the vertical coordinate, positive upward; and t [T] is time. This equation is developed by consideration of conservation of mass. The first term represents the change in storage of liquid mass and the second term is mass flux divergence, or the change in flux over space. The second term contains fluxes due to the matric potential gradient ($K(\psi)\, \partial\psi/\partial z$) and gravitational potential ($K(\psi)\, \partial z/\partial z$). The flux term is developed from the generalization of Darcy's law for water flow in porous media,

$$q = -K(\psi)\frac{\partial \phi}{\partial z} = -K(\psi)\frac{\partial(\psi+z)}{\partial z} = -K(\psi)\left[\frac{\partial \psi}{\partial z} + 1\right] \qquad (2\text{-}2)$$

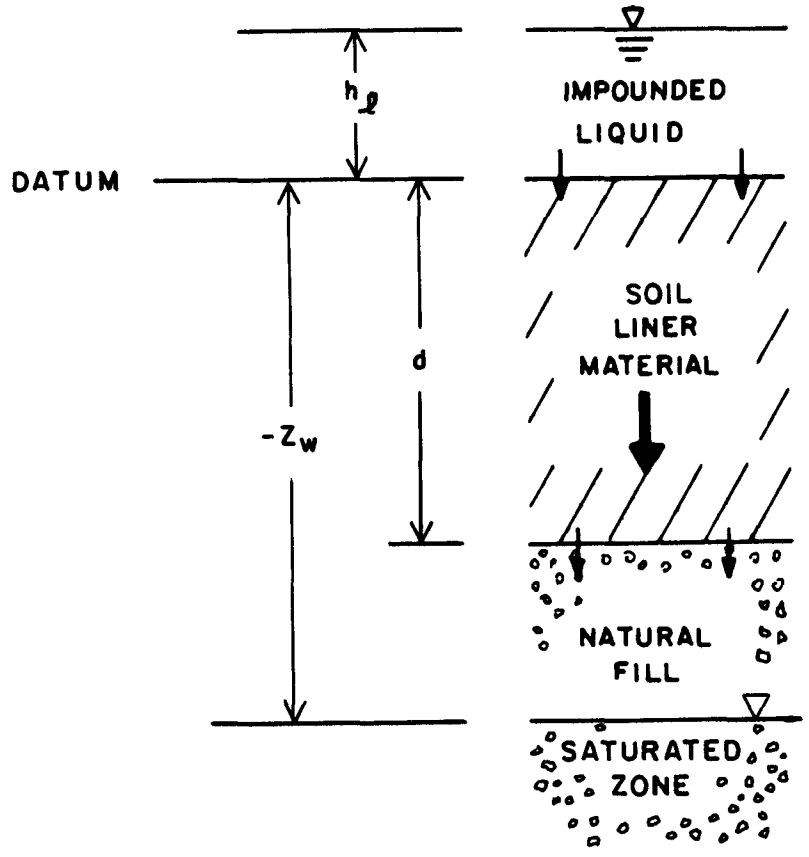

Figure 2-1. Flow domain for liner breakthrough.

in which q [LT^{-1}] is flux. Some assumptions implicit in (2-1) are that the fluid has constant density and does not freeze, that the medium does not deform, that the air phase is always at a spatially constant atmospheric pressure, and that the water flow is unaffected by temperature gradients or by solute concentration gradients.

Equation (2-1), derived for unsaturated flow, is also applicable to modeling temporarily or permanently saturated soil zones. In that case, ψ is known as the pressure head, $d\theta/d\psi$ becomes the specific storativity, and $K(\psi)$ is equal to K_s.

2.2.2 Boundary Conditions--

At the top of the liner, z=0, the liquid pressure is controlled by the level of liquid in the impoundment (see Figure 2-2). In terms of piezometric head, the matric potential at the liner top is fixed:

$$\psi = \phi_{z=0} - z \qquad \text{at } z=0 \tag{2-3}$$

Since the piezometric head is constant in space (hydrostatic) in the ponded liquid,

$$\phi_{z=0} = \phi_{z=h} = h_\ell \tag{2-4}$$

and, since z=0, (2-3) becomes:

$$\psi = \phi_{z=0} - 0 = h_\ell \qquad \text{at } z=0 \tag{2-5}$$

This is the fixed pressure Dirichlet boundary condition applied at the top of the soil column.

By definition, the matric potential at the water table is equal to zero; thus at the column bottom, $z = z_w$, the Dirichlet boundary condition is:

$$\phi = z_w \text{ or } \psi = 0 \qquad \text{at } z = z_w \tag{2-6}$$

This water table boundary condition is assumed to be controlled by local ground water flow and to be unaffected by the amount of liquid discharging through the liner. That is, the water table elevation is assumed to be constant.

The matric potential matching condition between the liner soil and the site soil is [see Bear, 1979, p. 206]:

$$\psi = \psi_s \qquad \text{at } z = -d \tag{2-7}$$

where ψ and ψ_s, refer to liner and site soil respectively. This is simply a condition of pressure continuity. This condition is incorporated into the governing equation (2-1) and is implicitly satisfied.

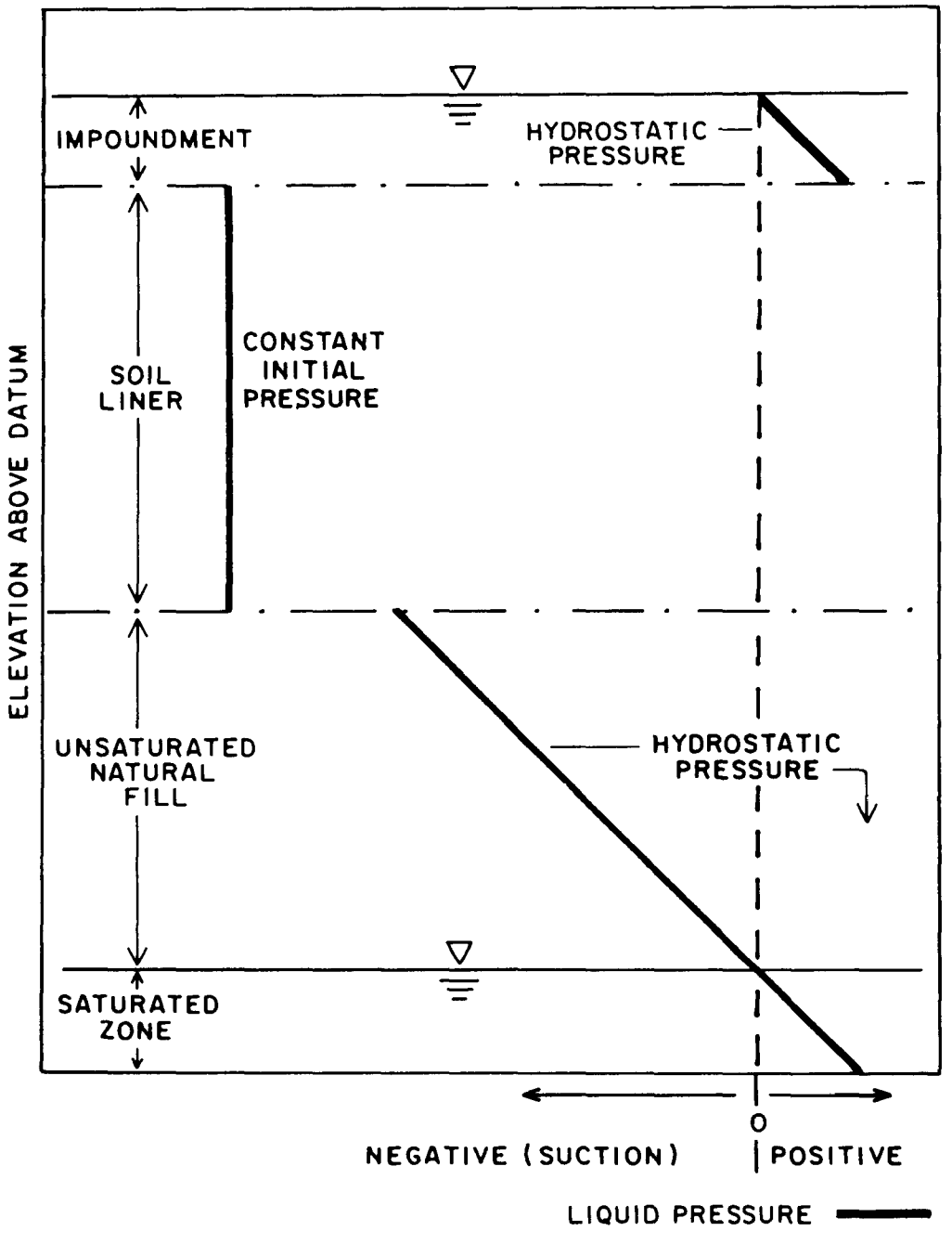

Figure 2-2. Schematic of initial capillary liquid pressure distribution.

2.3 Soil Moisture Characteristics

Liquid is held in the pore space of an unsaturated porous medium by capillary and adsorptive forces [Hillel, 1971, p. 57]. In a soil column at static equilibrium, these surface tension and adsorptive forces among the liquid, the solids, and the air exactly oppose the force of gravity pulling the liquid down. In general, the smaller the pore size, the more weight these forces can support. For the liquid to be at static (no flow) equilibrium, the piezometric head must be constant ($\phi = \psi + z$ = constant) over the entire column. Thus, the matric potential decreases linearly with height:

$$\psi = \phi_{\text{constant}} - z \tag{2-8}$$

At and below the water table $\phi = z_w$ and above the water table

$$\psi = z_w - z \tag{2-9}$$

This static pressure profile is shown in Figure 2-2.

Figure 2-3 shows typical soil moisture characteristic curves for a sandy and a clayey soil. Clays hold more liquid at lower pressures (or, in a hydrostatic situation, higher elevations above the water table) because of their smaller pore size. Although the porosity of a clay may be higher than that of a sandy soil, the individual pores are much smaller.

To evaluate the storage term of the governing equation (2-1), we must define the soil specific moisture capacity $C(\psi)$ $[L^{-1}]$:

$$C(\psi) \equiv \frac{d\theta}{d\psi} \tag{2-10}$$

which is the derivative of the moisture retention function

$$\theta = \theta(\psi) \tag{2-11}$$

that describes the relationship between moisture content and matric potential, shown in Figure 2-3.

Several mathematical expressions have been proposed for the moisture retention function, or characteristic curve. Brooks and Corey [1964] collected moisture retention data on many granular media and developed a power law relationship:

$$\theta(\psi) = \begin{cases} n & \psi > \psi_b \\ \theta_r + (n - \theta_r)\left[\dfrac{\psi}{\psi_b}\right]^{-\lambda} & \psi < \psi_b \end{cases} \tag{2-12}$$

in which θ_r [-] is residual (nonreducible) moisture content, ψ_b [L] is bubbling or air entry pressure at which air first enters the draining column, n [-] is porosity, and λ is a fitted parameter. The experimental data to develop this model included pressures of $0 \geq \psi \geq -500$ cm. The corresponding specific moisture capacity is:

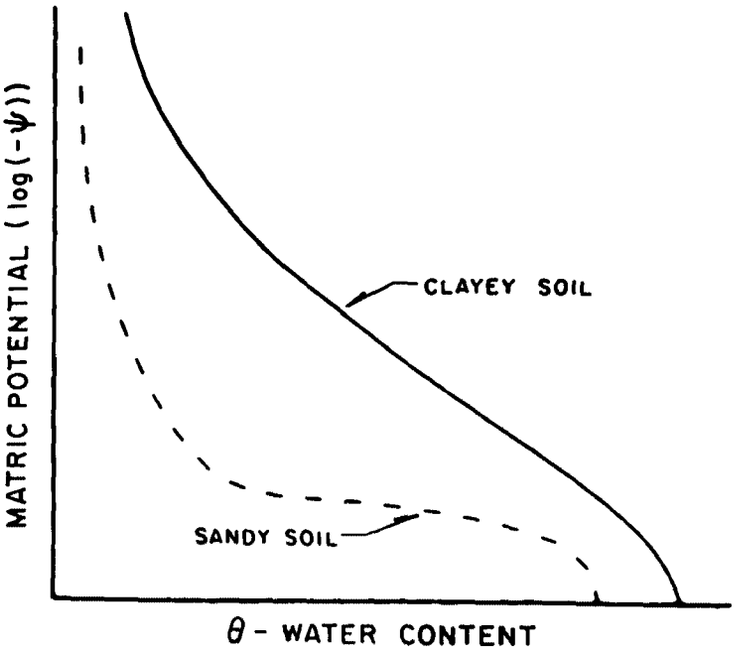

Figure 2-3. The effect of texture on soil moisture characteristics (after Hillel, 1971).

$$C(\psi) = \begin{cases} -\lambda(n-\theta_r)\,\dfrac{1}{\psi}\left|\dfrac{\psi}{\psi_b}\right|^{-\lambda} & \psi < \psi_b \\ 0 & \psi \geq \psi_b \end{cases} \qquad (2\text{-}13)$$

This function is discontinuous at saturation, $\psi = \psi_b$. Clapp and Hornberger [1978] amended this model to include gradual air entry near saturation and to provide a continuous relation.

King [1965] fit a hyperbolic function to moisture retention data for several soil types with pressures down to ψ = -100 cm:

$$\theta = n\delta \left[\frac{\cosh\left[(\psi/\psi_o)^{\beta} + \varepsilon\right] - \gamma}{\cosh\left[(\psi/\psi_o)^{\beta} + \varepsilon\right] + \gamma}\right] \qquad (2\text{-}14)$$

in which δ, ψ_o, β, ε, and γ are fitted parameters. This model was used by Gillham et al. [1976] to provide data for numerical computations.

Rogowski [1971] proposed a simple model requiring few input parameters. This model is:

$$\begin{aligned} \theta &= n + \alpha \ln(\psi_b - \psi + 1) && \psi \leq \psi_b \\ \theta &= n && \psi > \psi_b \end{aligned} \qquad (2\text{-}15)$$

in which

$$\alpha = (\theta_{15} - n) \,/\, \ln(\psi_b - \psi_{15} + 1) \qquad (2\text{-}16)$$

where $\psi_{15} = 1.5 \times 10^4$ cm (15 bars) and θ_{15} is moisture content when $\psi = \psi_{15}$. Again, this model is discontinuous at saturation ($\psi = \psi_b$) but only requires three measured parameters: n, ψ_b, and θ_{15}. This model performed well for several soil types, including a clay.

McQueen and Miller [1974] proposed a linear relationship between pF $\equiv$ log (-ψ), with ψ in cm, and moisture content. The three straight segments were a capillary segment from saturation to pF 2.5, an adsorbed segment from pF 2.5 to 5.0 and a tightly adsorbed segment from pF 5.0 to 7.0. As pointed out by McQueen and Miller [1974], their fitting procedure allows convenient approximation of the entire moisture characteristic curve from few data points.

Milly and Eagleson [1980] developed a related continuous function, considering only two unsaturated segments:

$$\begin{aligned} \theta(pF) = \frac{1}{M} \ln\left[\exp\left\{M\,(a_1 - s_1\,pF)\right\} + \exp\left\{M\,(a_2 - s_2\,pF)\right\}\right] \\ - \frac{1}{M'} \ln\left[\exp\left\{M'\,(a_2 - s_2\,pF)\right\} + \exp\left\{M'\theta_u\right\}\right] + \theta_u \end{aligned} \qquad (2\text{-}17)$$

in which a_1, a_2, s_1, s_2 and θ_u are defined by Figure 2-4, and M and M' control the curvature of the joining segments. On a linear portion of the capillary range between pF_{min} and pF_0, this function can be approximated as:

$$\theta(\psi) = a_2 - s_2 \log(-\psi) \tag{2-18}$$

and the specific moisture capacity is approximately

$$C(\psi) = -\frac{s_2}{\ell n(10)} \frac{1}{\psi} \tag{2-19}$$

Since (2-17) has continuous slope, the exact form of (2-19), for all ψ, is also continuous and can be written:

$$C(\psi) = \frac{1}{M}\left[p_1 (-\psi)^{q_1} + p_2 (-\psi)^{q_2}\right]^{-1} \left[-p_1 q_1 (-\psi)^{q_1 - 1} - p_2 q_2 (-\psi)^{q_2 - 1}\right] - \frac{1}{M'}\left[p_3 (-\psi)^{q_3} + p_4\right]^{-1} \left[-p_3^{q_3} (-\psi)^{q_e - 1}\right] \tag{2-20}$$

where:

$$p_1 = e^{M a_1} \qquad q_1 = -M s_1 \log(e)$$

$$p_2 = e^{M a_2} \qquad q_2 = -M s_2 \log(e) \tag{2-21}$$

$$p_3 = e^{M' a_2} \qquad q_3 = -M' s_2 \log(e)$$

$$p_4 = e^{M' u}$$

Equations (2-17) and (2-20) are plotted for sandy and clayey soils in Figure 2-5.

The moisture content of a soil is not a unique function of matric potential; this relationship varies widely between wetting and drying processes. This effect is called hysteresis and is important in determining redistribution of moisture in a soil column when some spaces are being wetted and later dried [Hillel, 1971]. During infiltration under ponding, the effect of hysteresis is small if the wetting history of different points in the soil is similar and all pores are wetting [see Morel-Seytoux, 1973, p. 176; Dane and Wierenga, 1975].

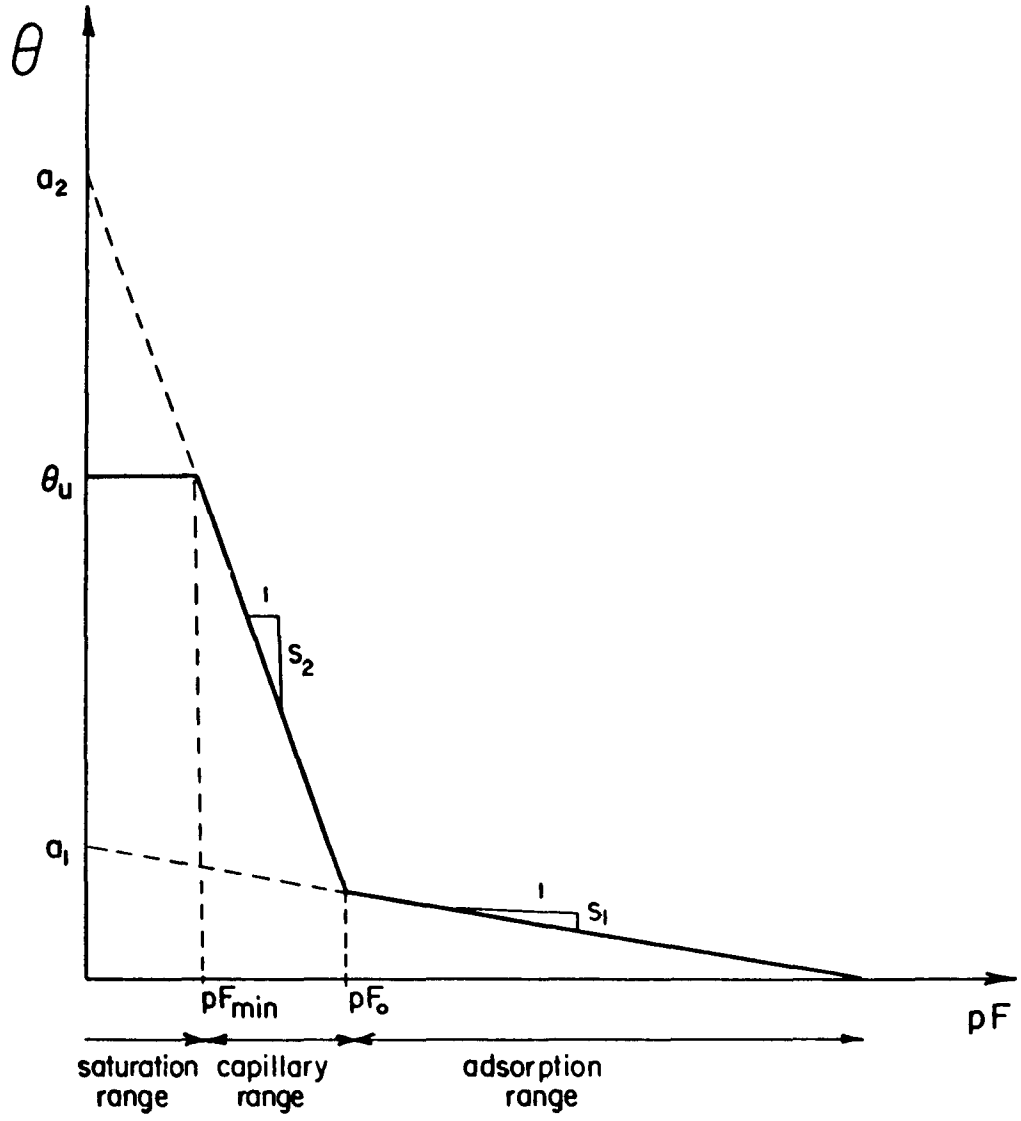

Figure 2-4. A piecewise linear relation between moisture content and the logarithm of suction (after Milly and Eagleson, 1980).

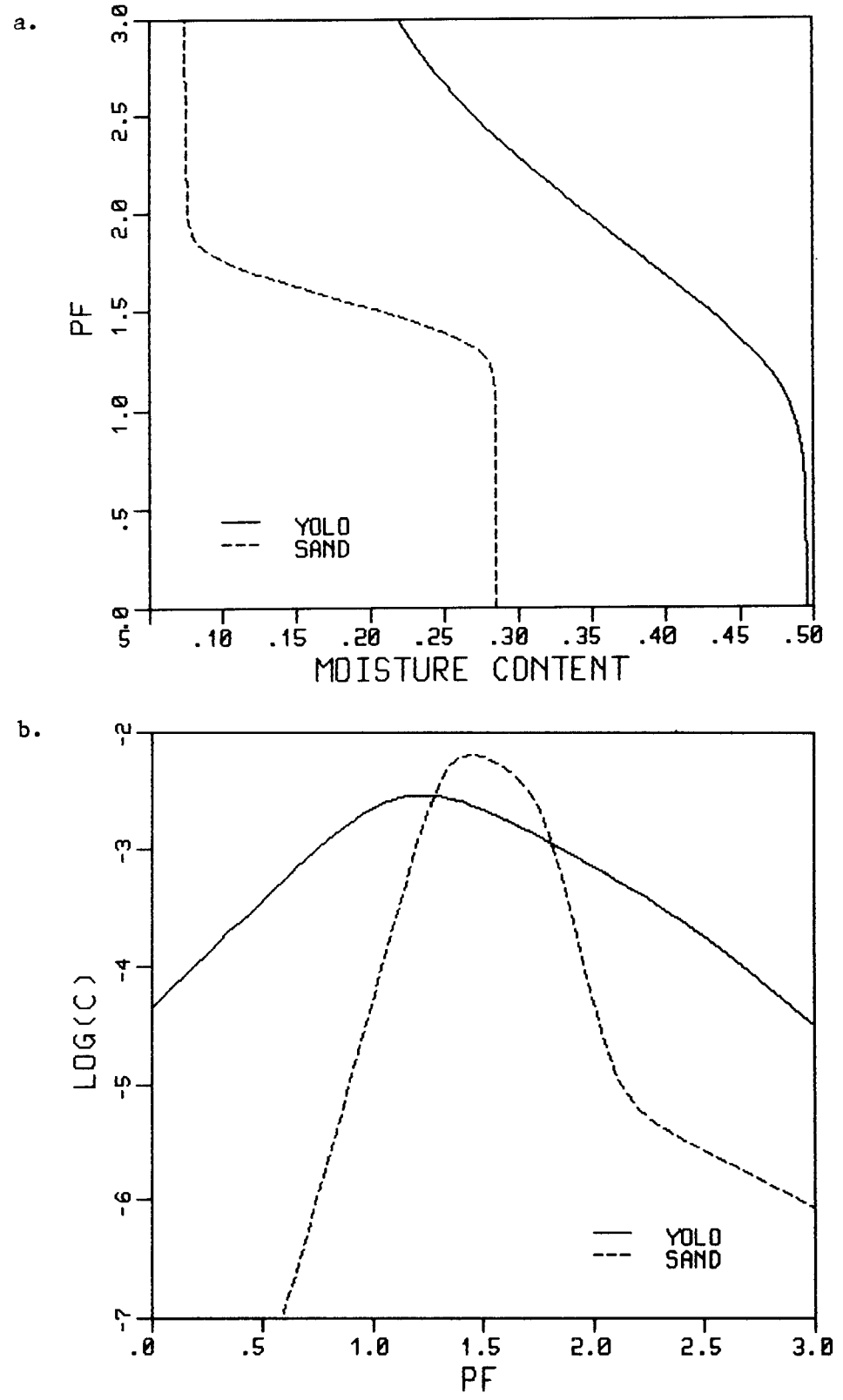

Figure 2-5. Sandy and clayey soil moisture characteristics computed from a continuous functional relationship developed by Milly and Eagleson (1980), a. moisture content and b. log of specific moisture capacity (cm^{-1}) vs. PF = $\log(-\psi)$, ψ in cm.

2.4 Unsaturated Hydraulic Conductivity

Darcy's law for flow in porous media states that the flux rate is proportional to the total piezometric head gradient times the hydraulic conductivity [Bear, 1979]:

$$q = -K(\psi) \frac{\partial \phi}{\partial z} \tag{2-22}$$

Hydraulic conductivity is a function both of the soil type and of the fluid. In this analysis, hydraulic conductivity will refer to the value applicable when the fluid is the proposed impoundment leachate. Furthermore, it will be assumed that the properties (density and viscosity) of the leachate do not differ significantly from those of the native water. This assumption can be relaxed in a more general approach to the problem.

For a given soil, the hydraulic conductivity is dependent on the moisture content or matric potential in the soil. As a function of moisture content, θ, the hydraulic conductivity function shows little hysteresis [Bear, 1979; Mualem, 1976] and since, as stated above, $\theta(\psi)$ hysteresis for this infiltration problem is ignored, the hydraulic conductivity as a function of matric potential can also be determined uniquely. Figure 2-6 shows a schematic of typical relationships between hydraulic conductivity and matric potential for sandy and clayey soil.

Numerous functional relationships have been proposed for the unsaturated hydraulic conductivity. These models include

$$\text{Gardner [1958]:} \quad K(\psi) = a \,/\, (b + (-\psi)^m) \tag{2-23}$$

where a, b, and m are constants, ($m \cong 2$ for clay);

$$\text{Gardner [1958]:} \quad K(\psi) = K_s \exp(-a\psi); \tag{2-24}$$

$$\text{Brooks and Corey [1964]:} \quad K(\psi) = K_s \left(\frac{\psi}{\psi_e}\right)^{-m} \qquad \psi \leq \psi_e \tag{2-25}$$

where m is an index of pore-size distribution; and

$$\text{Mualem [1978]:} \quad K(\psi) = K_s (S_e)^{0.015\, w + 3.0} \tag{2-26}$$

where Se is effective saturation:

$$S_e = \frac{\theta - \theta_r}{n - \theta_r}$$

and

$$w = \int_{\psi+\infty}^{\psi=0} \gamma_w \psi \; d\theta \tag{2-28}$$

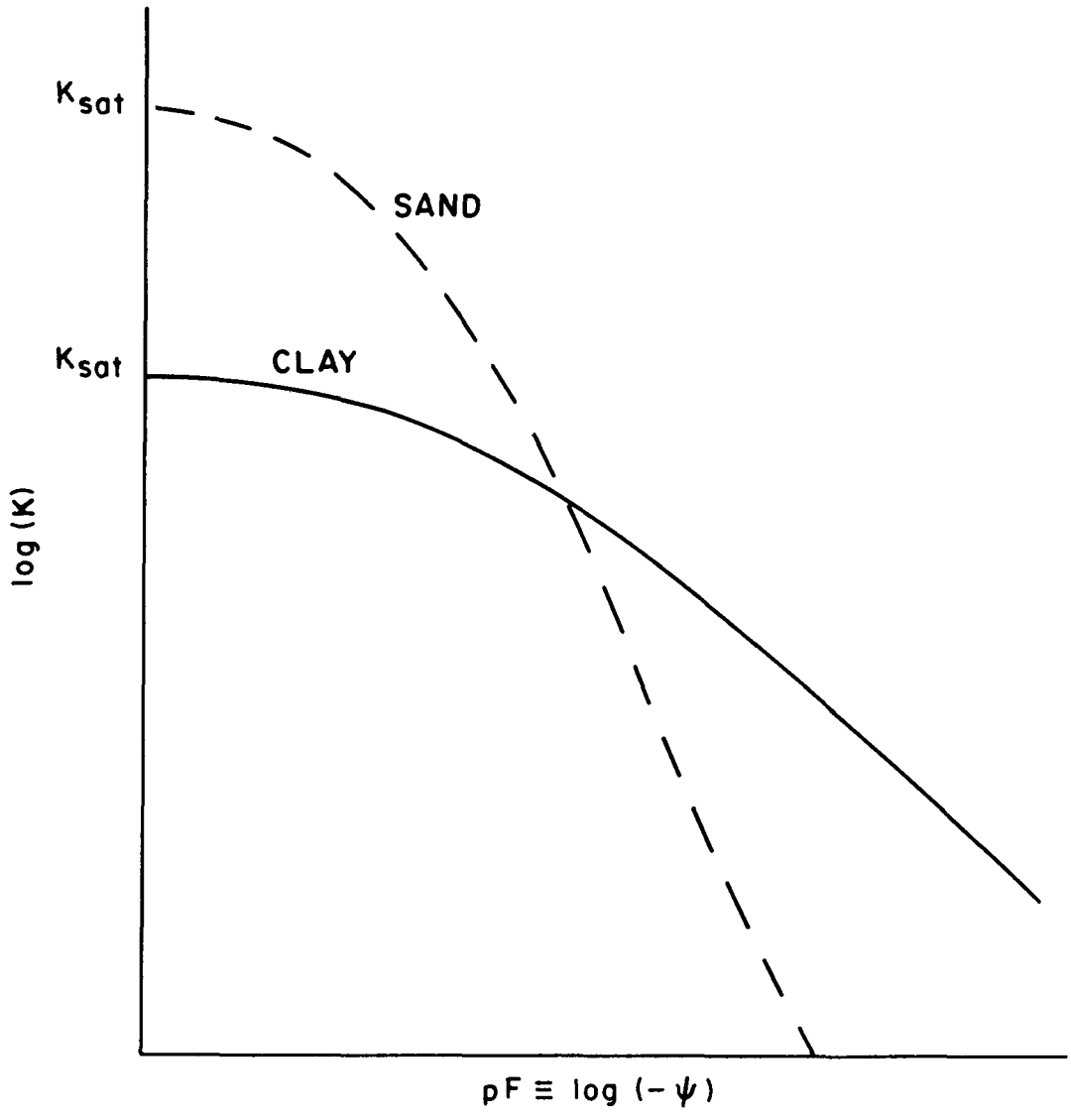

Figure 2-6. Schematic of unsaturated hydraulic conductivity for a sand and a clay soil.

in which γ_w is the specific weight of water. These formulas (2-26 - 2-28) require use of cgs units. Equation (2-28) "represents the amount of work required to drain a unit volume of a saturated soil" [Mualem, 1978]. Thus, (2-26) is dependent on the moisture characteristic curve. This model was shown to improve the prediction of unsaturated hydraulic conductivity for fine-grained soil [Mualem, 1978] relative to previous techniques.

There are several integral techniques which, as (2-26 - 2-28) above, derive the hydraulic conductivity function from the moisture characteristic curve [see Mualem 1976; Elzeftamy and Cartwright 1981; Jackson et al., 1965]. Such techniques are especially attractive when used in conjunction with numerical models because of the numerical integration required. The accuracy of these methods, of course, depends on the accuracy of the soil moisture characteristic curve, and on the applicability of the physical assumptions made by a particular technique.

2.5 Verification of Conceptual Model

Several investigators have shown that the presented governing equation for vertical unsaturated flow (2-1) accurately described the infiltration of moisture into soil. This verification has included comparison of laboratory and field experiments to analytical, finite difference, finite element, and other numerical solutions, all based on the conceptual model (2-1).

The agreement between Philip's [1958; 1969] quasi-analytical solution and experimental water content profiles reported by Davidson et al. [1969] is shown in Figure 2-7 [after Swartzendruber, 1969]. Youngs [1957] reported good agreement between theoretical and observed profile shape in laboratory experiments. Nielsen et al. [1961] compared solutions of (2-1) to the results of field studies and showed fair agreement.

The governing equation for vertical infiltration (2-1) has been solved numerically by many authors. Green et al. [1970] showed good agreement between a finite difference model of (2-1) and field measurements (see Figure 2-8). Giesel et al. [1973], Elzeftawy and Dempsey [1976], Haverkamp et al. [1977], and Ragab et al. [1982] compared results of laboratory experiments and finite difference solutions. Kunze and Nielsen [1982], Haverkamp et al. [1977], and Reeder et al. [1980] show excellent agreement between finite difference solutions and Philip's [1958; 1969] quasi-analytical results. The finite element technique was applied to the horizontal unsaturated flow equation with functional soil properties and compared to laboratory measurements by Hamilton et al. [1981]. Milly [1982] and Segol [1976] showed the agreement between results from finite element models and Philip's [1958; 1969] quasi-analytical infiltration solution (Figure 2-9).

As described above, the analysis herein considers only vertical flow. Practically speaking, the liner thickness at a typical impoundment will be two to three orders of magnitude smaller than the horizontal dimensions. Horizontal flow may be significant near the edges of the impoundment, but this effect should slow vertical movement. Jeppson et al. [1975] compared a numerical solution of the one-dimensional governing equation (2-1) to a

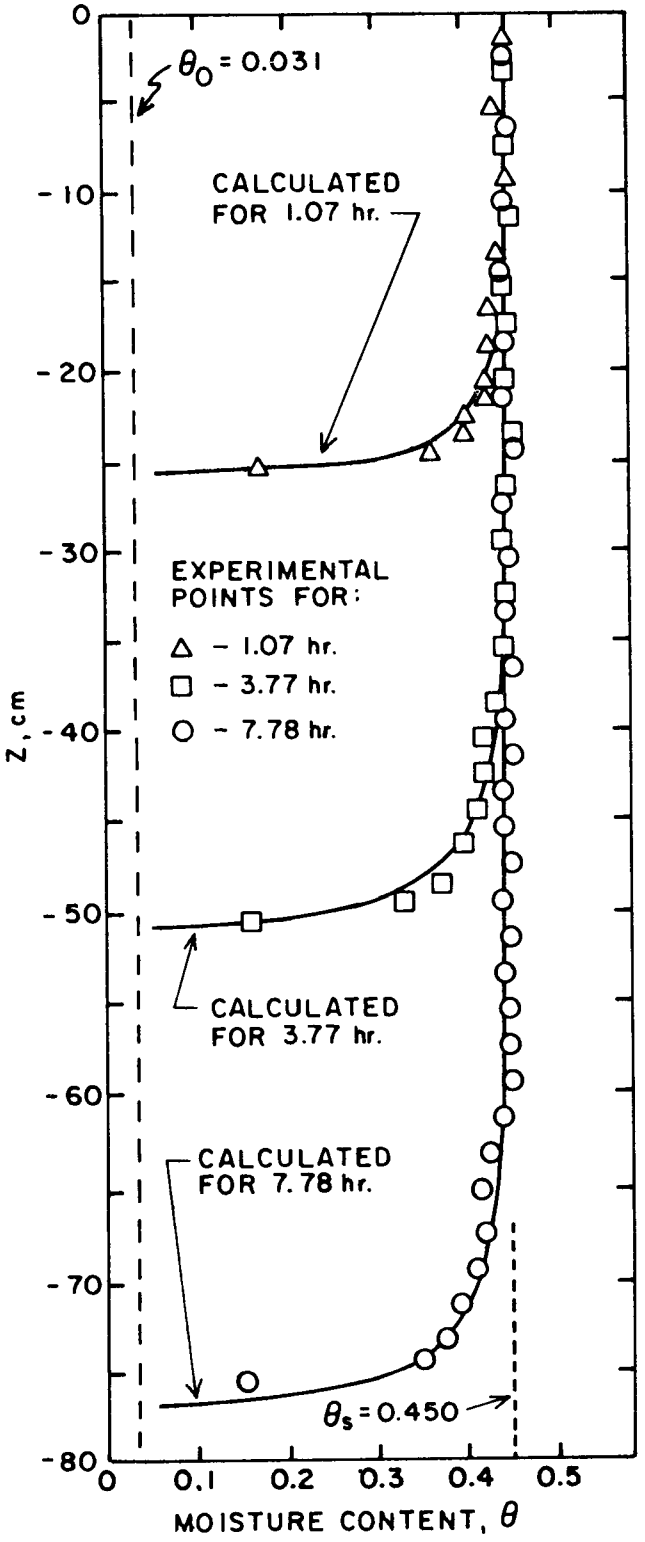

Figure 2-7. Experimental and theoretical moisture content profiles for Columbia silt loam (after Swartzendruber,(1969), data of Davidson et al. (1969)).

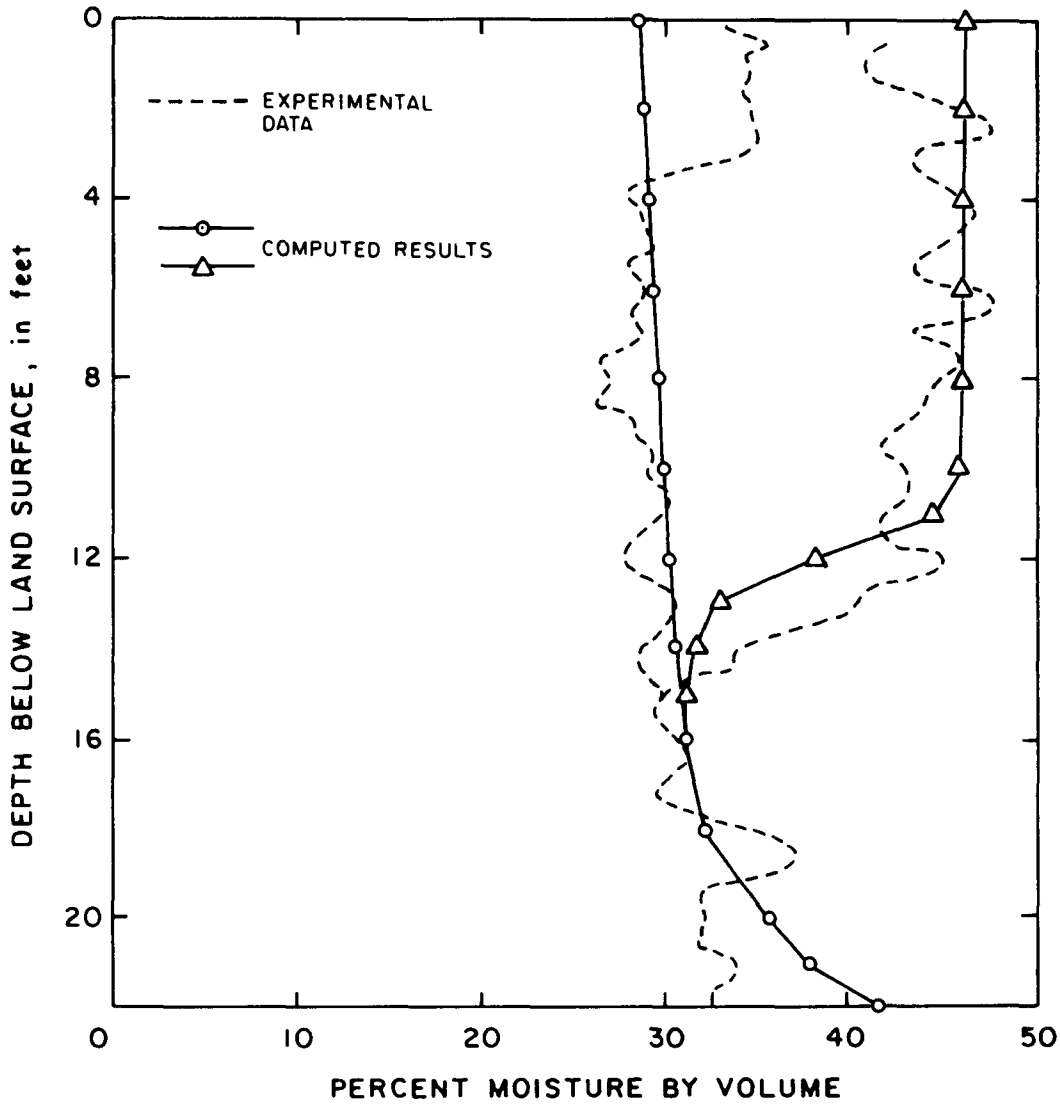

Figure 2-8. Computed (FDM) and measured field soil moisture profiles before and after 9 1/3 hours infiltration, constant properties (after Green et al., 1970).

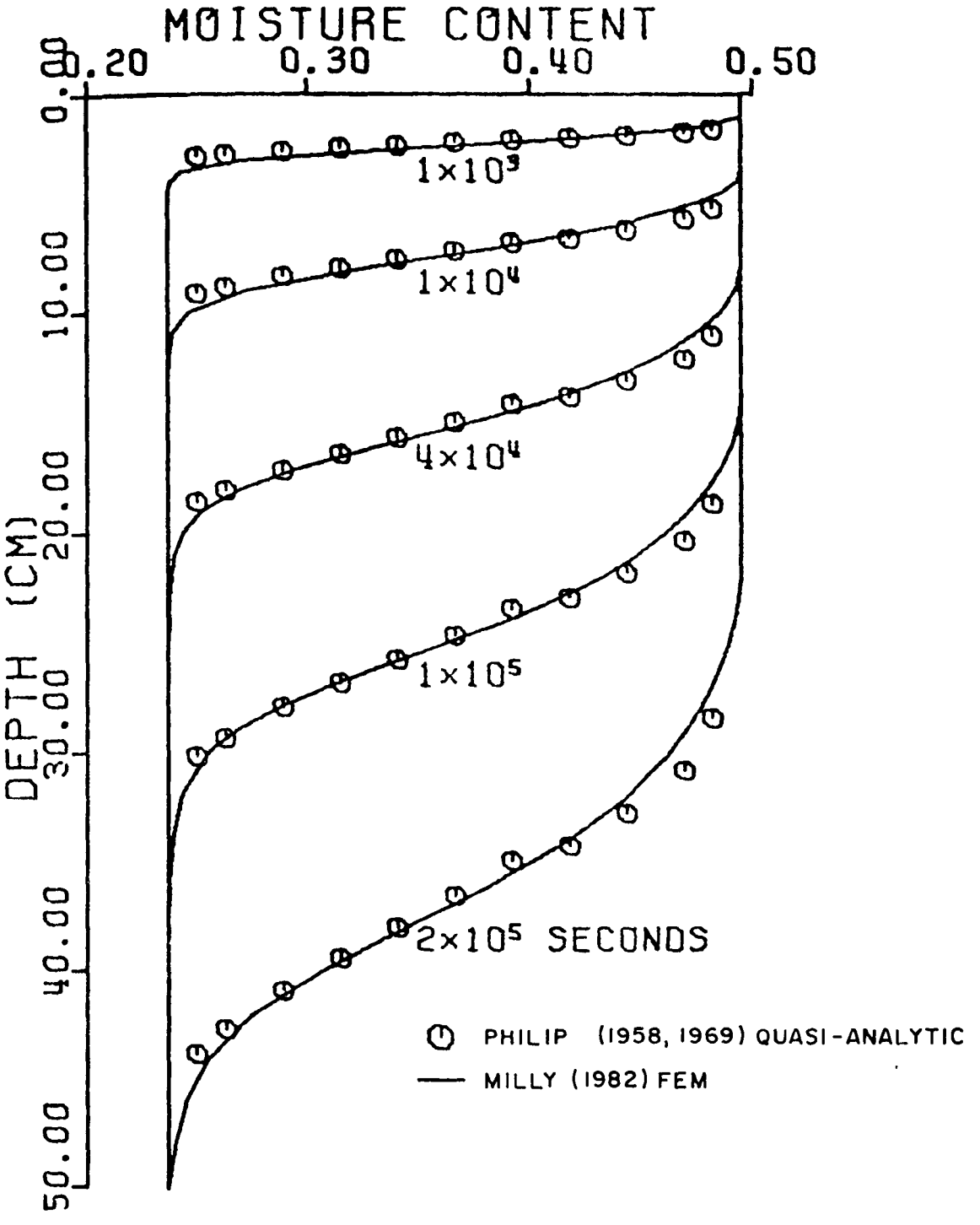

Figure 2-9. Comparison of computed infiltration into Yolo light clay with ponding by FEM and quasi-analytic methods (after Milly, 1982).

numerical solution of two-dimensional axisymmetric infiltration from a finite diameter circular area. As shown in Figure 2-10, the wetting front at the centerline of the axisymmetric solution advances slightly slower than the wetting front from the one-dimensional solution. Thus, in homogeneous soils, the one-dimensional analysis in conservative. For anisotropic layered soils, with horizontal hydraulic conductivities higher than vertical, Siegel and Stephens [1980], showed that lateral spreading can greatly reduce the vertical rate of moisture front movement, and the one-dimensional analysis is even more conservative.

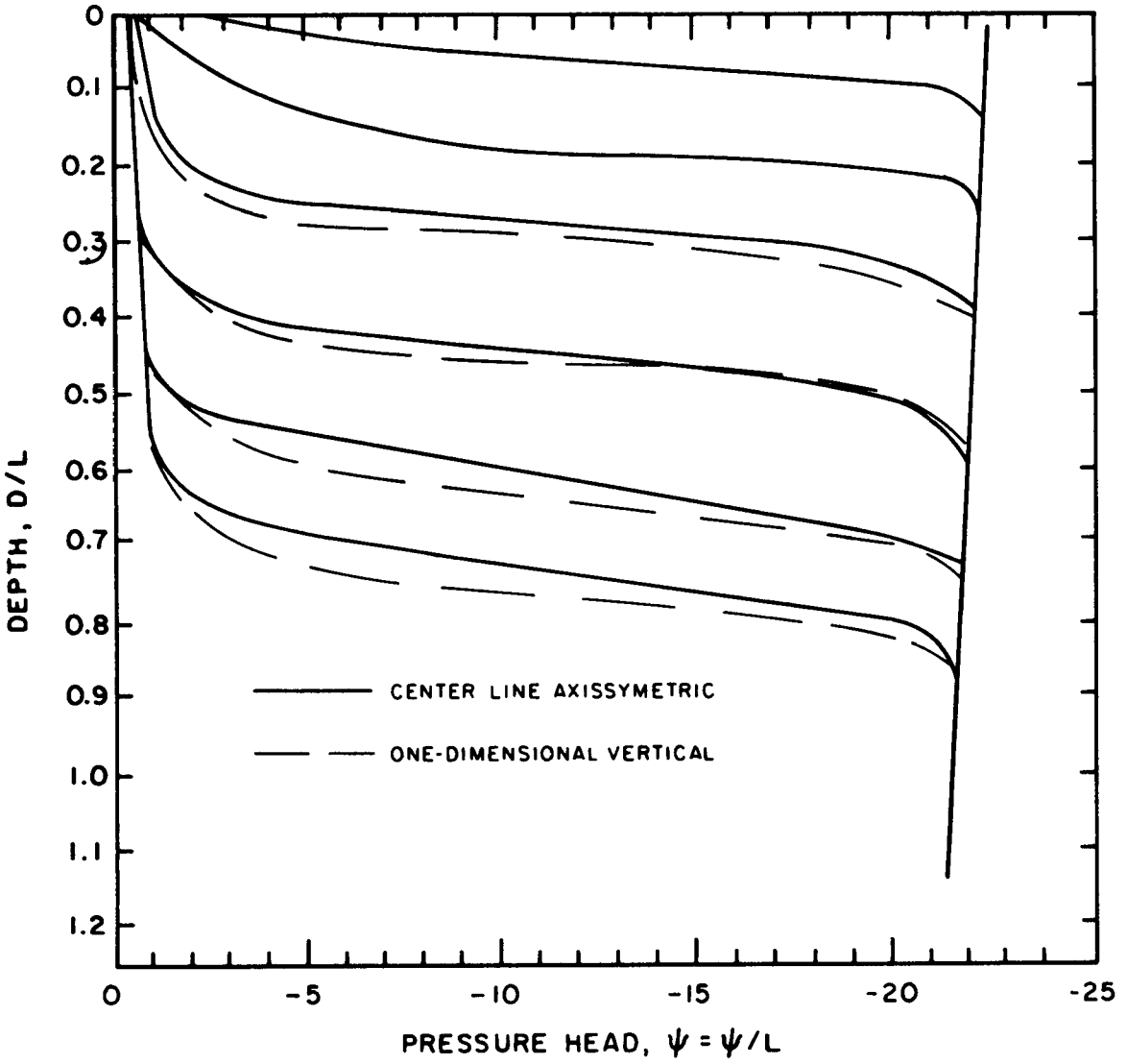

Figure 2-10. Computed dimensionless pressure head as a function of depth and time for infiltration from an axisymetric infiltrometer (after Jeppson et al., 1975).

3. DETERMINATION OF SOIL HYDRAULIC PROPERTIES

3.1 Introduction

The design of an adequate impoundment liner is grounded not only on the conceptual model of flow developed but also on accurate assessment of the soil properties of the liner and of the underlying site soil. Two such properties are particularly relevant to the model's execution. These are the moisture characteristic and the unsaturated hydraulic conductivity. This section defines these properties and discusses their empirical determination.

Although well-documented and cost-effective methods exist for laboratory determination of soil hydraulic properties, the accuracy of laboratory-obtained values should be scrutinized (Roberts, 1982; Olson and Daniel, 1981). Of foremost concern is the use of soil or permeant samples which may not be representative of field conditions. Sampling and handling techniques may significantly alter soil microstructure. In addition, field investigation and statistical sampling, if inadequate, may fail to document macroscopic features (i.e., fissures, root holes, sand seams or lenses) that significantly influence local hydraulic properties. Finally, soil tests should be conducted using a permeant similar to that to be impounded in order to include effects of chemical and physical interactions in the values assessed for hydraulic properties. Any additional cost associated with the adoption of *in situ* measurement techniques should be weighed against the cost of using inaccurate empirical parameters in the liner design. This section will refer to and compare both field and laboratory testing procedures.

3.2 The Soil Moisture Characteristic

The soil moisture characteristic, described in Section 2.3, expresses the relationship between water content of a soil and negative pressure or suction. As sufficient negative pressure is applied--that is, as an outward force is exerted and exceeds the capillary force which retains water in soil pores--these pores begin to drain. Increasing suction causes drying as smaller and smaller interstices empty. The moisture characteristic, a hysteretic curve, illustrates that water is harder to withdraw from soil once wet than it is to absorb once dry.

Hillel (1980) discusses methods that can be used in the laboratory or *in situ* to measure soil moisture content continuously or intermittently. These include neutron scattering, gamma-ray absorption, and electrical resistance of porous blocks; the former two are suitable for use in field studies. Once equipment is installed and calibrated, testing by these methods requires considerably less time and effort than laboratory oven-drying techniques which may yield erroneous results.

Tensiometers, pressure plates, and thermocouple psychrometers, each accurate over different ranges of suction, can be used to monitor suction continuously. Tensiometers are generally limited to suctions less than 0.9 atm in order to avoid cavitation of air bubbles in the device. The

pressure plate is a modification of the tensiometer design capable of accurately measuring suctions from 1 to 15 atm. While inaccurate for suctions lower than 1-2 atm, psychrometers, by measuring the relative humidity of pore air, can be used to determine suctions up to about 80 atm. When one of these methods are used to obtain readings over time in conjunction with moisture content readings, the wetting moisture characteristic for a design liner and waste liquid can be constructed.

3.3 Unsaturated Hydraulic Conductivity

Hydraulic conductivity, $K(\psi)$, described in Section 2.4, is a highly variable soil property exhibiting a range of values over 14 orders of magnitude from gravel to clays. The presence of organic solvents has been documented as increasing the conductivity of clays (Haxo, 1976), sometimes with no apparent tendency to reach maximum values (Brown & Anderson, 1982). Although many techniques have been developed to measure hydraulic conductivities over this range, only a few are feasible for measurement of conductivity in the type of unsaturated fine-grained soils that are suitable for liners.

3.3.1 Laboratory Methods--

Olson and Daniel (1981) selected two tests for determination of conductivity in unsaturated fine-grained soils.

A. The instantaneous profile test (Weeks and Richards, 1967, Watson, 1966). A soil sample is arranged in a column at equilibrium. By imposing a constant or time-dependent suction or fluid flow, unsteady-state seepage develops within the sample. Probes inserted at different depths in the column measure water content and suction values over time. A steady-rate of inflow test requires about 2 weeks to run.

B. The pressure plate method (Klute, 1965). This method entails placing a soil sample on a saturated porous plate in a pressure vessel. After a known air pressure is applied, water pressure in the plate is kept at atmospheric pressure and the system allowed to equilibrate. Then, by steps, the air pressure in the vessel is abruptly altered, which causes excessive pore water pressure and the drainage of water through the porous plate.

Olson and Daniel (1981) also discuss sources of error in laboratory conductivity tests of partially saturated soils. They recommend as the best laboratory techniques:

(1) At 0-0.9 atm of suction, the instantaneous profile method with tensiometers;

(2) At 2-80 atm of suction, the instantaneous profile method with psychrometers;

(3) At 1-15 atm of suction, pressure plate outflow.

3.3.2 Field Methods--

Olson and Daniel (1981) suggest that although in situ unsaturated soil field testing methods have only recently been developed, there are two techniques available that can be used for the case of ponded fluids. Roberts (1982) also presents an overview of these techniques, and related in situ methods are described in Method 9100 of EPA guidance.

A. The instantaneous profile method has been adapted for field use. In a diked test plot, probes for measuring water and suction pressure are inserted at selected depths. The plot is flooded with the test permeant and, after the permeant has soaked into the ground, covered to prevent evaporation. If an appropriate moisture characteristic has been previously constructed, moisture content probes or suction probes alone can be used and the other value inferred from the wetting branch of the characteristic (cf. Baker et al., 1974; Rose and Krishman, 1967). Testing times may be long in relatively impervious soils.

B. Infiltration through impeding layer (Gardner, 1970; Hillel and Gardner, 1970; Bouma, et al., 1971). A column of soil is isolated by pushing a thin-walled tube into the soil and then capped with a relatively impervious porous stone or membrane. (This procedure thus also may be conducted in the laboratory). Water is ponded on top of the stone and a small constant head maintained to develop steady-state seepage. Rate of flow through the stone is measured with a Mariotte bottle. Tensiometers inserted into the soil are used to measure suction and to confirm a hydraulic gradient of unity directly beneath the stone. Given this unit gradient the hydraulic conductivity is equivalent to the infiltration rate. Olson and Daniel (1981) point out that for fine-grained soils, not only may it be impractical to wait for steady state seepage to develop but the stone impedance would have to be so great that accurate flow rate measurements would be difficult to obtain.

4. NUMERICAL SIMULATION OF UNSATURATED FLOW

Due to the nonlinearities of the unsaturated flow equation, exact analytical solutions have not been obtained except for a few simple cases. Numerical techniques are available to solve the unsaturated flow equations. These techniques, primarily finite difference and finite element methods, provide solutions of the governing equations that take into account the inherent nonlinearities of the system and the nonhomogenicity of soil types and initial conditions. They all rely on the basic concept of solving for the moisture state at a finite number of points in space and time. Available computer-programs range from those treating basic flow [Bruch, 1975, Johnson, et al., 1982] to coupled heat and moisture transport with vapor transport and moisture hysteresis [Milly, 1982]. Using such programs, it is possible to predict the performance of specific liner designs, with parameters from field and laboratory tests.

4.1 Finite Difference Method

Finite Difference Methods (FDM) have been successfully applied to a wide range of problems in groundwater flow and soil physics. The FDM consists of first breaking the solution domain of a differential equation into subdomains. This process is called discretization. For each subdomain, continuous differential terms in the governing equation are replaced by approximate expressions based on the values of the state variable in the subdomains. Typically, one or more equations are solved for each subdomain. This technique is relatively simple to understand in practice, and is applied to both spatial and temporal differential terms. Freeze and Cherry [1979] describe the application of finite difference techniques to vertical unsaturated flow.

In application to the vertical unsaturated flow equation, the vertical column is divided up into a row of short vertical segments. This row of segments is called a grid. For mesh-centered grids, the values of matric potential (ψ) are evaluated at nodes which are located at the ends of each segment (Figure 4-1a). For a block-centered grid, these nodes are located at the center of each segment (see Figure 4-1b). Likewise, solutions in time are obtained by breaking time into discrete steps. Solutions at new times are obtained (at the nodes) using the previous solution(s). In general, the accuracy of this method improves as the grid spacing (Δz) and the time step (Δt) decrease in size.

4.1.1 FDM Spatial Difference Approximations--

The spatial domain of the vertical unsaturated flow equation (2-1) is the soil column, from the top of the impoundment liner down to the water table. This domain includes the liner and the underlying site soil. This domain is discretized as shown in Figure 4-1 in which subscript i represents the node number. Values of the state variable (matric potential, ψ), and soil properties (hydraulic conductivity, $K(\psi)$, and moisture capacity, $C(\psi)$) are approximated by values at a node i: ψ_i, K_i, and C_i. Note that K_i and

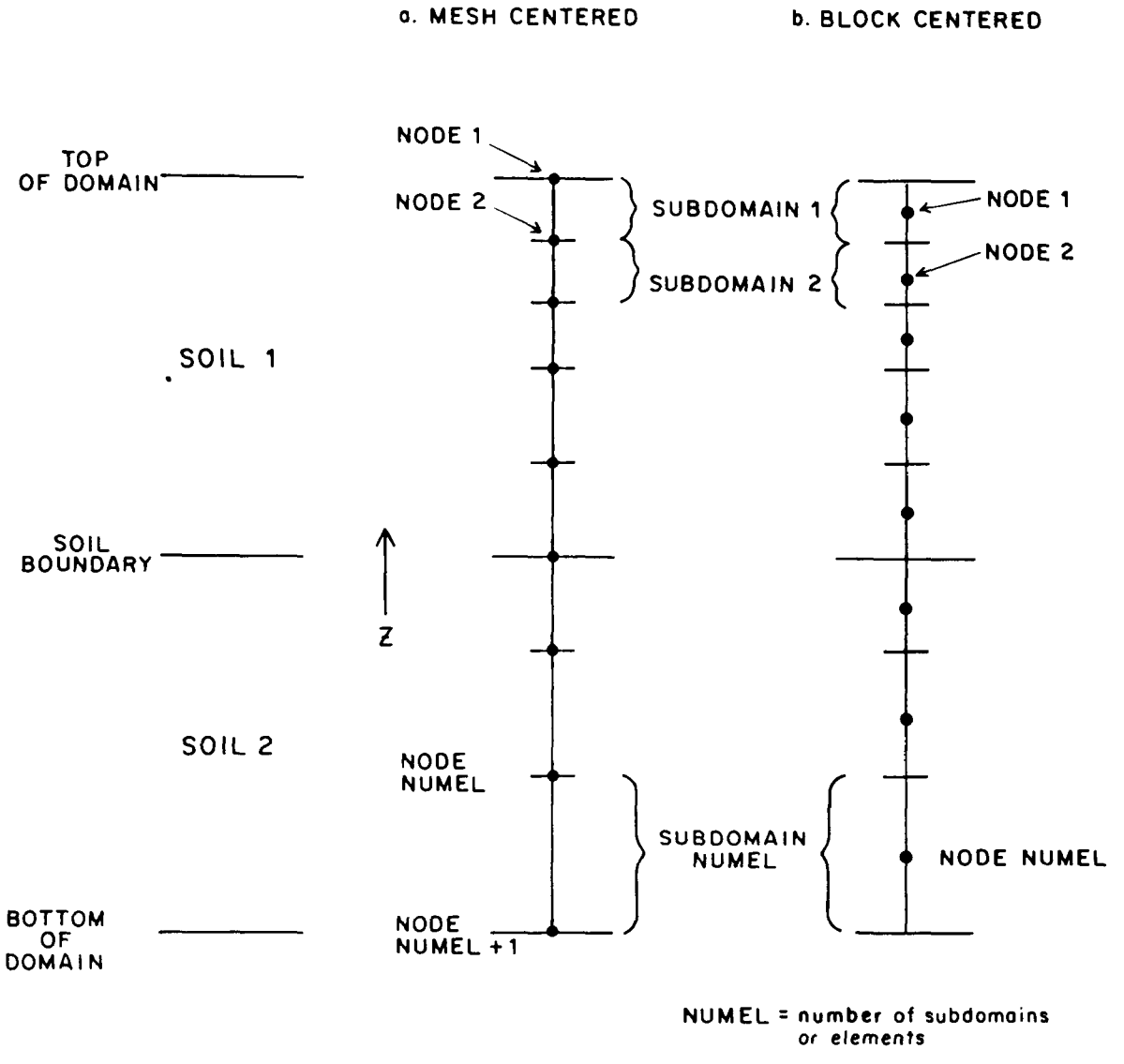

Figure 4-1. Finite difference method spatial discretization grids.

C_i are functions of ψ_i. These values are used to approximate the derivatives in (2-1). The first term in (2-1), representing pressure driven flux, can be replaced by:

$$\frac{\partial}{\partial z}\left[K\frac{\partial \psi}{\partial z}\right] = \left[K_{i+1/2}\frac{\psi i+1 - \psi i}{\Delta z} - K_{i-1/2}\frac{\psi i - \psi i-1}{\Delta z}\right]\frac{1}{\Delta z} \qquad (4\text{-}1)$$

in which $\Delta z = z_{i+1} - z_i$ is the constant node spacing and

$$K_{i+1/2} = \frac{1}{2}(K_i + K_{i+1})$$
$$K_{i-1/2} = \frac{1}{2}(K_i + K_{i-1}) \qquad (4\text{-}2)$$

are the arithmetic average hydraulic conductivities between nodes. The gravitational flux term can be expressed as:

$$\frac{\partial K(\psi)}{\partial z} = \frac{K_{i+1} - K_{i-1}}{2\Delta z} \qquad (4\text{-}3)$$

Equations (4-1) and (4-3) are centered difference approximations [see Pinder and Gray, 1977]. These expressions assume that the node spacing, Δz, is constant, although that is not a general requirement. With constant node spacing (4-3) is second order accurate. This means that if conductivity $K(\psi)$ is a liner function of z and z^2 only, then (4-3) is exact.

4.1.2 FDM Temporal Derivative Approximations--

The temporal domain of the vertical unsaturated flow equation (2-1) is time, $t > 0$, after infiltration into the liner begins. Time is broken down into time level subdomains as shown in Figure 4-2 in which superscript n represents time level. The nodal values of properties and state variables, which are actually continuous in time, are approximated by values at discrete time levels: $\psi^n{}_i$, $K^n{}_i$, and $C^n{}_i$. The storage term in (2-1) can be written:

$$C\frac{\partial \psi}{\partial t}_{n+\alpha} = \alpha\left[C\frac{\partial \psi}{\partial t}\right]_{n+1} + (1-\alpha)\left[C\frac{\partial \psi}{\partial t}\right]_n = \frac{\psi^{n+1} - \psi^n}{\Delta t}\, C^{n+\alpha} \qquad (4\text{-}4)$$

in which $C^{n+\alpha} = \alpha C^{n+1} + (1-\alpha)\, C^n$; $0 \leq \alpha \leq 1$ is a temporal weighting parameter, and $\Delta t = t^{n+1} - t^n$ is the time step size. Subscripts have been dropped for convenience. If $\alpha = 0$, (4-4) is

$$C\frac{\partial \psi}{\partial t}\Big|_n = \frac{\psi^{n+1} - \psi^n}{\Delta t}\, C^n \qquad (4\text{-}5)$$

which is forward differencing. When solving for ψ^{n+1}, all other terms of (4-5) are known from the last time step and thus ψ^{n+1} is solved <u>explicitly</u>. If $\alpha=1$, (4-4) is:

$$C\frac{\partial \psi}{\partial t}\Big|_{n+1} = \frac{\psi^{n+1} - \psi^n}{\Delta t}\, C^{n+1} \qquad (4\text{-}6)$$

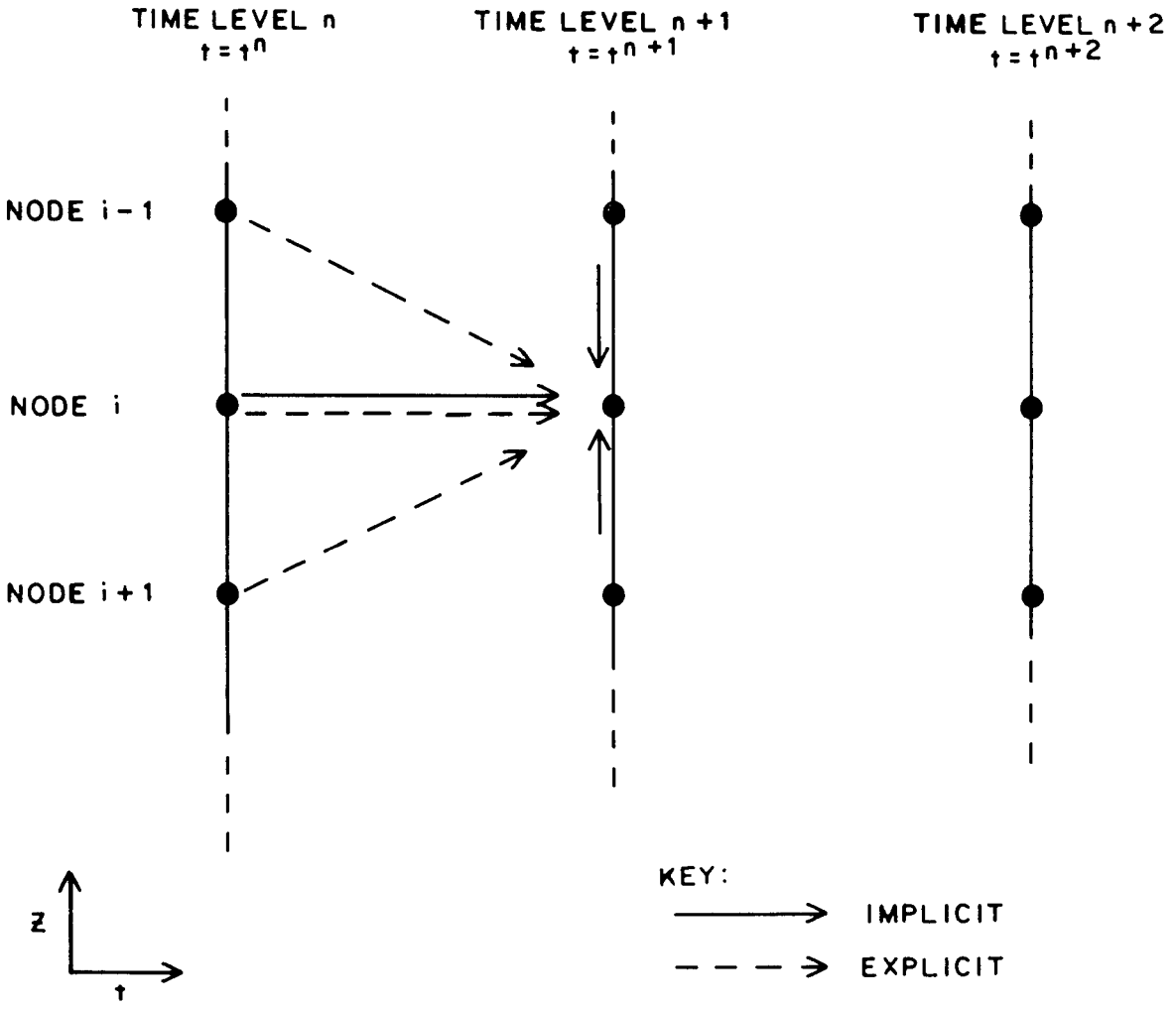

Figure 4-2. Finite difference method temporal discretization for node i at time level n + 1 showing explicit (dash) and implicit (solid) relationships.

Both sides of (4-6) contain terms which must be evaluated at the current timestep, t^{n+1}, and depend on the solution ψ^{n+1}, thus (4-6) is implicit in ψ^{n+1}. Another standard time differencing scheme is the Crank-Nicolson procedure obtained by setting $\alpha=0.5$ in (4-4).

The explicit scheme ($\alpha=0$) is conditionally stable (the solution will not always converge) and should only be used with small time steps. The fully implicit scheme ($\alpha=1$) is unconditionally stable although accuracy is greatly affected by time step size. The Crank-Nicolson scheme ($\alpha=0.5$) is also unconditionally stable and is more accurate for many flow problems [Pinder and Gray, 1977]. Theoretically, any $0 \leq \alpha \leq 1$ is first order accurate except $\alpha=0.5$, which is second order accurate for constant time steps.

Application of FDM to the governing flow equation results in a system of equations to be solved each time step for the unknown nodal values of matric potential. This equation, written in matrix notation, is

$$\left(\frac{\underline{A}^{n+\alpha}}{\Delta t} + \alpha \underline{B}^{n+\alpha}\right) \underline{h}^{n+1} = \left(\frac{\underline{A}^{n+\alpha}}{\Delta t} - (1-\alpha)\underline{B}^{n+\alpha}\right) \underline{h}^{n} + \underline{f}^{n+\alpha} \qquad (4\text{-}7)$$

where h^n is the vector of known values of potential at the last time step and h^{n+1} is the unknown vector to be determined. The matrix A is determined by the grid geometry and by the storage coefficients, $C(\psi)$. The matrix B is a function of hydraulic conductivity and of the grid geometry. The vector f is a forcing vector that accounts for boundary conditions. It also includes gravity flow terms. For a one-dimensional problem, the matrix B is tridiagonal, i.e.,

$$\underline{B} = \begin{bmatrix} q_1 & r_1 & 0 & & & & \\ p_2 & q_2 & r_2 & 0 & \text{All 0's} & & \\ 0 & p_3 & q_3 & r_3 & & & \\ & & & & & & 0 \\ \text{All 0's} & & & & & p_{n-1} & q_{n-1} & r_{n-1} \\ & & & & & 0 & p_n & q_n \end{bmatrix} \qquad (4\text{-}8)$$

while A is diagonal (only the diagonal elements are nonzero). Thus for $\alpha = 0$, the i'th line of (4-8) expresses an implicit relation among the new potential at node i (through q_i), the new potential at node i-1 (through p_i), and the new potential at node i+1 (through r_i). For $\alpha=0$, the i'th equation gives the new potential at node i explicitly.

Equation (4-7) is not a linear equation for the unknown, h^{n+1}, since the storage and flux matrices, A^{n+1} and B^{n+1}, are themselves functions of h^{n+1}. In order to solve (4-7) at a given time step, therefore, a variety of

linearization and iteration schemes have been developed. The resulting linear matrix equation can be solved either directly or iteratively, the former being more economical in one-dimensional applications.

4.1.3 FDM Application to Vertical Unsaturated Flow--

The FDM has been applied to vertical unsaturated flow by many authors. Freeze [1969] investigated natural ground water recharge and discharge mechanisms. Brutsaert [1971] used a two-dimensional vertical model in a study of soil moisture flow beneath drains and irrigation ditches. Cooley [1971] investigated flow to a pumping well using an axisymmetric two-dimensional vertical model. For one-dimensional vertical flow, the FDM has been verified by, among others, Green et al. [1970], Ragab et al. [1982]. Giesel et al. [1973], and Elzeftawy and Dempsey [1976]. Kunze and Nielson [1982], Haverkamp et al. [1977], and Reeder et al. [1980] show excellent agreement between finite difference solutions and Philip's [1958, 1969] quasi-analytical results.

4.2 Finite Element Method

The Finite Element Method (FEM) has only more recently become a common tool in ground water flow simulation. This method is conceptually more difficult to grasp and is practically speaking more complicated than the FDM. Nonetheless, it has several advantages including flexibility in grid design, and improved accuracy for many nonlinear and frontal (sharp changes) problems.

Like the FDM, the FEM also involves discretization, breaking the flow domain into subdomains. For the FEM, these spatial subdomains are called elements and are delineated by nodes (see Figure 4-3). Whereas the FDM approximates the governing equation with discrete difference terms, the FEM uses an integral approach. First, the governing equation is converted to an integral equation, including the boundary conditions. Next, the dependent variable (matric potential) is approximated using the values at the nodes and interpolation functions between nodes on the elements. This approximate potential profile is substituted into the integral equation which can be evaluated over each element. The resulting element integrals are combined and a system of equations is developed relating the rate of change of matric potential at each node to the values at all nodes and to the boundary conditions. Although the FEM can then also be applied to the integration of the solution in time, the FDM is most commonly applied to the time derivative, as described above. Pinder and Gray [1977] describe the FEM and its application to unsaturated flow problems.

4.2.1 FEM Spatial Approximation--

The vertical flow domain is discretized as shown in Figure 4-3. In this domain, the matric potential is approximated as

$$\psi \simeq \sum_{i=1}^{n} N_i \, \psi_i \qquad (4\text{-}9)$$

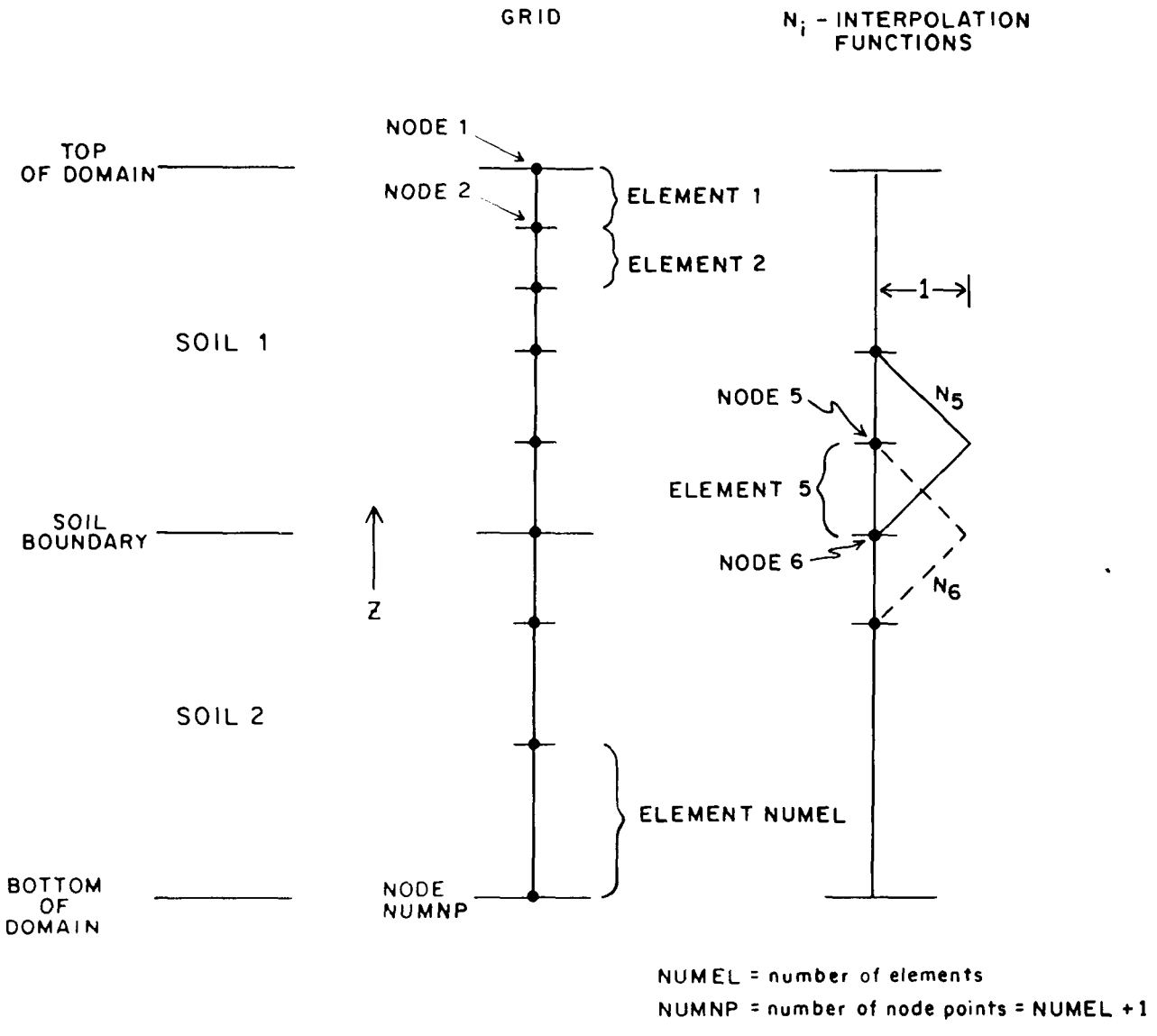

Figure 4-3. Finite element method discretization and linear interpolation functions.

where N_i is an interpolation function (see Figure 4-3) which is a function of space, z, and ψ_i is the approximate value of pressure head at node i. A common type of interpolation function is the linear or chapeau (hat) function. On any element, defined by the end nodes, the pressure head then varies linearly between these two nodes (see Figure 4-3). Thus, when all the ψ_i's are known, the pressure distribution is a continuous function made up of piece-wise linear (straight) segments. Quadratic interpolation, an alernative approach, uses three nodes per element and results in curved segments.

In any weighted residual method, the governing equation is multiplied by a weighting function and the results integrated over the spatial flow domain. The weighted residual method most commonly used in ground water and soil physical models is that of Galerkin, which uses the interpolation functions in (4-9) as weighting functions also. This representation of (2-1) can be written:

$$\int N_k \left\{ C \frac{\partial \psi}{\partial t} - \frac{\partial}{\partial z} K \frac{\partial \psi}{\partial z} - \frac{\partial K}{\partial z} \right\} dz = 0 \quad \text{for each k} \tag{4-10}$$

Equation (4-10) can be integrated by parts to yield:

$$\int \left\{ N_k \, C \frac{\partial \psi}{\partial t} + K \frac{\partial N_k}{\partial z} \frac{\partial \psi}{\partial z} - \frac{\partial N_k}{\partial z} K \right\} dz$$

$$- N_k \left[K \frac{\partial \psi}{\partial z} + K \right]_{z=o}^{z=z_w} = 0 \qquad \text{for each k} \tag{4-11}$$

The second part of (4-11) is non-zero only at the boundary elements. If a flux boundary condition is used, this term, which is simply the moisture flux at the boundary, is specified. If the fixed pressure boundary condition is used at node k, then no solution is required at that node. At an internal node, this term can be dropped for notational simplicity:

$$\int_{\text{internal}} \left\{ N_k \, C \frac{\partial \psi}{\partial t} + K \frac{\partial N_k}{\partial z} \frac{\partial \psi}{\partial z} - \frac{\partial N_k}{\partial z} K \right\} dz = 0 \tag{4-12}$$

The value of $C(\psi)$ and $K(\psi)$ can also be approximated using the interpolation (or other) functions:

$$C(\psi) = \sum_{j=1}^{n} N_j C_j; \qquad K(\psi) = \sum_{j=1}^{n} N_j K_j \tag{4-13}$$

where subscript j implies the value at node j. Inserting (4-9) and (4-13) into (4-12) we obtain:

$$\sum_{(e)} \int_{(e)} \left\{ N_k \sum_j N_j C_j \frac{\partial \sum_i N_i \psi_i}{\partial t} + \sum_j N_j K_j \left(\frac{\partial N_i}{\partial z} \frac{\partial N_i \psi_i}{\partial z} + 1 \right) \right\} dz = 0 \tag{4-14}$$

where the summation is over all elements.

There are n equations, indexed by k, for n unknowns, indexed by i, in (4-14). The time integration of (4-14) is treated in the same way as already discussed for the FDM. The result is a nonlinear system for algebraic equations,

$$\left(\frac{\underline{A}'^{\,n+\alpha}}{\Delta t} + \alpha \, \underline{B}'^{\,n+\alpha} \right) \underline{h}^{n+1} = \left(\frac{\underline{A}'^{\,n+\alpha}}{\Delta t} - (1-\alpha) \, \underline{B}'^{\,n+\alpha} \right) \underline{h}^{n} + \underline{f}'^{\,n+\alpha} \qquad (4\text{-}15)$$

in which h^{n+1} is the vector of unknown values of matrix potential. This equation and its solution are perfectly analogous to (4-7) for the FDM. The most significant difference is that A', unlike A, is tridiagonal. This means that (4-15) never gives an explicit set of equations for the new pressures, even when α is zero.

4.2.2 FEM Applications to Vertical Unsaturated Flow--

Finite elements have been applied to vertical unsaturated flow problems by many authors, including Neuman [1973], Johnson et al. [1982], Yeh and Ward [1980], Hamilton et al. [1981], and Segol [1976]. Maslia and Johnston [1982] used a two-dimensional saturated-unsaturated finite element model to investigate ground water flow beneath a failed landfill. Trautwein, et al. [1982] investigated leakage from a waste pond using a one-dimensional finite element model of unsaturated vertical flow. The FEM for vertical unsaturated flow has been verified by Segol [1976] and Milly [1982], who showed agreement of FEM results with Philips [1958, 1969] quasi-analytical infiltration solution.

4.3 Discretization of Flow Domain

The first step of modeling is to discretize the flow domain, in this case the vertical coordinate and time. In general, the accuracy of numerical techniques increase with smaller subdomains. A consistent technique converges to the exact solution as subdomain size becomes infinitely small [Pinder and Gray, 1977]. By varying the size of these subdomains to suit a particular simulation, accuracy can be maximized while retaining large subdomains in less critical areas.

4.3.1 Grid Design--

The simplest grid divides the liner and site soil into equally sized subdomains. These elements may be fairly large if there are only small variations of moisture content in the profile, such as occurs under conditions of equilibrium. However, if large gradients of moisture (e.g., a wetting front) occur, the size of the elements should be smaller. In order to economize on the total number of elements, it is important in such cases to use a variably-sized set of elements in order to concentrate nodes in the region of greatest variations, as discussed below.

For the transient infiltration problem, the initial distribution of matric potential varies gradually everywhere, except at the top of the liner (see Figure 2-2). As infiltration proceeds, this sharp front moves into the

soil and is gradually smoothed as it moves down the soil column. By the time the moisture front reaches the bottom of the liner, it is sufficiently dispersed to relax the subdomain size requirement. This variation suggests a grid with small subdomains at the top of the liner and a gradation of subdomain size moving down the column. Figure 4-4 shows two graded grids of this general design. In the first, the gradient involves blocks of segments which become larger in steps. The second example has subdomains which vary in size continuously from the liner top to the water table. In this second grid, the bottom subdomain is about 10 times as large as the top one. The extent of gradation and the ease of incorporating this into the model data depend on the particular program being used. In general, the FEM is particularly well suited for graded grids of the second type.

It is difficult to specify a general criterion for the size of grid spacing. The subdomain size and gradation are usually determined during the initial simulations. Many models are very sensitive to this discretization and care should be taken. A good test of the effect of subdomain size on the solution is to compare the change in simulated matric potential obtained using smaller and smaller grid spacings. When the change between two simulations is unaffected by grid spacing, the larger size can probably be used.

4.3.2 Time Stepping--

The considerations in selecting time step sizes are analogous to those in grid design. One efficient numerical scheme uses very small time steps at the beginning of infiltration, when the matric potential gradients are highest, and gradually increases the time step size as the moisture front advances into the soil liner and disperses. Many computer programs incorporate this feature directly into their integration procedures. Again, the initial time step size and the rate of gradation are usually determined during initial simulations of the problem at hand. Given that initial time steps may be as low as one second, or less, a variable time step size is imperative to maintain cost effectiveness during long-term simulation.

4.4. Soil properties in numerical models

During numerical solution of the governing equation or vertical unsaturated flow, the specific moisture capacity, $C(\psi)$, and unsaturated hydraulic conductivity, $K(\psi)$ must be determined. The values must be evaluated for each value of matric potential at the node points. There are two general methods for incorporating these continuous functions into the numerical model. The first is by specifying a table of points from the data curves. The computer program then interpolates between these tabular values when needed for additional points. The second method is to directly compute soil properties using functional relationships such as those presented above in sections 2.3 and 2.4.

4.4.1 Tabular Interpolation--

The continuous moisture characteristic $\theta(\psi)$, and hydraulic conductivity $K(\psi)$, curves can be represented by a table of values. The specific moisture capacity, $C(\psi) = d\theta/d\psi$, is then determined from the input $\theta(\psi)$ curve. This

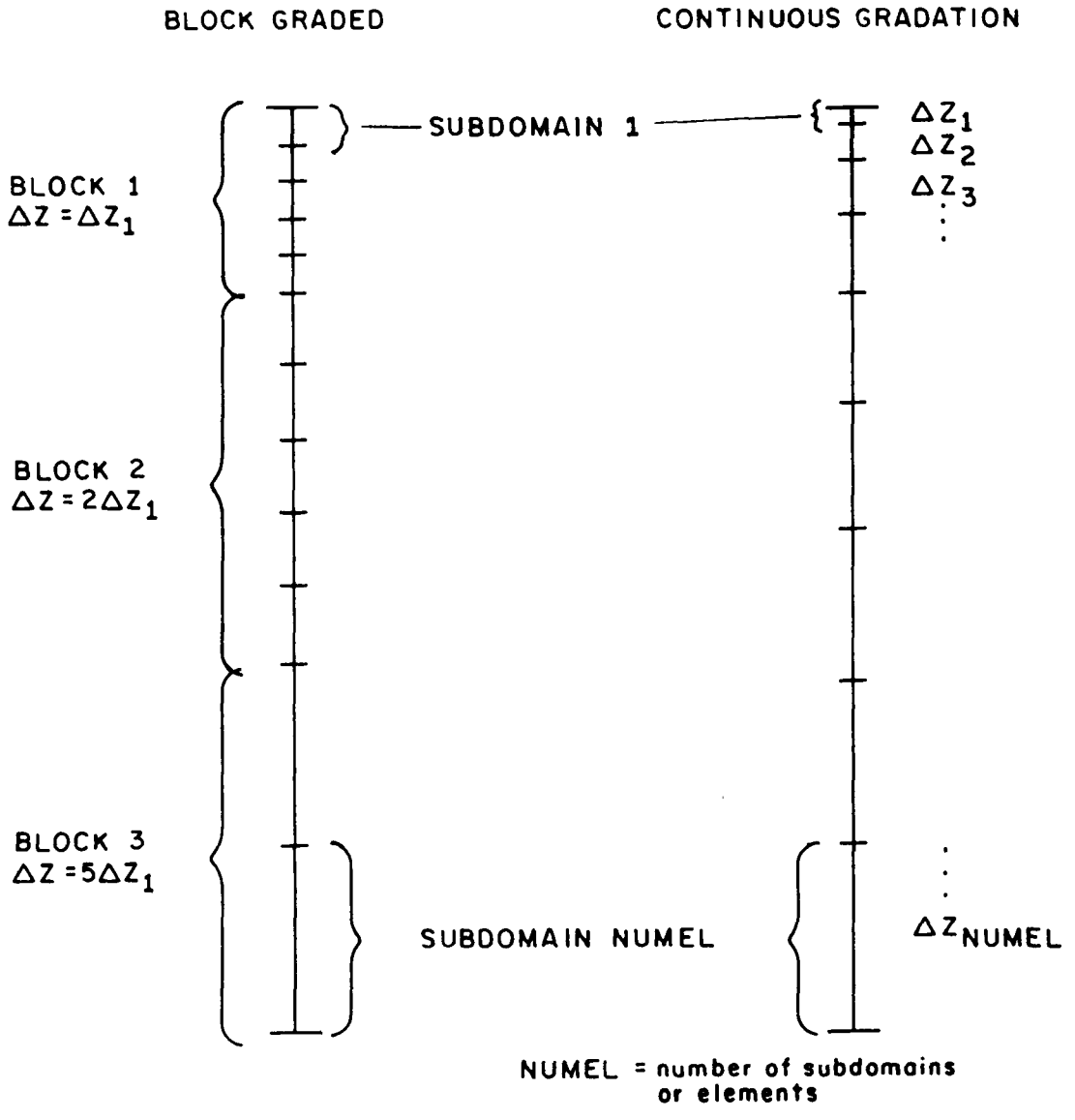

Figure 4-4. Two vertical grids with variable subdomain sizes.

table contains a list of values of matric potential with the corresponding moisture contents and conductivities. When the matric potential falls between two of these tabular points, the moisture content or conductivity is obtained by interpolating between the respective tabular values. The computationally simplest interpolation procedure is linear weighting. Using this procedure, the moisture content at a given matric potential can be written:

$$\theta(\psi) = \theta(\psi_m) + \frac{\psi-\psi_m}{\psi_{m+1}-\psi_m}\left[\theta(\psi_{m+1}) - \theta(\psi_m)\right] \qquad (4\text{-}16)$$

where ψ_m and ψ_{m+1} are two values of matric potential from the input table, with $\psi_m \leq \psi \leq \psi_{m+1}$, and $\theta(\psi_m)$ and $\theta(\psi_{m+1})$ are corresponding values of moisture content. The specific moisture capacity for this curve is:

$$C(\psi) = \frac{\theta(\psi_{m+1}) - \theta(\psi_m)}{\psi_{m+1} - \psi_m} \qquad (4\text{-}17)$$

Note that this parameter, which is the storage term in the governing equation, is constant between the tabular values and is discontinuous when $\psi = \psi_m$. This is shown in Figure 4-5. Some programs actually use tabular values of specific moisture capacity $C(\psi_m)$, $C(\psi_{m+1})$ and linearly interpolate for $C(\psi)$. Unfortunately, this form is not the derivative of (4-16) and mass balance errors may occur. This error will decrease as the spacing between the tabular values decreases.

The unsaturated hydraulic conductivity can also be determined by linear interpolation:

$$K(\psi) = K(\psi_m) + \frac{\psi - \psi_m}{\psi_{m+1} - \psi_m}\left[K(\psi_{m+1}) - K(\psi_m)\right] \qquad (4\text{-}18)$$

where $K(\psi_m)$ and $K(\psi_{m+1})$ are the conductivities corresponding to the input matric potentials ψ_m and ψ_{m+1}.

Log-linear interpolation is suggested by the form of functional relationships discussed in Section 2. The moisture content between two input points can be determined using semi-logarithmic weighting:

$$\theta(\psi) = \theta(\psi_m) + \frac{\log(-\psi) - \log(-\psi_m)}{\log(-\psi_{m+1}) - \log(-\psi_m)}\left[\theta(\psi_{m+1}) - \theta(\psi_m)\right] \qquad (4\text{-}19)$$

The corresponding specific moisture capacity for this representation is:

$$C(\psi) = \frac{\theta(\psi_{m+1}) - \theta(\psi_m)}{\log(-\psi_{m+1}) - \log(-\psi_m)}\left[\psi \ln(10)\right]^{-1} \qquad (4\text{-}20)$$

which is not constant between tabular values, but is still discontinuous as shown in Figure 4-5. Linear (4-16) and semi-logarithmic (4-19) interpolation for moisture characterization are compared in Figure 4-5 and Figure 4-6 for the same input table of values. Linear interpolation produces smoother changes in $C(\psi)$.

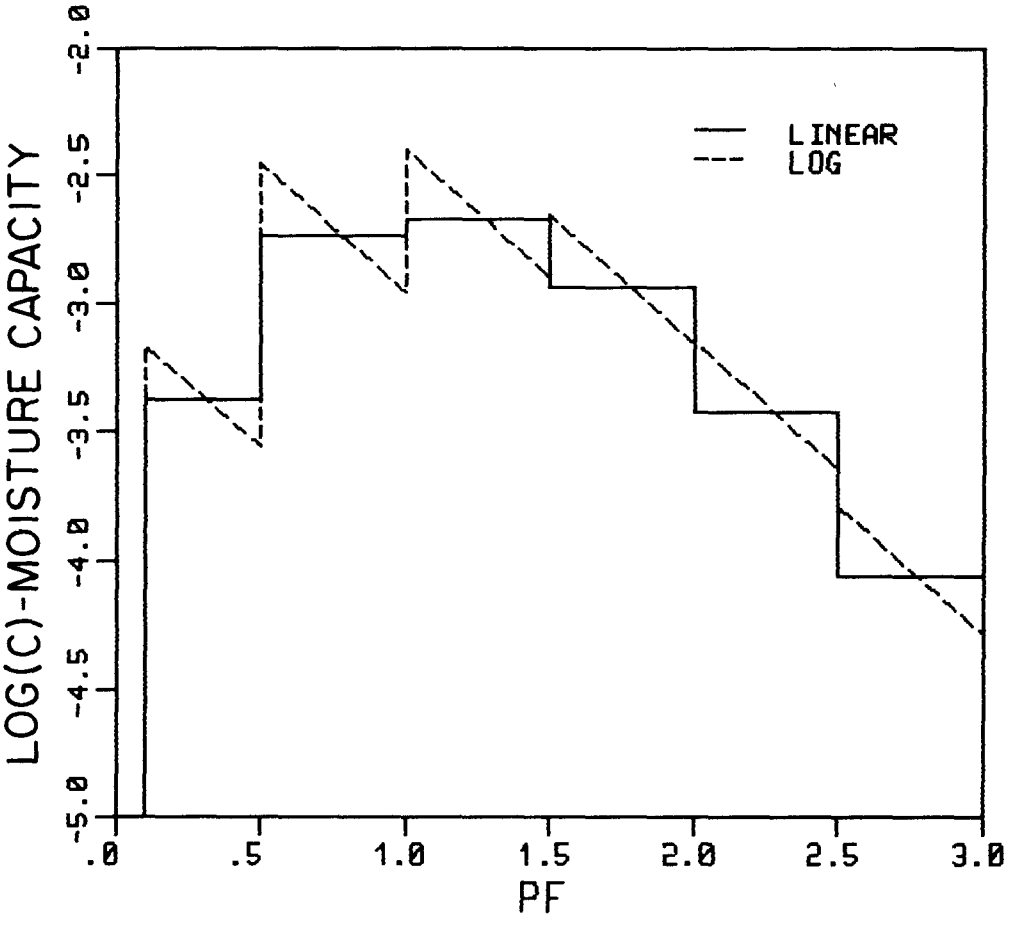

Figure 4-5. Interpolation of specific moisture capacity from table of values 0.5 pF apart, pF = log (-Ψ), Ψ in cm.

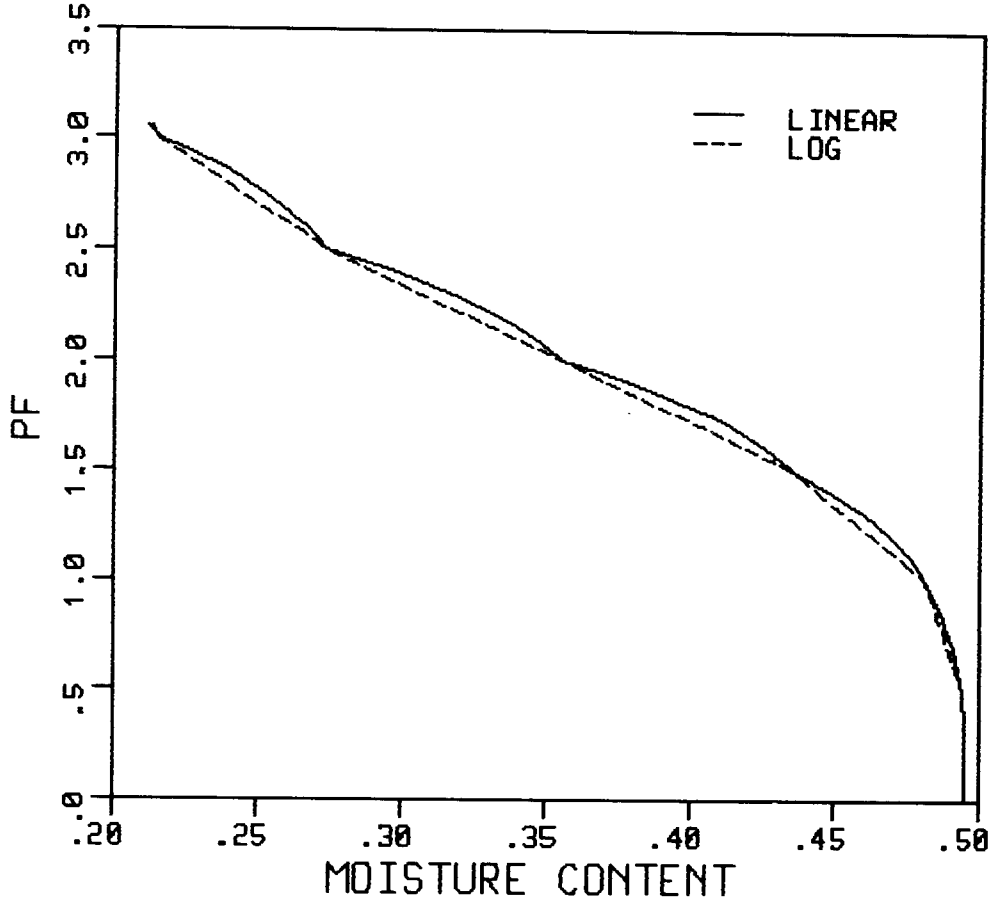

Figure 4-6. Interpolation of moisture content from table of values 0.5 pF apart, pF = (-Ψ), Ψ in cm.

Log-log interpolation is suggested for the unsaturated hydraulic conductivity. This can be written:

$$K(\psi) = K(\psi_m) \left(\frac{\psi}{\psi_m}\right)^{\beta} \tag{4-21}$$

where

$$\beta = \frac{\log[K(\psi_{m+1})/K(\psi_m)]}{\log[\psi_{m+1}/\psi_m]}$$

Linear (4-18) and log-log (4-21) interpolation for unsaturated hydraulic conductivity are compared in Figure 4-7 using the same input table of values. The improved representation of conductivity using log-log interpolation is obtained at a small additional computational cost.

Higher order techniques are available for interpolation. These prove most useful in determining the specific moisture capacity from input values of moisture content. Hamilton [1979] used cubic spline interpolation to produce a moisture content curve, from input tabular values, that was continuous in both first ($d\theta/d\psi = C(\psi)$) and second derivatives ($d^2\theta/d\psi^2 = dC/d\psi$). Thus, the computed specific moisture capacity is smooth and continuous. This procedure fits the input data to a polynomial with 4(NP-1) parameters where NP is the number of tabular values. The cost effectiveness of this method decreases as the number of input data points increases.

4.4.2 Functional Relationships--

Any of the functional relationships presented in sections 2.3 and 2.4 could be directly incorporated into a computer program. Examples of this are Milly and Eagleson [1980] and Yeh and Ward [1980]. Two advantages of this method are that normally few input variables are needed and it is possible to have continuous smooth curves. The latter is a particular advantage in developing the specific moisture capacity curve, $C(\psi) = d\theta/d\psi$. The disadvantages of this method are that it can often require much more computation than an interpolation procedure and that the functional parameters must be determined.

The functional relationship used must closely match the soil property data. Not only must the parameters of the function be determined, but the functional relationship to be used must be selected. For a given function, the parameters are adjusted to minimize some measure of the deviation between the soil properties predicted by the model and the observed properties. For example, a least-squares fit minimizes the sum of the squared deviations:

$$\varepsilon = \sum_{i=1}^{nd} \left[K(\psi)_{pred.} - K(\psi)_{data}\right]^2 \tag{4-22}$$

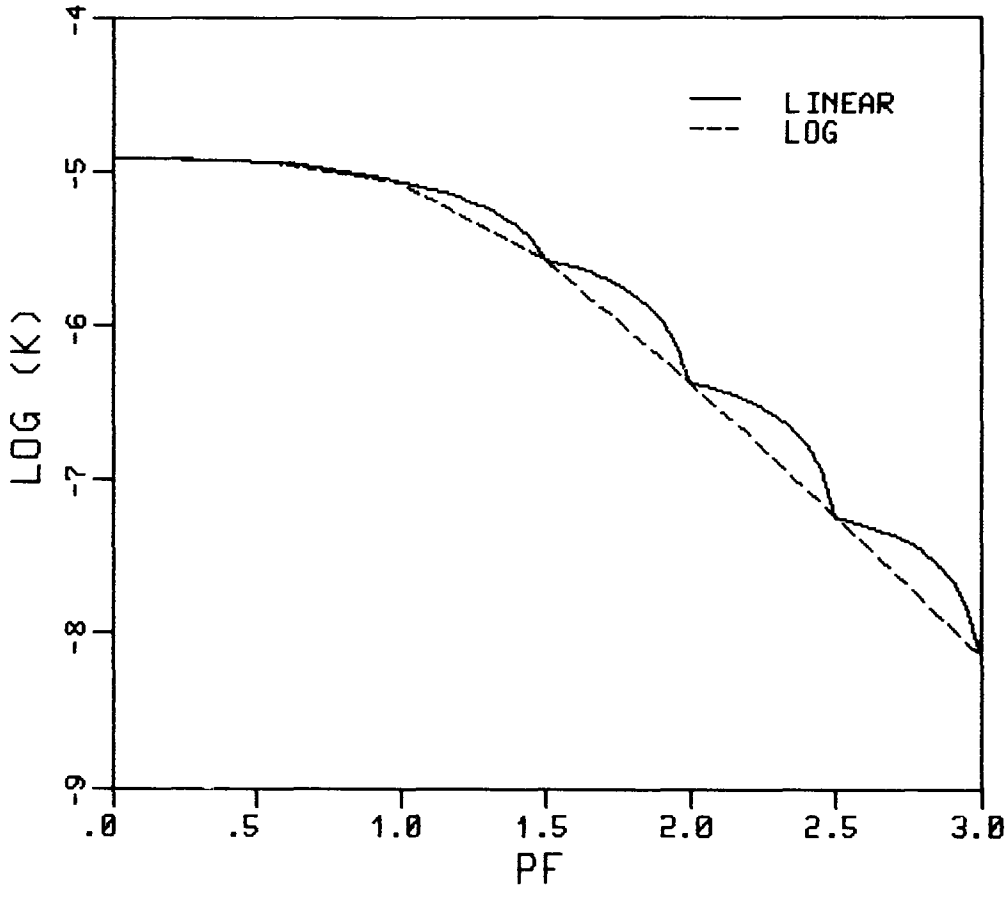

Figure 4-7. Interpolation of unsaturated hydraulic conductivity (K, cm/s) from values spaced 0.5 pF apart, pF = log(-Ψ), Ψ in cm.

in which $K(\psi)_{pred.}$ is the conductivity predicted by the model, $K(\psi)_{data}$ is the measured conductivity, and ε is the sum of the squared errors. This fit should be performed only over the data range to be simulated. For example, if the lowest matric potential expected in the field is ψ = -1000 cm, the fit should be performed for properties corresponding to potentials between -1000 cm and 0 cm, saturation. Finally, the fitted function should be graphically compared to the measured values.

Unsaturated hydraulic conductivity is more difficult to measure than moisture retention. Several functional relationships have been developed which determine unsaturated conductivities from the saturated conductivity and measured moisture retention [see for example, Elzeftawy and Cartwright, 1981, and Mualem, 1978]. Nonetheless, it is extremely valuable to have actual measurements of unsaturated conductivity with which to compare the models.

The use of functional relationships in numerical simulations and their ability to match measured soil properties are discussed by, among others, Mualem [1976], Jackson et al. [1965], and Ragab et al. [1982].

4.5 Example Computer Program

SOILINER, an available computer program which solves the vertical unsaturated flow equation, is an example of the computer implementation of the finite difference method (FDM). This program will be used below in Section 5 to design a hypothetical soil liner. This program was chosen for example simulations primarily because it is designed to solve only the equation considered in this study, vertical unsaturated flow, and because it uses the FDM which is conceptually simpler than finite element methods (FEM). However, the discussion below in Section 5 is not limited to SOILINER, but applies equally to any program which solves the same governing equation (see Appendix B).

The remainder of this section briefly describes the numerical technique and the soil property representations employed by SOILINER, and verification of the computer program by comparison to analytical solutions.

4.5.1 Numerical Technique--

The governing equation for vertical unsaturated flow (see Section 2) can be written:

$$C(\psi)\,\frac{\partial \psi}{\partial t} - \frac{\partial}{\partial z}\left[K(\psi)\,\frac{\partial \psi}{\partial z} + K(\psi)\right] = 0 \qquad (4\text{-}23)$$

in which $C(\psi) = \partial\theta/\partial\psi$ [L^{-1}] is specific moisture capacity, where θ[-] is volumetric moisture content; ψ[L] is matric potential or capillary pressure head; $K(\psi)$ [LT^{-1}] is vertical unsaturated hydraulic conductivity; z [L] is the vertical coordinate, positive upwards; and t [T] is time. For notational purposes, the second term in (4-23) which is flux divergence, is denoted by:

$$V(\psi) = \frac{\partial}{\partial z} K(\psi)\,\frac{\partial \psi}{\partial z} + \frac{\partial K(\psi)}{\partial z} \qquad (4\text{-}24)$$

and by (4-23)

$$V(\psi) = C(\psi) \frac{\partial \psi}{\partial t} \tag{4-25}$$

thus V $[T^{-1}]$ can be thought of as the rate of storage change at any point.

Standard centered finite difference expressions can be used to evaluate V in (4-24). The spatial domain is discretized into a mesh centered grid (see Figure 4-1a) with node points on the boundary between soil elements. Substituting the FDM represetations for the two flux terms (see (4-1) and (4-3)) into (4-24) we have:

$$V_i(\psi) = \left[K_{i+1/2} \frac{\psi_{i-1} - \psi_i}{\Delta z_{i+1/2}} - K_{i-1/2} \frac{\psi_i - \psi_{i-1}}{\Delta z_{i-1/2}} \right] \frac{1}{\Delta z_i} + \frac{K_{i+1/2} - K_{i-1/2}}{\Delta z_i} \tag{4-26}$$

where subscript "i" designates node number and

$$\begin{aligned} \Delta z_{i+1/2} &= z_{i+1} - z_i \\ \Delta z_{i-1/2} &= z_i - z_{i-1} \\ \Delta z_i &= 1/2 \ (z_{i+1} - z_{i-1}) \end{aligned} \tag{4-27}$$

are the lengths of the two elements on each side of node i and the length associated with node i, respectively. The element conductivities are evaluated as geometric averages:

$$\begin{aligned} K_{i+1/2} &= [K(\psi_{i+1}) \times K(\psi_i)]^{1/2} \\ K_{i-1/2} &= [K(\psi_i) \times K(\psi_{i-1})]^{1/2} \end{aligned} \tag{4-28}$$

A weighted temporal difference expression is obtained by substituting (4-25) into (4-4):

$$C^{n+\alpha} \frac{\psi^{n+1} - \psi^n}{\Delta t} = \times V(\psi^{n+1}) + (1-\alpha) \ V(\psi^n) \tag{4-29}$$

in which $0 \leq \alpha \leq 1$ is the weighting parameter; and

$$C^{n+\alpha} = \alpha C^{n+1} + (1-\alpha) \ C^n \tag{4-30}$$

These expressions apply at each node and subscripts have been dropped for convenience.

Equation (4-29) is a FDM expression of the governing equation (4-23) at a node. Since both C^{n+1} and K^{n+1} depend on the solution, ψ^{n+1}, (4-29) is nonlinear in ψ. An iterative procedure is used to solve for ψ^{n+1}. The solution at a new iteration can be expressed as the solution from the last iteration plus a correction computed at the new iteration

$$\psi^{k+1} = \psi^{k} + \Delta\psi^{k+1} \tag{4-31}$$

in which all terms are at node i and time step n+1 and superscript k is iteration level. The left hand side (LHS) of (4-29) becomes:

$$C^{n+\alpha}\left(\frac{\psi^{n+1} - \psi^{n}}{\Delta t}\right) = C^{k,n+\alpha}\left(\frac{\psi^{n+1} - \psi^{n}}{\Delta t}\right) + C^{k,n+\alpha}\left(\frac{\Delta\psi^{k+1}}{\Delta t}\right) \tag{4-32}$$

The second term on the right hand side (RHS) of (4-29) is known from the last time step. The first RHS term is evaluated by substituting (4-31) into (4-26):

$$V_i\ (\psi^{k+1}) = \left[K^{k}_{i+1/2}\left(\frac{\psi^{k}_{i+1} + \Delta\psi^{k+1}_{i+1} - \psi^{k}_{i} - \Delta\psi^{k+1}_{i}}{\Delta z_{i+1/2}}\right) - K_{i-1/2}\left(\frac{\psi^{k}_{i} + \Delta\psi^{k+1}_{i} - \psi^{k}_{i-1} - \Delta\psi^{k+1}_{i-1}}{\Delta z_{i-1/2}}\right)\right]\frac{1}{\Delta z_i} + \frac{K^{k}_{i+1/2} - K^{k}_{i-1/2}}{\Delta z_i} \tag{4-33}$$

or

$$V_i\ (\psi^{k+1}) = \left[K^{k}_{i+1/2}\left(\frac{\Delta\psi^{k+1}_{i+1} - \Delta\psi^{k+1}_{i}}{\Delta z_{i+1/2}}\right) - K^{k}_{i-1/2}\left(\frac{\Delta\psi^{k+1}_{i} - \Delta\psi^{k+1}_{i-1}}{\Delta z_{i-1/2}}\right)\right]\frac{1}{\Delta z_i} + V_i\ (\psi^{k}) \tag{4-34}$$

in which $V(\psi^k)$ is evaluated from the last iteration, and, again, superscript "k" or "k+1" represents iterative values at time step n+1.

The final form of the FDM governing equation is obtained by substituting (4-32) and (4-34) into (4-29) and grouping $\Delta\psi^{k+1}$ terms on the LHS:

$$C^{k,n+\alpha}_i\frac{\Delta\psi^{k+1}_i}{\Delta t} - \left[K^{k}_{i+1/2}\left(\frac{\Delta\psi^{k+1}_{i+1} - \Delta\psi^{k+1}_{i}}{\Delta z_{i+1/2}}\right) - K^{k}_{i-1/2}\left(\frac{\Delta\psi^{k+1}_{i} - \Delta\psi^{k+1}_{i-1}}{\Delta z_{i-1/2}}\right)\right]\frac{1}{\Delta z_i} = -C^{k,n+\alpha}_i\frac{\psi^{k}_i - \psi^{n}_i}{\Delta t} + V_i(\psi^{k}) + (1-\alpha)\ V_i(\psi^{n}) \tag{4-35}$$

All terms on the RHS of (4-35) are known from the last time step, "n", or the last iteration, "k" at the new time step "n+1". Equation (4-35) is solved directly for $\Delta\psi^{k+1}$ using the Thomas algorithm for tridiagonal matrix equations (see Pinder and Gray, 1977).

A flow chart for the computer program SOILINER's solution procedure is shown in Figure 4-8. SOILINER allows variable node spacing and computes a new time step such that the maximum change in pressure head is near some specified value.

4.5.2 Soil Property Representations--

SOILINER uses functional expressions for unsaturated hydraulic conductivity, moisture content, and specific moiture capacity. For each element, the saturated hydraulic conductivity, the porosity, and the soil type code (1,2,3, etc.) is input. The hydraulic conductivity is computed as the relative conductivity of each element's soil type (as a fraction of 1) times the saturated value for that element. Likewise, the functions for moisture content and specific moisture capacity allow the porosity to change for different elements of the same soil type. The listing of SOILINER in Appendix C shows three soil types are used, but the number of soil types is limited only by the number of functional relationships inserted into the soil property subroutine and by the number of grid blocks.

4.5.3 Verification--

In order to verify the numerical technique used by SOILINER, the model's results are compared to analytical solutions for three physically realistic problems. The first two simulations are for steady state unsaturated flow and the third is for infiltration under ponding into an unsaturated clay.

Two grids were used for SOILINER's simulations. Node 1 is at the column top, z = 0, and the last node is at the column bottom, z = 50 cm. The first grid divided this 50 cm column into 50 1 cm elements (51 node points). The second grid divided the soil column as follows: the first 5 cm was divided into 10 elements; the next 25 cm into 25 elements; and the final 20 cm into 10 elements for a total of 45 elements and 46 nodes.

No-flow steady state--

The governing equation for steady state saturated flow is:

$$\frac{\partial}{\partial z} K(\psi) \frac{\partial \psi}{\partial z} + \frac{\partial K(\psi)}{\partial z} = 0$$

or

$$\frac{\partial}{\partial z}\left\{ K(\psi) \left| \frac{\partial \psi}{\partial z} + 1 \right| \right\} = 0 \qquad (4\text{-}36)$$

which states that the flux is constant in space. The pressure boundary conditions to (4-36) determine the direction and rate of flow.

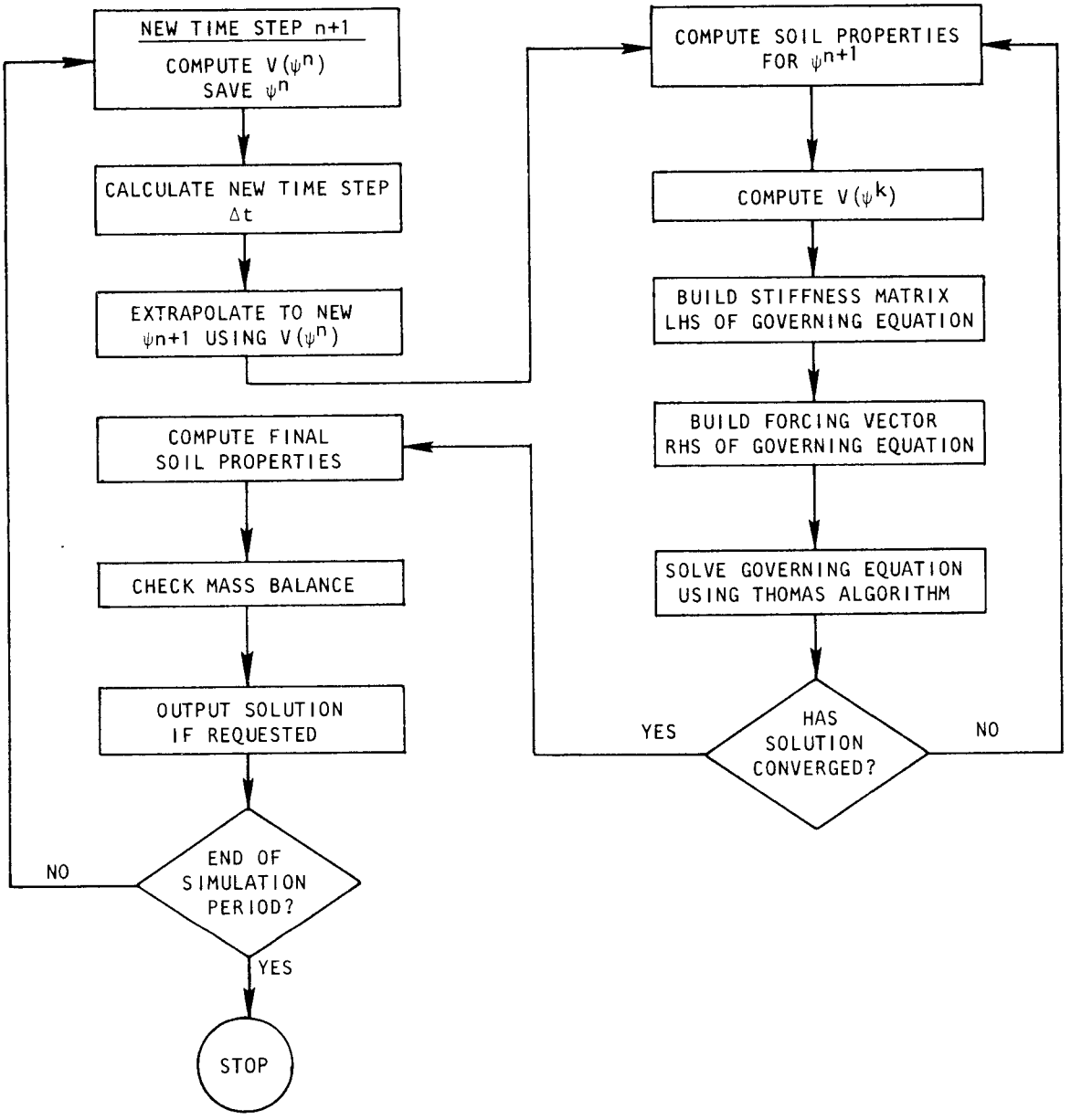

Figure 4-8. SOILINER solution procedure flowchart.

At steady state no-flow, the piezometric gradient is zero:

$$\frac{\partial \phi}{\partial z} = \frac{\partial(\psi+z)}{\partial z} = 0 \qquad (4\text{-}37)$$

Thus, the capillary pressure head gradient is equal to -1:

$$\frac{\partial \psi}{\partial z} = -\frac{\partial z}{\partial z} = -1 \qquad (4\text{-}38)$$

The boundary conditions for this situation are

$$\psi = 0 \qquad z = z_w \qquad (4\text{-}39)$$

at the water table at the bottom of the soil column and

$$\psi = z_w - z_t \qquad z = z_t \qquad (4\text{-}40)$$

at z_t, the soil column top. Between the column bottom and top, capillary pressure head is inversely proportional to elevation:

$$\psi = z_w - z \qquad z_w \leq z \leq z_t \qquad (4\text{-}41)$$

Equation (4-41) is an analytical solution to (4-36) with boundary conditions (4-39) and (4-40).

For the SOILINER simulations, the top node ($z_t = 0$) capillary pressure head is $\psi = -50$ cm and the bottom node ($z_w = -50$) capillary pressure is $\psi = 0$ cm. Simulations with both constant node spacing and variable node spacing produce the exact analytical solution to five significant digits.

Steady state evaporation flow upward--

Gardner [1958] developed analytical solutions for steady state unsaturated flow when the unsaturated hydraulic conductivity follows the following form:

$$K(\psi) = \frac{a}{(-\psi)^n + b} \qquad (4\text{-}42)$$

where a and b are constants, and n is 1, 1/2, 2, 3, or 4. For n = 4, the analytical solution to (4-36) is given implicitly by:

$$z = \frac{1}{r}\left[\frac{1}{4\rho^3\sqrt{2}} \ln\left(\frac{\psi^2 - \rho\psi\sqrt{2} + \rho^2}{\psi 2 + \rho\psi\sqrt{2} + \rho 2}\right) + \frac{1}{2\rho^3\sqrt{2}} \tan^{-1}\left(\frac{\rho\psi\sqrt{2}}{\psi^2 - \rho^2}\right)\right] + W \qquad (4\text{-}43)$$

in which

$$r = q/a$$

$$\rho^4 = \beta/r$$

$$\beta = rb + 1$$

where q is the discharge rate, constant in space and time, and W is a constant of integration. For a water table at an elevation of z_w = -50 cm and flow upward, W = -50 cm.

Using (4-42) for the functional soil hydraulic conductivity, SOILINER was run with boundary conditions of

$$\psi = 0 \text{ at } z_w = -50 \text{ cm}$$

and (4-44)

$$\psi = -200 \text{ at } z = 0$$

The flux computed by SOILINER was then used to compute Gardner's solution (4-43) using the computer program listed in Appendix F.

Figure 4-9 shows the agreement between SOILINER simulations with a regular grid (Test 2A) and a graded grid (Test 2C) and Gardner's analytic solution.

Transient infiltration--

Philip [1958, 1969] developed a quasi-analytical solution to transient infiltration into unsaturated soil and applied this technique to simulate infiltration into the Yolo light clay with a porosity of 0.495 and a saturated hydraulic conductivity of 1.23×10^{-5} cm/s. The functional relationships for the unsaturated hydraulic conductivity and moisture characteristic were taken from Haverkamp et al. [1977] and are shown in Milly [1982]. The initial boundary conditions for this problem are

$$\psi = -600 \text{ cm} \qquad \text{all } z,\ t \leq 0$$

$$\psi = 25 \text{ cm} \qquad z = 0,\ t > 0$$

$$\psi = -600 \text{ cm} \qquad z = -\infty,\ t > 0$$

The soil is initially at a constant moisture content and capillary pressure over its entire thickness. For the SOILINER simulations, the initial time step was 0.1 sec and subsequent time steps were automatically calculated to keep the maximum pressure change between time steps at any node to about 10 cm.

Figure 4-10 shows a comparison of SOILINER using a regular grid with Philip's quasi-analytic solution. The agreement for this highly nonlinear problem is very reasonable. Figure 4-11 shows the similar accuracy of SOILINER with a graded grid. The graded grid has fewer nodes, but because of

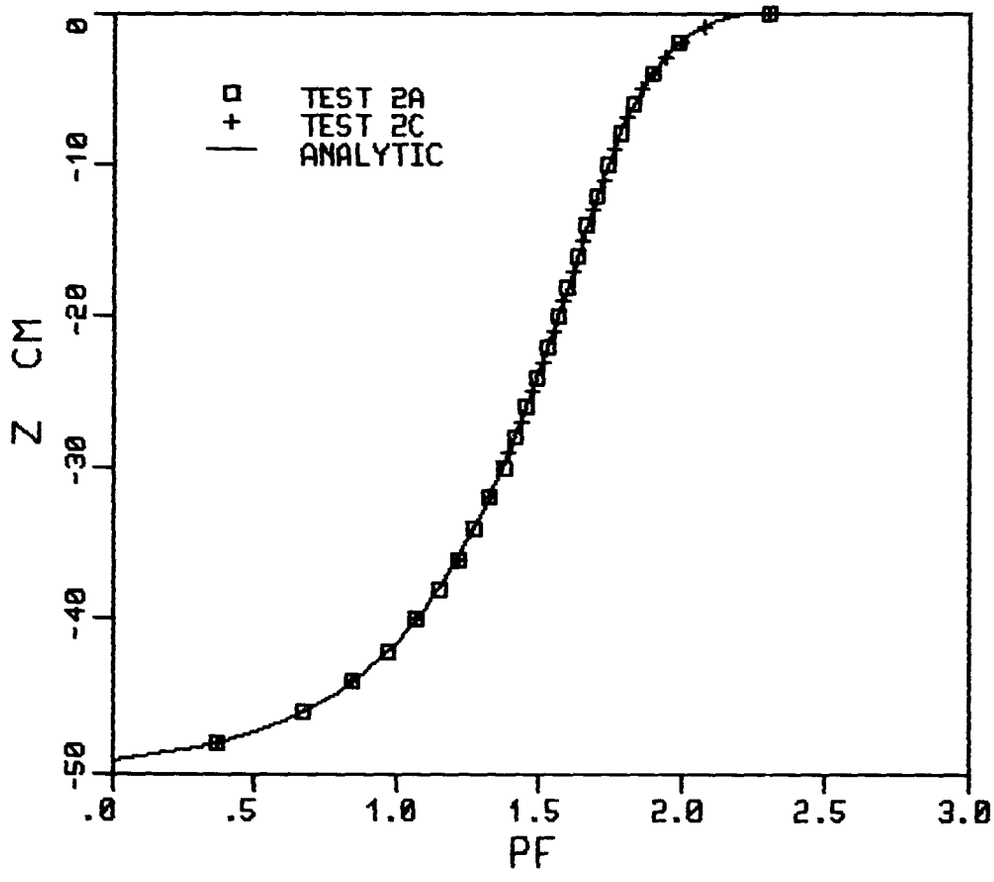

Figure 4-9. Comparison of solutions for steady state vertical flow upward from a water table: solid curve is analytical solution of Gardner (1958); symbols are SOILINER numerical solutions at every other node. Test 2A(□) is a regular spaced grid with 50 nodes, Test 2C(+) is a variable spaced grid with 46 nodes. (pF = log $(-\psi)$, ψ in cm.)

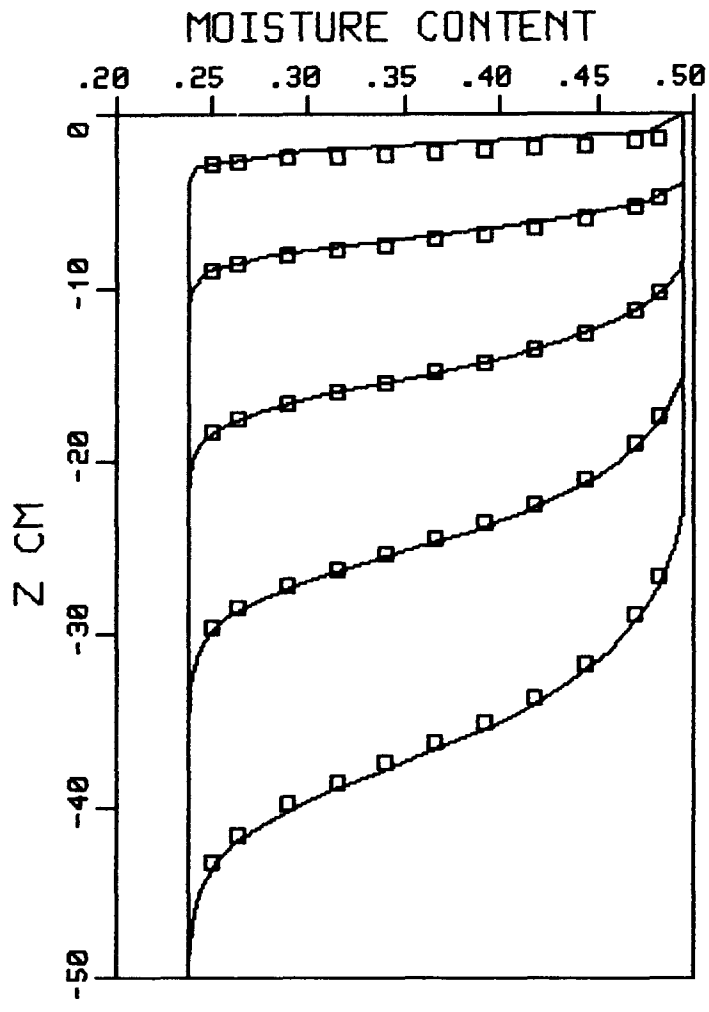

Figure 4-10. Comparison of Philip's quasi-analytic solution (□) and SOILINER regular grid solution (solid line) for infiltration into Yolo light clay under ponding. Curves are at 10^3, 10^4, 4×10^4, 10^5, and 2×10^5 sec.

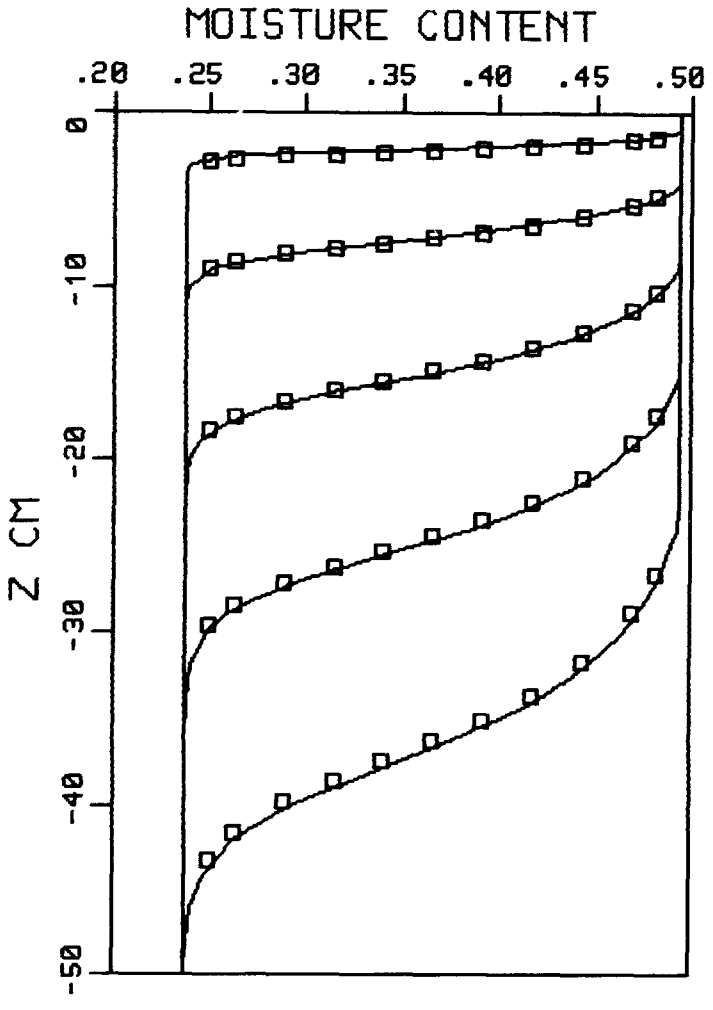

Figure 4-11. Comparison of Philip's quasi-analytic solution (□) and SOILINER graded grid (46 nodes) solution (solid line) for infiltration into Yolo light clay under ponding. Curves are at 10^3, 10^4, 4 x 10^4, 10^5, and 2 x 10^5 sec.

smaller node spacings at the top of the column, the initial moisture profile is closer to Philip's results, demonstrating the value of variable grid spacing.

SOILINER is shown to accurately simulate the flow of moisture in a vertical unsaturated column using both regular and graded grids. The infiltration test is very similar to the application of SOILINER in liner design. Successful completion of these verification runs using other computer models would similarily indicate their utility for soil liner design.

5. SOIL LINER DESIGN

5.1 Introduction

The usefulness of a numerical model for assessing the adequacy of soil liner designs can be demonstrated by analysis of a hypothetical liner performance problem. A temporary surface impoundment for storage of hazardous wastes is to be constructed on a sandy soil with a shallow water table 5 meters below the land surface. Site soil will be excavated to sufficient depth to install a natural soil liner. The top of the liner will correspond to the original land surface. The impoundment depth will be 1 meter. This impoundment is to be used to store hazardous wastes for 5 years, at which time the liquids are to be removed and all contaminated soils excavated. With the design life given, an accurate estimate of the required soil liner thickness and of the extent of release at closure is needed.

5.2 Discretization of the Flow Domain

The first step in the preparation of the computer-assisted numerical analysis and simulation is the discretization of the spatial domain, here the soil column through which vertical flow can occur. For the problem at hand, the soil column from the liner top to the water table can be discretized into 120 elements as follows: the first 5 cm is divided into 10 elements, the next 25 cm is divided into 25 elements, the next 50 cm into 25 elements, the next 120 cm into 30 elements, and the final 300 cm into 30 elements. Within each block of elements, the node spacing is constant. The computer model automatically determines the time step size each time step in such a way that the maximum change in pressure between time steps is about 25 cm. In addition, the maximum allowable time step size is 11.6 days.

5.3 Soil Properties from Data and Models

The site soil is a sand with a saturated hydraulic conductivity of 9.44×10^{-3} cm/s and a porosity of 0.287 (data from Haverkamp et al., 1977). The material for the soil liner is a heavy clay with a saturated hydraulic conductivity of 1×10^{-7} cm/s and a porosity of 0.495. These values are similar to a compacted bentonite clay and are more restrictive to flow than the Yolo light clay. The unsaturated conductivity and moisture characteristic curves for these two soils are shown in Figure 5-1. The site soil moisture is initially in static equilibrium with the water table. Under these conditions the pressure head at any point is the negative of the elevation above the water table. For example, at an elevation of 300 cm above the water table, the pressure is $\psi = -300$ cm. The clay liner is initially at a saturation of about 50 percent which corresponds to a moisture content of about 0.25 and a pressure head of -500 cm.

In actuality, soil property data will be gathered by methods referenced in Section 3 and prepared for the model as described in Sections 4.4 and 4.5.2. For this example, the computer program uses functional relationships for K, ψ, and C. These functions are described by Haverkamp et al. [1977]. The moisture characteristic and relative hydraulic conductivity for the clay

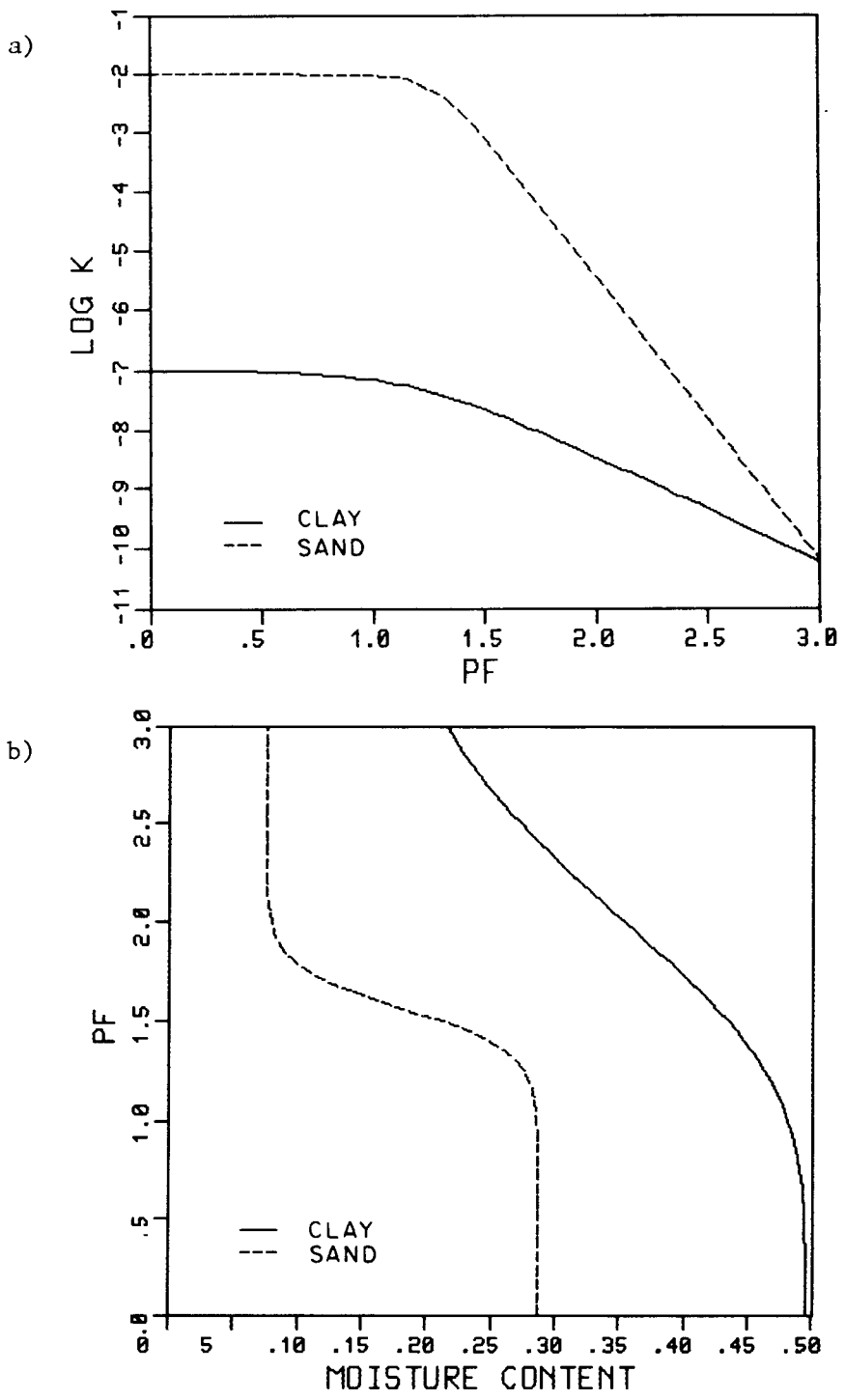

Figure 5-1. Soil properties of hypothetical clay (solid line) and sand (dashed line) for liner design. a) Unsaturated hydraulic conductivity (cm/s) as a function of capillary pressure (pF = $\log(-\psi)$, ψ in cm) b) Moisture content as a fuction of capillary pressure.

soil are those determined for the Yolo light clay. However, the saturated hydraulic conductivity has been reduced to represent a soil suitable for use as a liner.

5.4 Simulation

Table 5-1 shows estimates of liner thickness required for this system. The transit time and Green and Ampt models are simplified techniques which do not require numerical procedures (see Cogley et. al. [1982]).

5.4.1 Infiltration--

Figures 5-2 and 5-3 show the results of simulation of moisture movement into the liner system with a liner thickness of 180 cm. This initial thickness was determined by application of the Green and Ampt infiltration model with a wetting from pressure head of -32 cm. Figure 5-2 shows the capillary pressure at several locations in the liner over time. Moisture moves into the soil at a rate which decreases with time, reaching a depth of 45 cm in about 1/2 year but reaching a depth of 90 cm after about 1 1/2 years. Likewise, at a point 135 cm below the liner top, the soil does not approach saturation until over 3 1/2 years. The pressure at the bottom of the liner increases in early times because the initial pressure is lower than the pressure in the underlying sand, thus moisture actually moves up into the liner. The pressure at the bottom of the liner first responds to infiltration from the impoundment after about 5 years and is approaching its steady state value at 6 years.

Figure 5-3 is a plot of the moisture content profile in the clay liner and in the underlying sand at several times during infiltration. Before the wetting front reaches the bottom of the liner, moisture is flowing up into the clay from the sand due to the initial pressure gradients. The infiltration profile at 5 years just reaches the bottom of the liner. The profile at 6 years is essentially in steady state and will remain unchanged as long as the boundary conditions do not change. Under these conditions, there is a steady flow of water downward from the liner toward the water table.

5.4.2 Breakthrough--

At the end of 5 years, liquid is flowing out of the bottom of the liner at a discharge rate of 3.78×10^{-4} cm/day or 0.54 ft^3/day/acre. For an impoundment 1 acre in area, 0.54 ft^3 of liquid flows out of the liner in 1 day. Whether this rate is large enough to represent breakthrough of the liner is not clear. At this time, the moisture content in the clay at the liner bottom is 0.275. One year later the discharge rate at the liner bottom has increased to 1.36×10^{-2} cm/day or 19.5 ft^3/day/acre. The moisture content in the clay at the liner bottom is 0.31. At 6 years, this system is essentially in steady state and the moisture content at the liner bottom will not increase significantly. As shown in Figure 5-3, the increase in moisture content in the sand which occurs because of this infiltration between year 5 and year 6 is insignificant. The sand is so much more conductive to flow than the clay that only a small change in pressure gradients is sufficient to move all leakage from the liner down to the water table.

TABLE 5-1. COMPARISON OF SIMPLIFIED MODELS FOR 5-YEAR LINER

	Pressure parameter (cm)	Liner thickness (cm)
Transit time	$h_d = 0$	74.6
	$h_d = -10$	77.2
	$h_d = -100$	97.4
	$h_d = -500$	155
Green and Ampt	$\psi_c = -10$	164
	$\psi_c = -32$	175
	$\psi_c = -100$	205

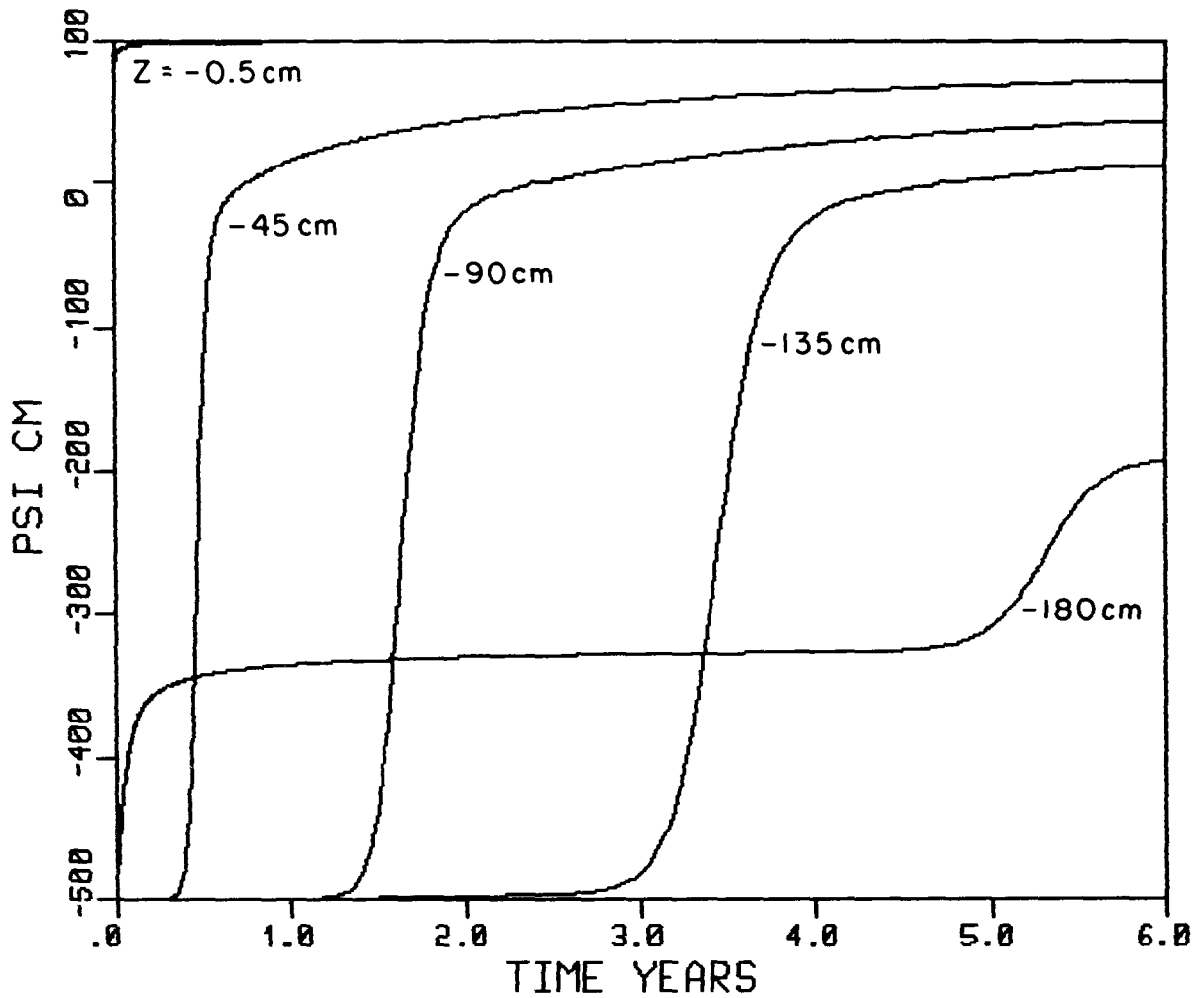

Figure 5-2. Simulated pressure versus time at several points in liner with initial moisture content of about 0.25.

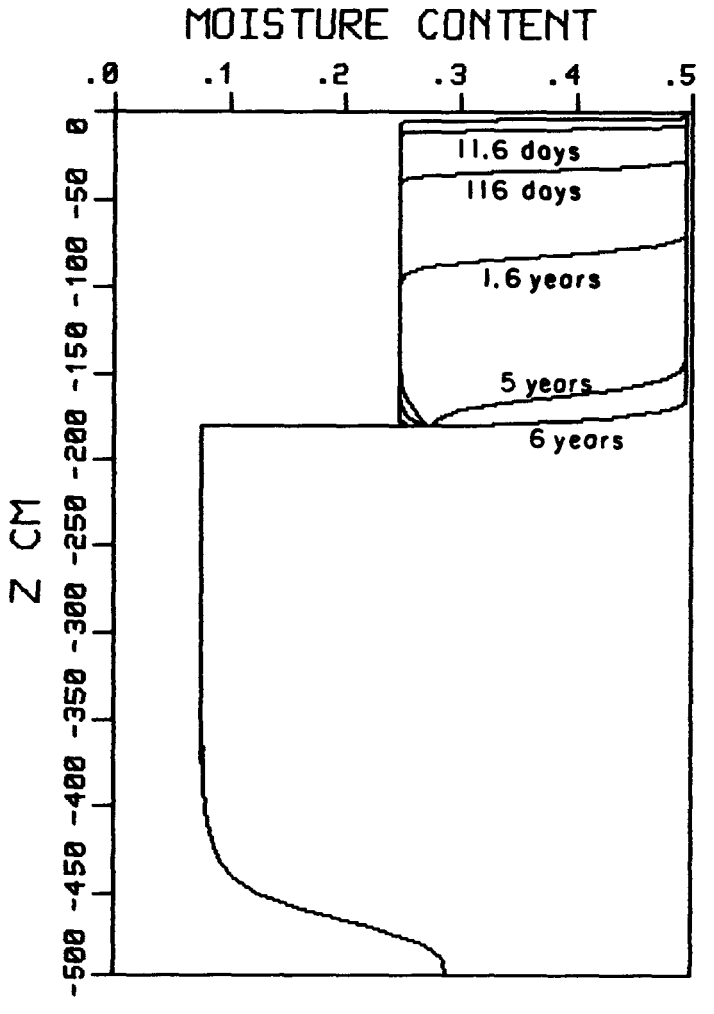

Figure 5-3. Simulated moisture content profile in liner and site soil with initial moisture content of about 0.25.

5.5 Adjusting Liner Specifications

The effect of initial moisture content in the soil liner can be investigated by simply changing the initial specifications on the clay soil liner. Figure 5-4 shows the results of simulation on the same liner system with an initial moisture content in the liner of about 0.30, which corresponds to a pressure head of -200 cm. The fact that pressure gradients will be less in this case might suggest that breakthrough would occur more slowly. However, as shown in Figure 5-4, the pressure at the liner bottom begins changing after 4 years as opposed to 5 years above. This is because the unsaturated hydraulic conductivity is higher at this higher initial capillary pressure, and there is less pore space which must be filled by the advancing moisture front. This liner reaches equilibrium after 5 years. Figure 5-4 also shows that the initial pressure gradient at the liner bottom has been reversed from that above. In this case, the pressure in the liner is higher and the initial flow is down into the site soil, thus reducing pressure at the liner bottom.

Use of the numerical model allows simulation of complex liner systems and variable boundary conditions. For this third simulation, the liner consists of a 60 cm thick layer of the site soil between two 60 cm layers of the liner clay. In addition, this simulation incorporates a change in the impoundment depth from 100 to 200 cm after 2 years. Figure 5-6 shows the liner moisture content profile at three times during infiltration. Before the moisture front reaches the upper sand layer, it has no effect on infiltration and the curve is identical to Figure 5-3. The profile at 1.6 years, after the moisture front has reached the sand layer, is down to about 1.5 meters below the liner top. This compares to less than 1 meter with a homogeneous liner. Leachate entering the sand layer quickly moves vertically down to the interface between the sand and clay. This interface could serve as an effective leachate collection point. The sand layer does not completely saturate until about 3 years after construction, at which time the system is essentially in steady state. Steady state discharge from the bottom clay liner into the underlying site soil is higher for this liner design, with a value of about 40 ft^3/day/acre, due in part to the increased impoundment depth.

5.6 Summary

The initial liner design, a homogeneous layer 180 cm thick, resulted in release of potentially hazardous liquids to the unsaturated zone above the water table after 5 years. If the design goal was a liner that released zero liquid at this time, the model could be run with a thicker liner, and the flow rate again examined at the liner bottom. In addition, numerical models can easily simulate different designs with various soil layers and the effect of variable boundary conditions. Soil properties may also vary from one node to another, thus allowing simulation of a liner with variable soil properties. The numerical model is also valuable in predicting the steady state moisture profile and discharge rates from the liner for any configuration.

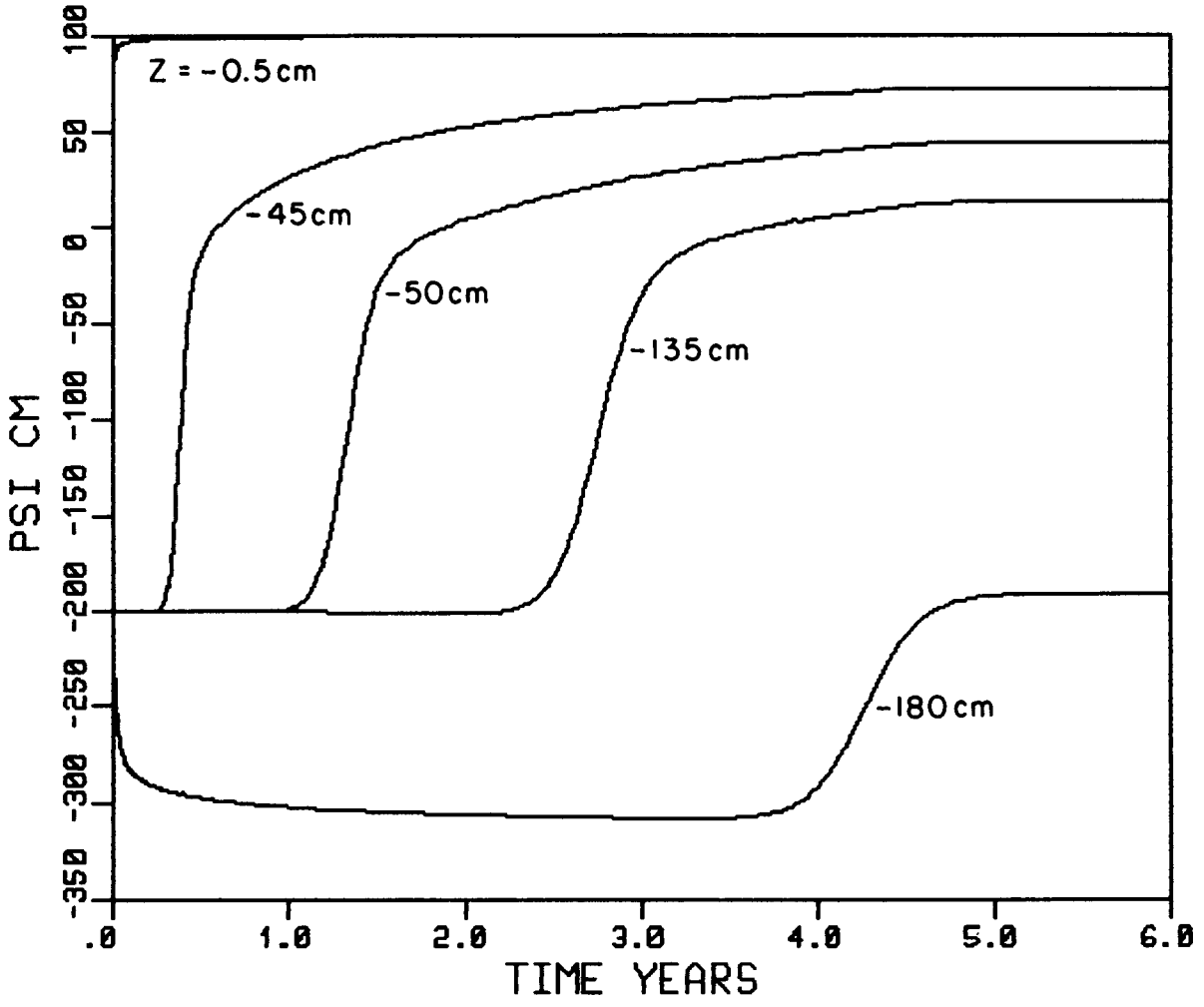

Figure 5-4. Simulated pressure versus time at several points in liner with initial moisture content of about 0.30.

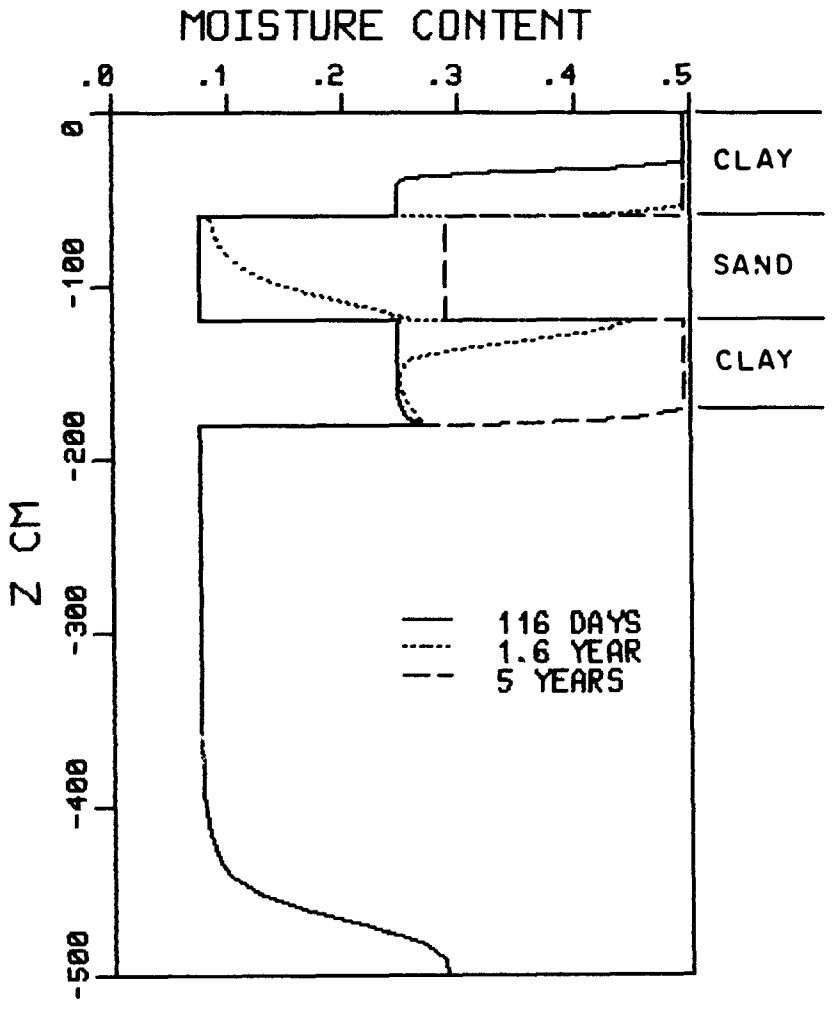

Figure 5-5. Simulated moisture content profiles in a three-layer liner and underlying site soil.

6. SUMMARY

Procedures for modeling flow through clay liners have been presented as accurate and flexible tools to assist in liner design. The conceptual model of vertical unsaturated flow has been reviewd. This non-linear partial differential equation has metric potential,or capillary pressure as its state variable, and requires the soils' unsaturated hydraulic conductivity and specific moisture capacity as functions of pressure. This conceptual model has been verified by comparison to laboratory and field tests. This one-dimensional model is conservative for homogeneous soils.

Laboratory and field tests to determine the required soil properties are available and have been discussed. Finite difference and finite element numerical procedures for solving the unsaturated flow equation have been presented. During numerical solution, soil properties are evaluated using tabular interpolation of functional forms. Discretization of the space and time domain for solution has been reviewed. An example computer program is presented and tested by comparison to analytical solutins of the unsaturated flow equation.

In order to illustrate procedures for assessing the adequacy of a single sort liner, an example computer program (SOILINER) was applied to a hypothetical liner system. This system consisted of a low conductivity clay soil underlain by pervious sand. Given the soil properties of this particular system and a design life of 5 years, a required liner thickness of two meters was estimated. Breakthrough can be defined as the exceedence of a particular flux rate at the liner bottom. Additional simulations demonstrated how numerical models can be used to simulate flow through complexly layered liner systems. Besides evaluating time to breakthrough on the basis of flux rate out of a given liner, the numerical model also allows prediction of the flux steady-state moisture profile and discharge rates from any soil layer of the system under study.

7. REFERENCES

Bear, J., Hydraulics of Groundwater, McGraw-Hill, New York, 1979.

General text with emphasis on mathematical expressions of moisture movement. Includes a description of finite elements applied to unsaturated flow equation.

Bouma, J, D. I. Hillel, F. D. Hole, and C. R. Amerman, Field measurement of unsaturated hydraulic conductivity by infiltration through artificial crusts, Soil Sci. Soc. Amer. Proc., 35, 262-264, 1971.

Brooks, R. H. and A. T. Corey, Hydraulic properties of porous media, Hydrology Paper No. 3, Colorado State University, Fort Collins, March 1964.

Brown, K. W. and D. C. Anderson, Effects of organic solvents on the permeability of clay soils, draft report in fulfillment of EPA Grant # R806825010, Cincinnati, OH, 1982.

Bruch, J. C., Jr., Finite element solutions for unsteady and unsaturated flow in porous media, California Water Resources Center, University of California, Contribution No. 151, 1975.

Brutsaert, W. F., A functional iteration technique for solving the Richards equation applied to two-dimensional infiltration problems, Water Resources Research 6(7), 1583-1596, 1971.

2-D vertical, non-steady, 5 different soil types, user-oriented, finite-difference model. New Mexico Tech., 1971.

Clapp, R. B., and G. M. Hornberger, Empirical equations for some soil hydraulic properties, Water Resources Research, 14, 601-604, August 1978.

Added continuous gradual air entry representation to Brooks & Corey power law model. Use Campbells relative conductivity formula. Applied model to Holtan et al lab data including clays.

Cogley, D. R., D. J. Goode, and C. W. Young, Review of transit time equation for estimating storage impoundment bottom liner thickness, final report in fulfillment of EPA Contract No. 68-02-3168. GCA/Technology Division, Bedford, MA, 1982.

Cooley, R. L., A finite difference method for unsteady flow in variably saturated porous media: application to a single pumping well, Water Resources Research, 7(6), 1607-1625, December 1971.

Finite difference on 2-D unsaturated equations and application to well hydraulics.

Dane, J. H., and P. J. Wierenga, Effect of hysteresis on the prediction of infiltration, redistribution and drainage of water in a layered soil, Journal of Hydrology, 25, 229-242, 1975.

Davidson, J. M., L. R. Stone, D. R. Nielsen, and M. E. Larue, Field measurement and use of soil-water properties, Water Resources Research, 5, 1312-1321, December 1969.

Elzeftawy, A. and K. Cartwright, Evaluating the saturated and unsaturated hydraulic conductivity of soils, in T. F. Zimmie and C. O. Riggs, eds., Permeability and Groundwater Contaminant Transport, American Society for Testing and Materials, 168-181, 1981.

Elzeftawy, A. and B. J. Dempsey, Unsaturated transient and steady state flow of moisture in subgrade soil. Transportation Research Rec. 612, 56-61, 1976.

Freeze, R. A., The mechanism of natural ground-water recharge and discharge: 1. One-dimensional, vertical, unsteady, unsaturated flow above a recharging or discharging ground-water flow system, Water Resources Research, 5(1), 153-171, February 1969.

Freeze, R. A. and J. A. Cherry, Groundwater, Prentice-Hall, Englewood Cliffs, NJ, 1979.

Gardner, W. R., Some steady-state solutions of the unsaturated moisture flow equation with application to evaporation from a water table, Soil Science, 85, 228-232, 1958.

Gardner, W.R ., Field measurement of soil water diffusivity, Soil Sci. Soc. Amer. Proc., 34, 832-833, 1970.

Giesel, W., M. Renger, and O. Strebel, Numerical treatment of the unsaturated water flow equation: comparison of experimental and computed results, Water Resources Research, 9, 174-177, February 1973.

Finite difference technique on pressure and experiment on sand column, one dimensional.

Gillham, R. W., A. Klute, and D. F. Heermann, Hydraulic properties of a porous medium: measurement and empirical representation, Soil Science Society of America Journal, 40, 203-207, March-April 1976.

Presents an empirical extension to King's [1965] hysteretic curve fitting model.

Green, D. W., H. Dabiri, and C. F. Weinaug, Numerical modeling of unsaturated groundwater flow and comparison of the model to a field experiment, Water Resources Research, 6, 862-874, June 1970.

Hamilton, J. M., Measurement of permeability of partially saturated soils, M. S. Thesis. Geotech Eng. Rep. GE 79-4, Univ. of Texas at Austin, 1979.

Hamilton, J. M., D. E. Daniel, and R. E. Olson, Measurement of hydraulic conductivity of partially saturated soils, in T. F. Zimmie and C. O. Riggs, eds., Permeability and Groundwater Contaminant Transport, American Society for Testing and Materials, 182-196, 1981.

Haverkamp, R., M. Vauclin, J. Touma, P. J. Wierenga, and G. Vachaud, A comparison of numerical simulation models for one-dimensional infiltration, Soil Science Society of America Journal, 41, 285-294, 1977.

Haxo, H. E., Jr., Evaluation of selected liners when exposed to hazardous wastes, 102-111, in Residual Management by Land Disposal, Proceedings of the Hazardous Waste Research Symposium, Tuscon, AZ, EPA-600/9-76-015, U.S. EPA, Cincinnati, OH, 1976.

Hillel, D. I., Soil and Water - Physical Principles and Processes, Academic Press, New York, 1971.

General text including description of unsaturated flow and moisture characteristics. Describes finite difference techniques applied to flow equation.

Hillel, D. I., Fundamentals of Soil Physics, Academic Press, N.Y., 1980.

Hillel, D. I., and W. R. Gardner, Measurement of unsaturated conductivity and diffusivity by infiltration through an impeding layer, Soil Sci., 109, 149-153, 1970.

Jackson, R. D., R. J. Reginato, and C. H. M. Van Bavel, Comparison of measured and calculated hydraulic conductivites of unsaturated soils, Water Resources Research, 1(3), 375-380, 1965.

Validated Child, Collis-George, Marshall, and Millington and Quirk models. Sand and loams.

Jeppson, R. W., W. J. Rawls, W. R. Hamon, and D. L. Schreiber, Use of axisymmetric infiltration model and field data to determine hydraulic properties of soils, Water Resources Research, 11, 127-138, February 1975.

Johnson, T. M., S. A. Rojstaczer, and K. Cartwright, Modeling of moisture movement through layered covers designed to limit infiltration at low-level radioactive waste disposal sites, Presented at American Geophysical Union Spring Meeting, Philadelphia, May 31-June 4, 1982.

King, L. G., Description of soil characteristics for partially saturated flow, Soil Science Society of America Proceedings, 29(4), 359-362, 1965.

Klute, A., Laboratory measurements of hydraulic conductivity of unsaturated soil, 253-261, in C. A. Black (ed.), Method of Soil Analysis, Amer. Soc. of Agronomy, Madison, WI, 1965.

Kunze, R. J. and D. R. Nielsen, Finite-difference solutions of the infiltration equation, Soil Science, 134(2), 81-88, August 1982.

Maslia, M. L., and R. H. Johnston, Simulation of ground-water flow in the vicinity of Hyde Park Landfill, Niagara Falls, New York, U.S.G.S. Open-file Report No. OF82-0159, April 1982.

McQueen, I. S. and R. F. Miller, Approximating soil moisture characteristics from limited data: empirical evidence and tentative model, Water Resources Research, 10(3), 521-527, June 1974.

Analysed moisture retention data from literature and developed a log-linear representation pF vs 0. This technique allows approximation of entire curve from sparse data.

Milly, P. C. D., Moisture and heat transport in hysteretic, inhomogeneous porous media: a matric head-based formulation and a numerical model, Water Resources Research, 18(3), 489-498, June 1982.

Milly, P. C. D., and P. S. Eagleson, The coupled transport of water and heat in a vertical soil column under atmospheric excitation, R. M. Parsons Laboratory for Water Resources and Hydrodynamics, M.I.T., Technical Report No. 258, July 1980.

Develops 1-D vertical finite element model and verifies by comparison to infiltration solutions. Good review of current soil moisture research.

Morel-Seytoux, H. J., Two-phase flows in porous media, 119-202, in V.T. Chon, ed., Advances in Hydroscience, Academic Press, N.Y., 1973.

Mualem, Y., A new model for predicting the hydraulic conductivity of unsaturated porous media, Water Resources Research, 12(3), 513-522, June 1976.

Integral expression using soil moisture data, comparison of technique to others (Childs, Collis-George, Averjanor, Gardner, Millington and Quirk) for 45 soils.

Mualem, Y., Hydraulic conductivity of unsaturated porous media: generalized macroscopic approach, 14(2), 325-334, April 1978.

Functional power law between Kr and Se using work integral from soil moisture curve, comparison with 50 soils.

Neuman, S. P., Saturated-unsaturated seepage by finite elements, Journal of the Hydraulics Division, ASCE, 99(HY12), 2233-2250, December 1973.

UNSAT II. Computes hydraulic heads, pressure heads, water content, boundary fluxes and internal sinks and sources in a saturated/unsaturated, nonuniform, anisotropic, porous medium under nonsteady state conditions.

Nielsen, D. R., D. Kirkham, and W. R. van Wijk, Diffusion equation calculations of field soil water infiltration profiles, Soil Science Society of America Proceedings, 25, 165-168, 1961.

Olson, R. E. and D. E. Daniel, Measurement of the hydraulic conductivity of fine-grained soils, in T. F. Zimmie and C. O. Riggs, eds., Permeability and Groundwater Contaminant Transport, American Society for Testing and Materials, 18-64, 1981.

Philip, J. R., The theory of infiltration: 6. Effect of water depth over soil, Soil Science, 85(5), 278-286, 1958.

Philip, J. R., Theory of infiltration, 215-297, in V. T. Chow, ed., Advances in Hydroscience, Vol. 5, Academic Press, New York, 1969.

Pinder, G. F. and W. G. Gray, Finite Element Simulation in Surface and Subsurface Hydrology, Academic Press, New York, 1977.

Advanced text including description of finite element application to unsaturated flow and examples. Good comparison between finite difference and finite element techniques.

Ragab, R., J. Feyen, and D. Hillel, Comparison of experimental and simulated infiltration profiles in sand, Soil Science, 133(1), 61-64, January 1982.

Compared experimental and simulated infiltration when conductivity data obtained from water desorption method and mercury intrusion method. Lab tests. Sand.

Reeder, J. W., D. L. Freyberg, J. B. Franzini, and I. Remson, Infiltration under rapidly varying surface water depths, Water Resources Research, 16(1), 97-114, February 1980.

Roberts, D. W., Soil properties, classification, and hydraulic conductivity testing, draft report in fulfillment of EPA Contract No. 68-03-3058, Cincinnati, OH, 1982.

Rogowski, A. S., Watershed physics: model of the soil moisture characteristic, Water Resources Research, 7(6), 1575-1582, December 1971.

Rose, C. W., and A. Krishnan, A method of determining hydraulic conductivity characteristics for non-swelling soils in situ and of calculating evaporation from bare soil, Soil Sci., 103, 369-373, 1967.

Segol, G., A three-dimensional galerkin-finite element model for the analysis of contaminant transport in saturated-unsaturated porous media, Finite Elements in Water Resources, Proceedings of 1st International Conference, Pentech Press, 1976.

Siegel, J. and D. B. Stephens, Numerical simulation of seepage beneath lined ponds, 219-232, in Symposium on Uranium Mill Tailings Management, Proceedings, Colorado State University, Fort Collins, Co., 1980.

Swartzendruber, D., The flow of water in unsaturated flows, 215-292, in R. J. M. DeWiest, ed., Flow Through Porous Media, Academic Press, New York, 1969.

Trautwein, S. J., D. E. Daniel, and M. W. Cooper. A case history study of water flow through unsaturated soils, Presented at American Geophysical Union Spring Meeting, Philadelphia, May 31-June 4, 1982.

Watson, K. K., An instantaneous profile method for determining the hydraulic conductivity of unsaturated porous materials, Water Resources Res., 2, 709-715, 1966.

Weeks, L. V., and S. J. Richards, Soil water properties computed from transient flow data, Soil Sci. Soc. Amer. Proc., 31, 721-725, 1967.

Yeh, G. T. and D. S. Ward, FEMWATER: a finite-element model of water flow through saturated-unsaturated porous media, Oak Ridge National Laboratories, Report No. ORNL-5567, October 1980.

User's manual and modifications to 2-D vertical flow model of Reeves and Duguid (1975). Based on pressure head.

Youngs, E. G., Moisture profiles during vertical infiltration, Soil Sci., 84(4), 283-290, 1957.

APPENDIX A

REVIEW OF THE TRANSIT TIME EQUATION FOR ESTIMATING STORAGE IMPOUNDMENT BOTTOM LINER THICKNESS

This report was prepared for the
Office of Solid Waste
under contract no. 68-02-3168

DISCLAIMER

This report was prepared by David R. Cogley, Daniel J. Goode, and Charles W. Young of GCA Corporation, Technology Division, Bedford, Massachusetts under contract no. 68-02-3168. This is a draft report that is being released by EPA for public comment on the accuracy and usefulness of the information in it. The report has received extensive technical review but the Agency's peer and administrative review process has not yet been completed. Therefore it does not necessarily reflect the views or policies of the Agency. Mention of trade names or commercial products does not constitute endorsement or recommendation for use.

CONTENTS

FIGURES

SECTION 1

INTRODUCTION

The Environmental Protection Agency is incorporating an alternative design concept into proposed regulations for hazardous waste disposal (Part 264, Subpart K) to allow construction of liquid storage impoundments with a single natural soil bottom liner of sufficient thickness to prevent liquid breakthrough during the operating life of the impoundment. At closure, liquid waste is to be removed along with the depth of bottom liner contaminated as a result of liquid waste seepage. The goal of incorporating this concept into the regulations is to provide flexibility to the prospective owner/operator in selecting a means of storing hazardous wastes prior to ultimate disposal. The Agency is considering the use of a transit time equation to provide a simple method of estimating necessary bottom liner thickness as a function of the design impoundment life.

This report evaluates the correctness of the transit time equation being considered by EPA for estimating liner thickness and is intended for insertion into the Administrative Record of Rulemaking. The review identifies the derivation of the equation, key assumptions and other criteria, applicability, reliability, inherent limitations, and possible modifications or improvements. Other models and experimental and engineering methods that can be used to estimate liner thickness are presented and compared. The complex and highly variable adsorption, molecular diffusion, and reactive properties of individual components and their effects on liner thickness have not been included in this review. Rather, the review concentrates on flow of a single fluid through the liner. Conclusions and recommendations are presented to illustrate regulatory needs.

The transit time equation under consideration is derived from Darcy's equation for one dimensional, steady state, saturated flow. Other basic assumptions include the use of total (versus effective) porosity, and constant hydraulic conductivity independent of moisture content. Thus, the intent is to estimate liner thickness using documented or measured values for hydraulic conductivity and soil porosity.

SECTION 2

ESTIMATION OF LINER THICKNESS

The derivation, applicability, and limitations of the transit time equation are highlighted in this section. Modifications to the expression are discussed including procedures to incorporate effective porosity and negative pore pressure at the liner bottom. A review of modeling efforts adopted by Pope-Reid Associates based on the Green-Ampt equation for movement of the wetting front through clays is then presented. An alternative mathematical model which attempts to address unsteady state conditions (using a linearized approximate solution) is presented. The merits and limitations of each of these alternatives are explained in this section. Based on this review and knowledge of the mechanics of liner wetting and saturation, we present in Section 3 a proposed approach for measuring liner breakthrough times in the laboratory and field and estimating liner breakthrough times by scaling up observed behavior.

DERIVATION, ASSUMPTIONS, AND CRITERIA FOR THE TRANSIT TIME EQUATION

The transit time equation under consideration by EPA was suggested by CMA in the development of guidance for the Part 267 permitting standards (A. Day correspondence, June 1982). The equation takes the form:

$$d = 0.5 \left[\frac{tK}{n} \left\{ \left(\frac{tK}{n} \right)^2 + 4 \left(\frac{tKh}{n} \right) \right\}^{1/2} \right] \qquad (1)$$

where:

d = necessary thickness of soil (feet)

n = total porosity

K = hydraulic conductivity (ft/yr) (which is a function of the soil medium and fluid flowing through it)

h = maximum fluid head on the liner (feet)

t = facility life from startup through closure (years)

and is derived based on the illustration and reasoning presented below:

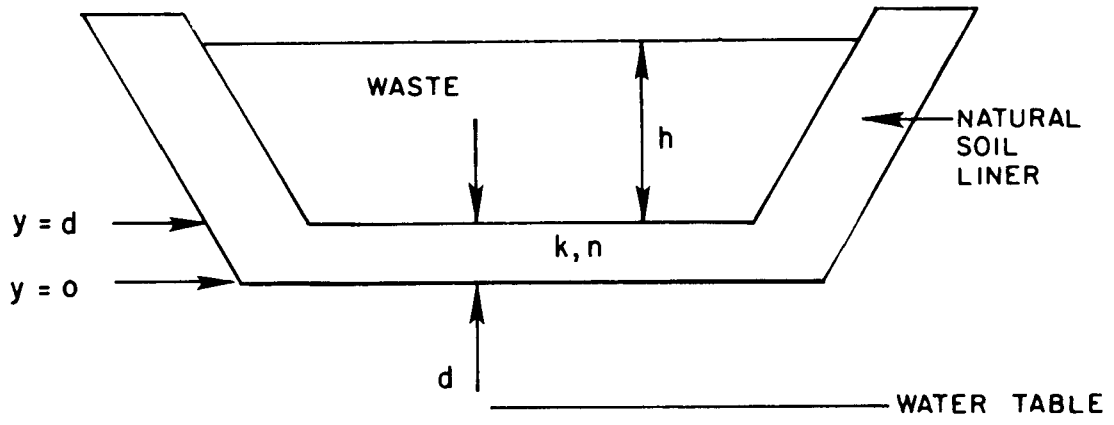

The transit time equation (1) is derived from Darcy's Law, which states:

$$v = \frac{K}{n} i \tag{2}$$

where:

v is the velocity and
i is the hydraulic gradient

If t is the desired containment time, then the liner thickness, d, is given by

$$d = v \cdot t = \frac{Kit}{n} \tag{3}$$

The hydraulic gradient, i, is given by

$$i = \frac{h + d}{d}, \text{ yielding} \tag{4}$$

$$d = \frac{K}{n}\left(\frac{h + d}{d}\right)t \tag{5}$$

Rearrangement to set the expression equal to zero gives:

$$d^2 - \frac{Kdt}{n} - \frac{Kht}{n} = 0 \tag{6}$$

which can be solved for d using the positive solution of the binomial equation, or

$$d = 0.5\left[\frac{tK}{n}\left\{\left(\frac{tK}{n}\right)^2 + 4\left(\frac{tKh}{n}\right)\right\}^{1/2}\right] \tag{7}$$

Key assumptions and criteria implicit in using the transit time equation are:

- saturated flow consistent with Darcy's Law
- one dimensional vertical liquid flow
- steady state conditions
- capillary tension (suction) = 0
- pore fluid pressure at bottom of liner is equal to atmospheric pressure
- mass transport by advection only (i.e., no dispersion or diffusion)

LIMITATIONS OF THE TRANSIT TIME EQUATION

The scenario under consideration requires provision of a single soil liner thick enough to contain all leachate within the basin and liner throughout the life of the storage impoundment. Therefore, an equation is required that can estimate the time to breakthrough of leachate at the liner bottom.

To accurately and reliably estimate the time to breakthrough for a given liner thickness, an equation is required that accounts for variable liner moisture content during wetting and associated variability in leachate conductivity and suction forces induced by capillary tension at any moisture content below complete saturation. Moore (SW-869, Sept. 1980) points out that:

"(1) during the early stages of wetting of a compacted clay liner, capillary attracton forces will predominate over gravitational forces; and

(2) as the clay liner becomes wetter the capillary forces decrease in importance; and, when the liner is saturated, these forces become negligible in comparison to gravitational forces."

The transit time equation under consideration is applicable (although limited) in describing leachate movement after wet up but is not appropriate to describe the first stage of liner wetting under capillary forces because:

- steady state conditions are assumed
- capillary tension is ignored
- conductivity is assumed constant independent of liner moisture content

The use of the saturated conductivity value, which is greater than unsaturated conductivity, results in higher values of liner thickness, and

partially offsets the neglect of capillary forces. As shown at the end of this section, this offset is not sufficient to render accurate predictions of required thickness (see Figure 5).

Although more applicable to the phase of leachate movement after initial wet up, additional limitations of the transit time equation must be recognized:

- total, rather than effective porosity is used
- liner homogeneity is assumed, thus ignoring localized failures such as liner cracking
- potential changes in liner conductivity or permeability as a function of long term waste liquid/liner interactions are not accounted for

The net effect of these limitations is certainly nonconservative, in that the resulting liner will be of insufficient thickness to contain leachate (avoid breakthrough) during the operating life of the storage impoundment.

POSSIBLE IMPROVEMENTS OR MODIFICATIONS TO THE TRANSIT TIME EQUATION

Within the general framework of a steady-state advective transport analysis, modifications to the proposed equation and its application could increase its usefulness. These modifications are not an attempt to change the basic assumptions which are:

- steady state Darcy flow
- fully saturated flow
- advective transport only
- homogeneous liner

The proposed liner thickness equation is modified to include the effects of:

- effective porosity instead of total porosity
- negative fluid pressure at liner bottom

The steady state saturated vertical flow equation in the liner can be written (see Bear 1979):

$$\frac{\partial}{\partial z} \rightarrow K \frac{\partial \phi}{\partial z} K = 0 \qquad (8)$$

where K [L/T] is the vertical saturated hydraulic conductivity, $\phi = \frac{p}{\gamma} + z$ [L] is the piezometric head, p [F/L^2] is the fluid pore pressure, γ[F/L^3] is

the fluid's specific weight, and z [L] is the vertical Cartesian coordinate, positive upward. Hydraulic conductivity is a function of both the porous medium matrix and the pore fluid. Assuming K is constant over z, equation (8), and Darcy's law give:

$$K \frac{\partial \phi}{\partial z} = \text{constant} = q \tag{9}$$

where q [L/T] is specific discharge, or volume flux per unit area of the porous media. The fluid velocity is obtained by dividing the specific discharge by the ratio of active fluid flow area to total area. This ratio is equivalent to the effective porosity, n_e, which is less than total porosity, n, because of closed pores, dead-end pores and entrapped air pores which do not contribute to the flow area. Effective porosity is always less than or equal to total porosity. Thus, fluid velocity V [L/T], is

$$V = \frac{q}{n_e} \quad \frac{K}{n_e} \quad \frac{\partial \phi}{\partial z} \tag{10}$$

The fluid pressure boundary conditions (see Figure 1) on the liner can be used to evaluate (10). The piezometric head at the top of the liner is equal to the elevation of the impounded water free surface h_s[L]. At the liner bottom, the boundary condition is more ambiguous. If the fluid pressure is assumed to be in static equilibrium with the atmosphere ($p_b = 0$), then the piezometric head is equal to the elevation of the liner bottom:

$$P_b = \frac{p_b}{\gamma} + z_b = z_b \tag{11}$$

where subscript b, $(\ )_b$, implies liner bottom value.

An alternative boundary condition can be formulated based on capillary forces. Capillary rise is the phenomenon of a fully saturated zone above the p=0 horizon, where the pore pressure is less than zero (see Bear 1979). Likewise, at the liner bottom, the liner may be fully saturated and have negative pressures due to drainage to the underlying soil or vapor transport from the interface. In terms of pressure head (p/γ) this force is called, for example, critical capillary head, h_{cc} (Bear 1979) or displacement pressure head, h_d, (see McWhorter and Nelson 1979). Thus, the piezometric head at the bottom boundary is:

$$\phi_b = h_d + z_b \tag{12}$$

where h_d [L] is less than zero representing a suction. Evaluating $\frac{\partial \phi}{\partial z}$ from the boundary conditions (12) we have:

$$\frac{\partial \phi}{\partial z} = \frac{\phi_t - \phi_b}{z_t - z_b} = \frac{h_s - h_d - z_b}{z_t - z_b} \tag{13}$$

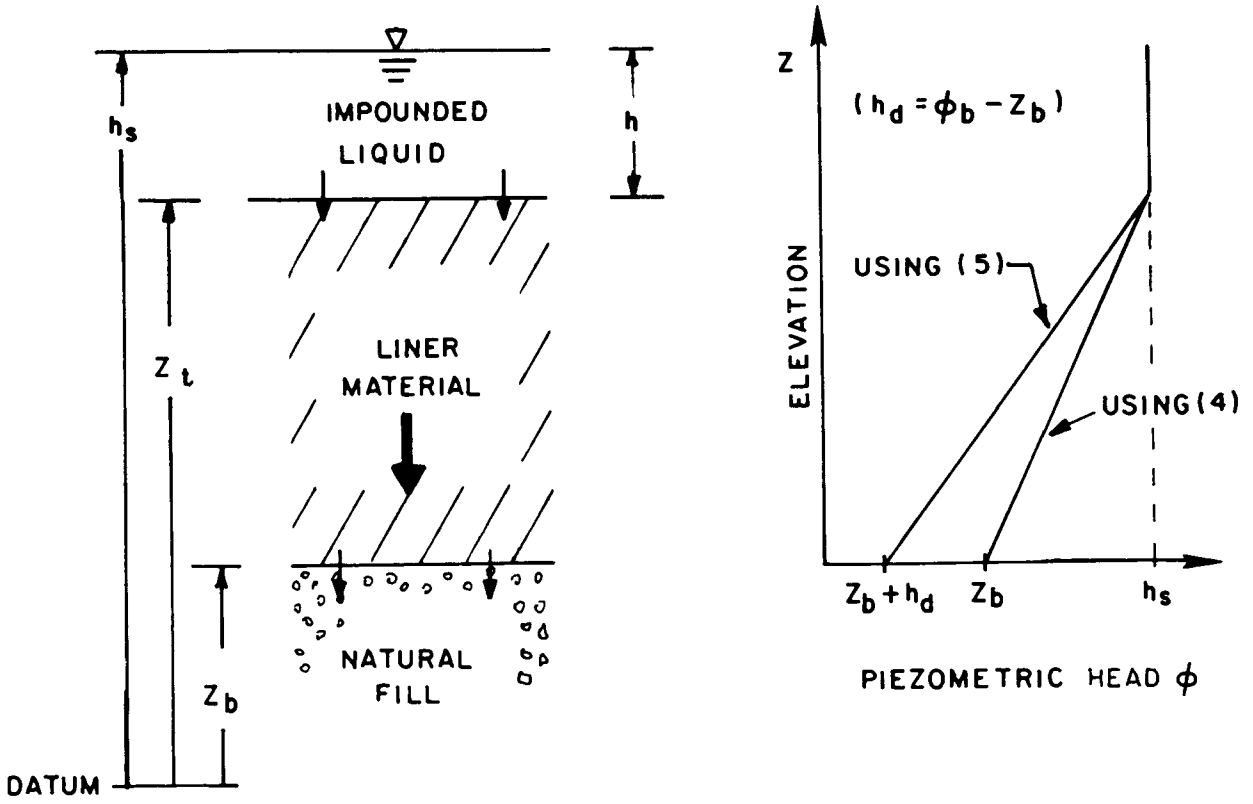

Figure 1. Definition sketch for proposed EPA Equation.

where z_t [L] is the elevation of the top of the liner. For no capillary forces (p = 0), $h_d = 0$.

Substituting (13) into (10), the fluid velocity is:

$$V = \frac{K}{n_e} \left(\frac{h_s - h_d - z_b}{z_t - z_b} \right) \tag{14}$$

Taking our datum at the bottom of the liner $z_b = 0$:

$$V = \frac{K}{n_e} \frac{h+d- h_d}{d} \tag{15}$$

where $d = z_t - z_b$ [L] is the liner thickness and $h = h_s - z_t$ is the ponded fluid depth. Assuming a design life t, the design thickness (to just contain fluid) is:

$$d = V.t = t \frac{K}{n_e} \left(\frac{h+d-h_d}{d} \right) \tag{16}$$

Rearranging and solving the binominal equation for d gives:

$$d = 1/2 \left[\frac{Kt}{n_e} + \left\{ \left(\frac{Kt}{n_e} \right)^2 + 4 \left(\frac{Kt(h-h_d)}{n_e} \right) \right\}^{1/2} \right] \tag{17}$$

This expression is identical to the unmodified equation (7) if the fluid pressure at the liner bottom is zero ($h_d = 0$) and effective porosity (n_e) is replaced by total porosity, n.

These two modifications,

- effective porosity instead of total porosity
- negative fluid pressure at liner bottom

both increase the design thickness, d, for a given design life.

GREEN-AMPT WETTING FRONT MODEL

Green and Ampt (1911) derived a simple model of infiltration which has been proposed as a design model for liner reliability (Pope Reid Associates Correspondense, 1982). As shown in Figure 2, the soil moisture profile is conceptualized as a square wave moving down the soil column. Above the wetting front, the soil is fully saturated, while below the wetting front the moisture content is equal to its initial value, θ_i. Assuming the pressure head at the front is a suction, ψ_c, [L] due to the partial initial saturation, Darcy flux q [L^3/T] in the saturated zone is: (see McWhorter and Nelson 1979).

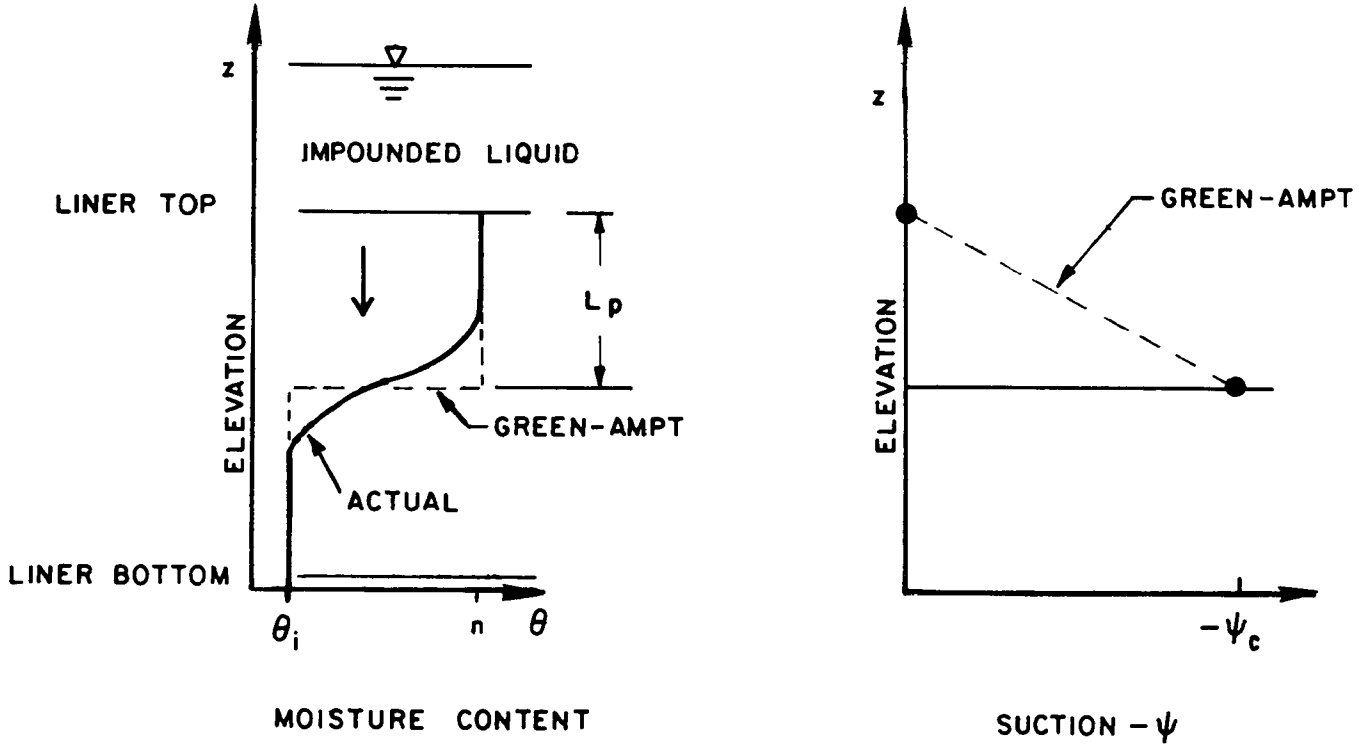

Figure 2. Green-Ampt Infiltration Model.

$$q = K \frac{(h+L_p-\psi_c)}{L_p} \tag{18}$$

where L_p [L] is the depth of penetration of the wetting front from the liner top. Conservation of volume of the pore fluid requires:

$$q = (n-\theta_i) \frac{dL_p}{dt} \tag{19}$$

Combining (18) and (19) and integrating:

$$t = \frac{n-\theta_i}{K} \left[L_p - (h-\psi_c) \ln \left(\frac{h+L_p-\psi_c}{h-\psi_c} \right) \right] \tag{20}$$

The design liner thickness is equal to $d = L_p$, when t equals the design life.

The Green-Ampt model approximates the dynamics of the liner infiltration event. Its major shortcomings are divergence at large times and the difficulty in estimating ψ_c. Estimates of ψ_c which are too low (more negative) yield thicker liners. (See PRA 1982.)

TRANSIENT LINEARIZED APPROXIMATE SOLUTION

Linearization of the highly nonlinear transient unsaturated flow equation can yield analytical solutions which can, in turn, be used to evaluate liner reliability. Although inherently an approximation, this technique captures much of the dynamics of the infiltration event. Moore (SW-869, 1980) has previously recommended this technique for impoundment liner evaluation.

Since the top boundary condition is ponded liquid (positive pressure), this model is developed in terms of pressure head (suction). The governing equation for vertical unsaturated flow can be written: (see Bear 1979, page 214).

$$\frac{\partial \psi}{\partial t} \frac{d\theta}{d\psi} - \frac{\partial}{\partial z} K \frac{\partial \psi}{\partial z} + \frac{dK}{d\psi} \frac{\partial \psi}{\partial z} = 0 \tag{21}$$

where [L] is the fluid pressure head, $\theta(\psi)$ [-] is moisture content, and $K(\psi)$ [L/T] is effective hydraulic conductivity. Note that z is positive downwards from the liner top ($z = 0$). Equation (21) is highly nonlinear due to the dependence of θ and K on ψ. These nonlinearities can be removed, and a solution obtained, by rearranging:

$$\frac{\partial \psi}{\partial t} - \frac{d\psi}{d\theta} \frac{\partial}{\partial t} K \frac{\partial \psi}{\partial z} + \frac{d\psi}{d\theta} \frac{dK}{d\psi} \frac{\partial \psi}{dz} = 0 \tag{22}$$

and substituting $D^* = \frac{d\psi}{d\theta} K$ and $K^* = \frac{d\psi}{d\theta} \frac{dK}{d\psi} = \frac{dK}{d\theta}$ resulting in:

$$\frac{\partial \psi}{\partial t} - D^* \frac{\partial^2 \psi}{\partial z^2} + K^* \frac{\partial \psi}{\partial z} = 0 \qquad (23)$$

Applying boundary conditions $\psi = h$ at the top ($z = 0$), where h is the depth of ponded liquid, and initial condition $\psi = \psi_i$ where ψ_i is the initial fluid pore pressure head, the solution is: (Bear 1979, page 268)

$$\psi = \psi_i + \frac{h-\psi_i}{2}\left[\operatorname{erfc}\left(\frac{z-K^*t}{2\sqrt{D^*t}}\right) + \exp\left(\frac{K^*z}{D^*}\right) \operatorname{erfc}\left(\frac{x+K^*t}{2\sqrt{D^*t}}\right)\right] \qquad (24)$$

where erfc is the complimentary error function (c.f. Crank 1975).

Equation (24) is presented graphically in Figure 3 with d = z. Unlike the proposed transit time equation or the Green-Ampt model, the transient linearized solution results in a continuous profile of soil moisture which is physically more accurate (see "Actual" moisture content curve in Figure 2). Thus there is no sudden increase in moisture content or reduction in suction pressure at the liner bottom. Rather, moisture content gradually increases from the initial value to saturation as the wetting front advances. This is consistent with the experimental observation that moisture flows out the bottom of the column before it is completely saturated (see McIntyre, et al., 1979). Since there is no explicit breakthrough, physically or mathematically, we must define this concept in terms of relative changes in moisture content or pressure. A common choice is 50 percent (see Figure 2) but obviously significant leachate has already reached the liner bottom at this time. A standard value of $(\psi-\psi_i)/(h-\psi_i)$, such as 0.1, could be chosen to represent break-through. Liner thickness is then found from Figure 3 iteratively by assuming a thickness, d, computing D*/K*d, and finding K*t/d on the bottom axis. Time t is then computed, and a new d assumed depending on whether t is less than or greater than the design life.

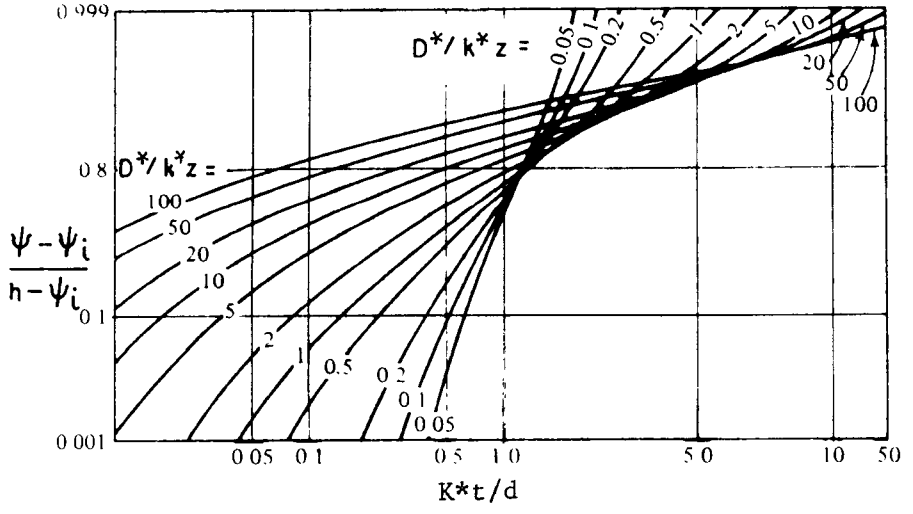

Figure 3. Graphical solution to linearized infiltration (after Ogata and Banks 1961).

The major fault with this method is determining D* and K* since the terms which define them, especially D*, vary over several orders of magnitude during saturation. Moore (1982) has outlined a method for determining K** and D** for the moisture content form of the linearized governing equation. (Note K** and D** are not numerically equivalent to K* and D* due to different governing equations.) Saturated conductivity is used for K**, and D** is determined by curve fitting results of laboratory column tests. It has not been verified that results of short-time small-scale lab tests can be adequately scaled to represent field behavior, and the fitted D** is a function of time and length (Daniel, 1982). This method does approximate the dynamic characteristics of the infiltration event, specifically, capillary forces, and decreased wetting front velocity with time.

MODEL COMPARISONS

The liner thickness design equations discussed above can be compared to a numerical finite element solution of the nonlinear unsaturated flow equation (Milly, 1982) and a quasi-analytical solution (Philip, 1958). Finite element solution of the nonlinear unsaturated flow equation is described in Section 3. It is considered that these two solutions are the most accurate, and serve as the "correct" result.

The liner material simulated is Yolo light clay. This material is not a particularly effective liner, but has been well studied and is presented for comparison. The soil properties are: $n = 0.495$, $\theta_i = 0.237$, and $K = 1.23 \times 10^{-5}$ cm/s. The liquid depth in the impoundment is $h = 25$ cm. The relative hydraulic conductivity ($K'(\ )/K$) and moisture retention functions are plotted in Figure 4. Breakthrough is defined by the ratio of suction pressure reduction at the liner bottom to the difference between initial pressure and the top boundary pressure. Results of the numerical and quasi-analytical solutions are plotted for 10 percent and 50 percent reduction in suction at the bottom of the liner (Figure 5) to illustrate the conservative effect of choosing values lower than 50 percent.

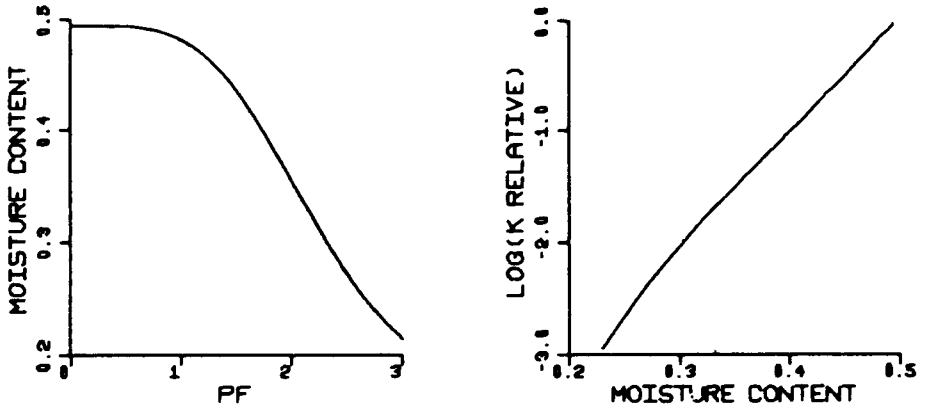

Figure 4. Hydraulic properties of Yolo light clay (pF = log (-), in cm).

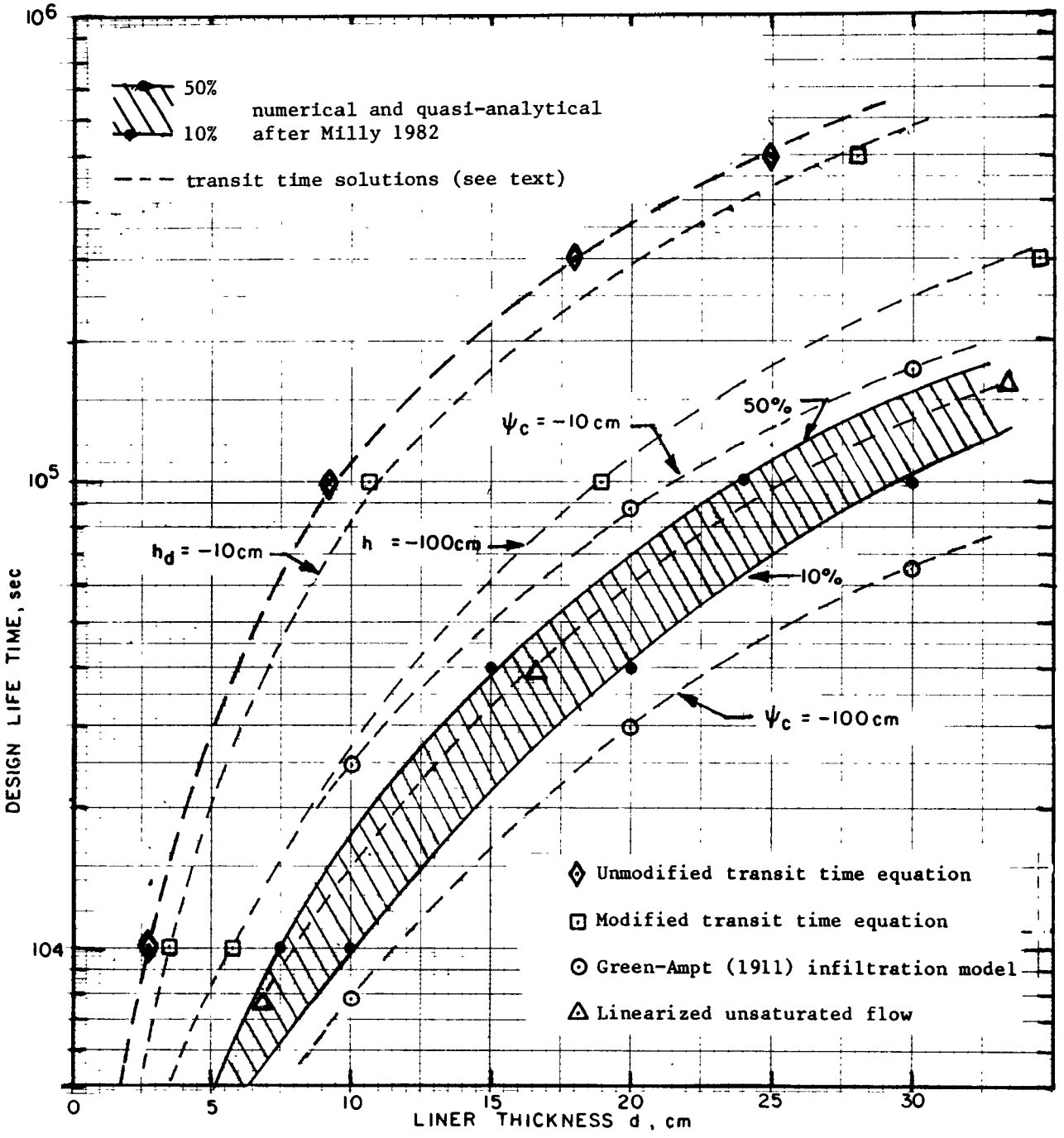

Figure 5. Comparison of Liner Thickness Equations

The unmodified EPA transit time equation (1) is used to calculate liner thickness. Design depth is plotted ($\diamond$) versus design life on a semi-log scale. The modified transit time equation (17) is applied to the liner ($\square$). The additional parameters needed for the modified form are taken as: $n_e = n = 0.495$, for the top line $h_d = -10$cm, and for the bottom line $h_d = -100$ cm.

Results of the Green-Ampt model (O) are plotted for two values of suction head, the top line is $\psi c = -10$ cm and the bottom line is $\psi c = -100$ cm.

The coefficients for the linearized unsaturated flow model are determined by fitting to the numerical results, $D^* = 10^{-2}$ and $K^* = 3 \times 10^5$. This model's results are plotted for one set of parameters (Δ).

As shown in Figure 5, solutions differ over a wide range. The EPA transit time equation underestimates liner thickness for given design life. The modified solution is also sensitive to h_d, a parameter which is an artifact of the approximations involved, and cannot be determined from field data. This error would be even more pronounced for a heavy clay, with lower conductivity. The Green-Ampt and linearized equation models are both very sensitive to parameters which, again, are artifacts of their respective approximations and cannot be accurately estimated from soil property data.

SECTION 3

UNSTEADY FLOW IN CLAY SOILS

Neither steady state models nor linearized unsteady flow models are capable of accurately predicting wetting phenomena for compacted clays. A brief recounting of soil suction for a variety of soils is presented here prior to a description of models which can properly account for unsteady flow phenomena.

SUCTION PROPERTIES OF SOILS

The relationship of soil suction and moisture content is illustrated for several soils. An apparatus for measuring soil suction is used to illustrate the concept of soil suction. This is followed by an explanation of units commonly used to express soil suction. Properties of a silty sand are used to illustrate soil suction values for a simple case. Properties of heavy clay are used to illustrate the effects of wetting, drying, and mixing on soil suction. Next, the behavior of a clay-sand interface is noted. Finally, requirements of a numerical model and its applicability to data from laboratory and field tests are discussed. It is concluded that flow of moisture out of the clay occurs not when the moisture content at the bottom of a liner begins to increase but rather when the clay is almost saturated. Regulations should address this saturation phenomena and not the arrival of the leading edge of the wetting front.

There are many techniques for measuring soil suction. One method is illustrated in Figure 6. A sample of soil is placed on a porous plate which is in contact with a water filled reservoir. The water is under a controllable vacuum (suction). At zero vacuum, the water meniscus moves toward the soil. As vacuum is applied, movement of the meniscus slows. When the vacuum equals the soil suction, the meniscus become stationary. This standard technique is described in Part 19 of ASTM Standards (D2325, D3152).

Several scales or units of suction are in common usage. Soil suction may be expressed in centimeters of water. A pF scale has been defined such that pF equals the logarithm to the base 10 of the soil suction in centimeters (of water). Soil suction values are also frequently expressed in atmospheres. The following values of soil suction are equivalent: 1 atmosphere, 14.7 pounds per square inch, 1,033 centimeters of water, pF 3.0

The relationship of soil suction to moisture content for a silty sand is illustrated in Figure 7. The drying curve is shown with open circles and the

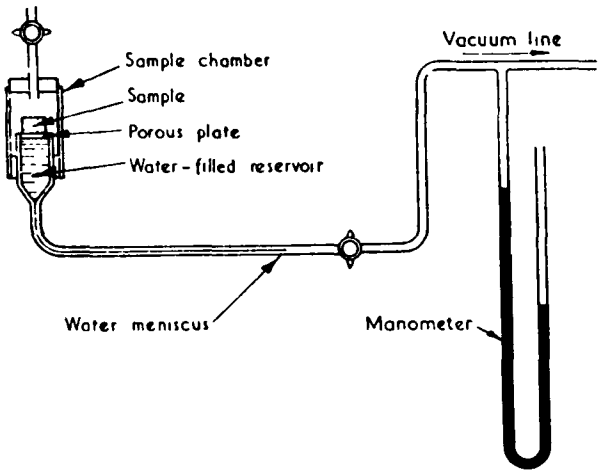

Figure 6. Method of measuring soil suction (Croney and Coleman).

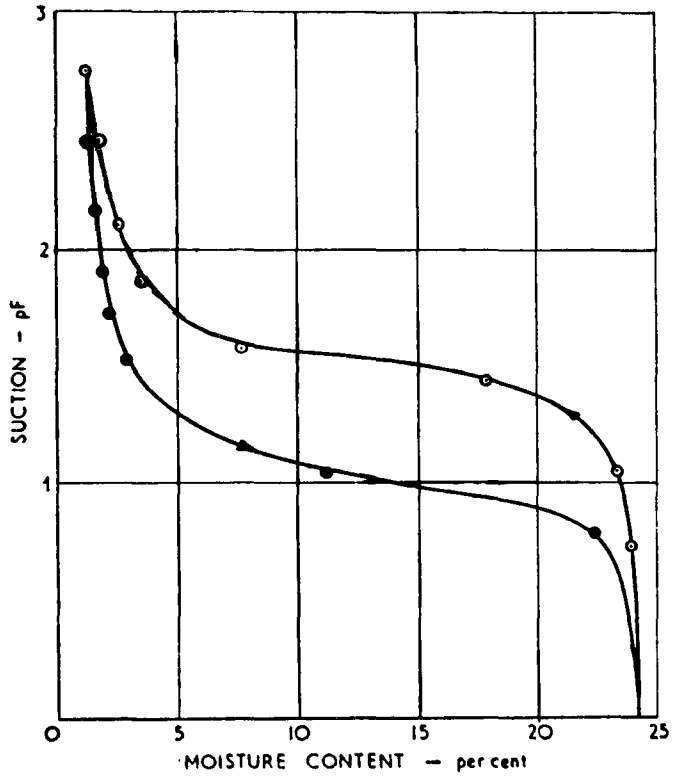

Figure 7. Relationships between suction and moisture content for a silty sand (Croney and Coleman).

wetting curve with filled circles. The observed hysteresis is typical of all soils. The important point is that for a variation of 1 pF unit in soil suction anywhere from 2 percent to 20 percent changes in moisture content (100 times weight of water divided by weight of dry soil) are observed. The greatest changes in moisture content occur for pF values in the vicinity of pF 1, i.e., 10 cm of water suction. For this particular sample of silty sand, very little water will enter the sand from adjacent soils if their suction values exceed pF 3.

Suction values of a heavy clay soil (plastic limit 27 percent, liquid limit 77 percent) subjected to a variety of experimental conditions were investigated by Croney and Coleman and their data are presented in Figure 8. Their explanation is excerpted below.

> "[Figure 8] shows the suction/moisture content relationships for a heavy clay soil (London clay). Curve A represents the "undisturbed" material drying from a suction close to zero. Inset is shown the shrinkage curve for the soil drying from the field-moisture condition... If the drying process is continued to oven-dryness and the suction is then decreased, the wetting condition of the soil over the range pF 1 - pF 7 is represented by the curve B [Figure 8]. On wetting to pF 1 the moisture content of the soil is appreciably lower than its value prior to oven-drying, showing that some irreversible structural change has occurred as a result of oven drying. On drying for a second time to pF 7 the suction relationship follows curve C, which forms a closed loop with curve B. Any subsequent wetting and drying cycles over the range pF 1 - pF 7 give suction curves corresponding to this loop, which appears therefore to be unique for the soil. When the structure of the clay is partially destroyed by thoroughly slurrying the soil at a high moisture content, and the slurried clay is subjected to an increasing suction, pF 0 - pF 7, curve D is obtained... If the slurried soil is dried to a suction less than pF 4.8 and the suction is then reduced progressively and subsequently again increased, closed hysteresis loops of the type E and F are obtained...
>
> "During the last few years several workers have attempted to ascribe pF values to the Atterberg limits... The heavy clay soil referred to [Figure 8] was thoroughly slurried with water to a moisture content well above the liquid limit. The number of blows required to close the groove, the suction of the soil immediately after the test, and the moisture content were all determined... Before each test the soil was thoroughly mixed in accordance with the standard procedure. The suction/moisture content points for various numbers of blows are shown [Figure 8]. The suction of the plastic limit was also determined... The liquid and plastic limit points were found to lie on the continuous dotted line, G. It was subsequently found that if the soil was disturbed without change of moisture content irrespective of its initial suction, it assumed a suction given by curve G at that moisture content... The broad conclusion is that if the suction/moisture content relationship of the soil is represented by a point above the line G, disturbance causes a

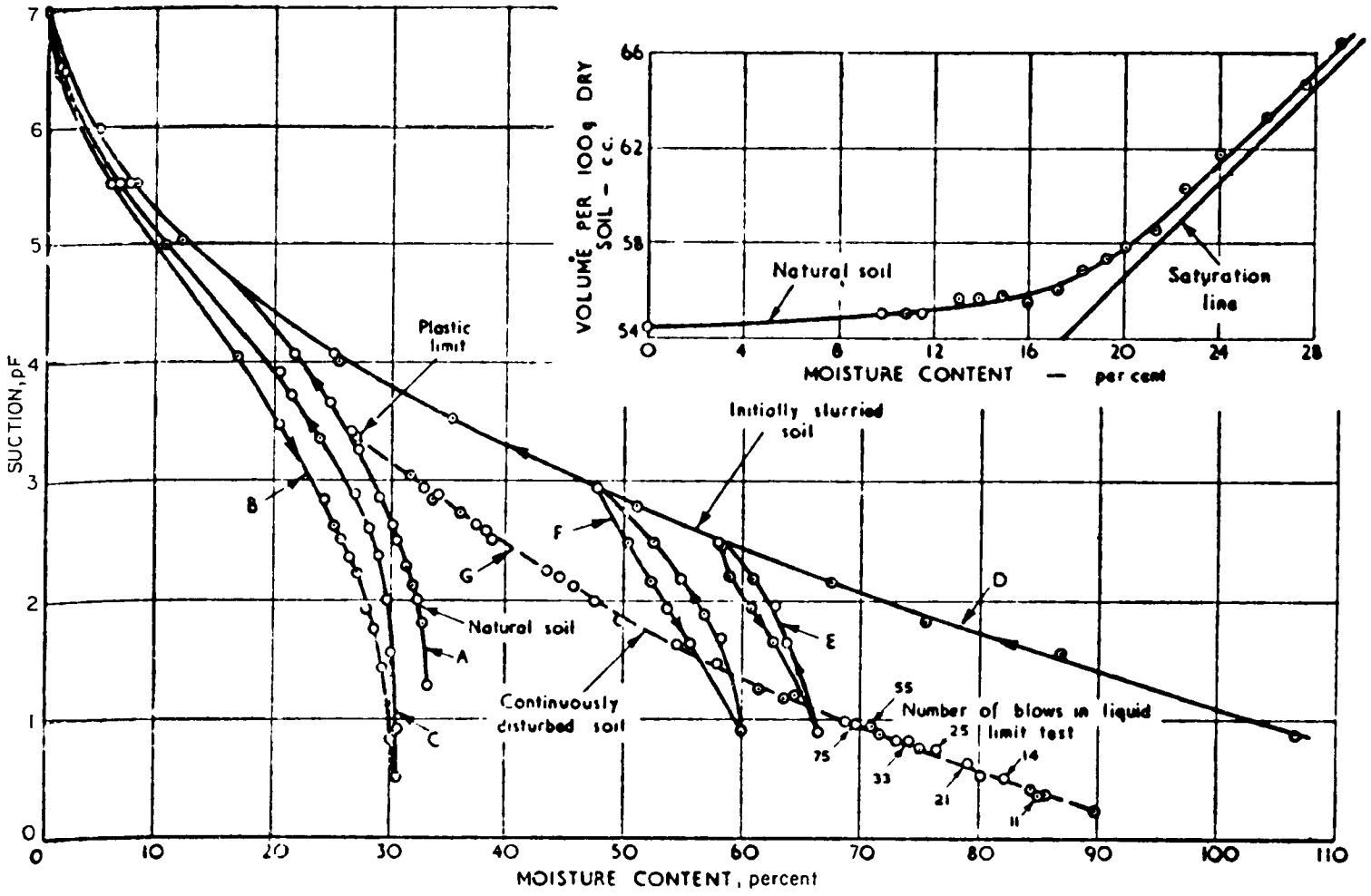

Figure 8. Suction/moisture content and shrinkage relationships for a heavy clay soil. (Croney and Coleman)

decrease in suction to the value given by the line at the moisture content of the sample. On the other hand, if the initial suction is represented by a point below line G, disturbance will be accompanied by an increase of suction. Tests on other heavy clays have shown that for each soil there is a unique suction/moisture content relationship."

The response of a clay/sand interface to wetting is illustrated in Figure 9 which is derived from curve B of Figure 8 and the wetting limb of Figure 7. Curve B of Figure 8 approximates the wetting curve for a heavy clay placed near optimum moisture content which is expected to be a few percent dry of the plastic limit. As discussed above, the sand will not absorb appreciable moisture until the suction aproaches pF 1. Thus, as the wetting front approaches the clay/sand interface, the suction will fall from high values toward pF 0. As the clay reaches pF 5, its moisture content is 10 percent and that of the sand is less than 2 percent. At pF 3, the moisture content is 23 percent for the clay and 2 percent for the sand. Between pF 1.5 and pF 0.5 the sand water content increases by 20 percent to 24 percent. Somewhere in this range gravity flow of water downward through the sand is expected. Thus, in the present case, flow of water through the sand is not expected until water content in the clay has risen from its initial value to 28 percent. See Figure 10 for an alternative display of this phenomenon.

For a waste impoundment with a clay soil liner underlain by unsaturated sand, it is important to determine, for the sand, the moisture content at which free drainage occurs and the corresponding pF value. Then, if one can model the wetting behavior of the clay, it should be possible to predict the breakthrough time at the sand/clay interface if the initial moisture content of the clay is known. A suitable model is available and is described in the next subsection. It is instructive to consider the theoretical basis for the model and then to determine how practical use may be made of the model using a limited number of laboratory and field tests.

Hamilton, Daniel and Olson (1981) describe the successful application of a Galerkin finite element model to the quantitative prediction of soil suction versus depth and time as moisture moves into a clay sample previously prepared at a low moisture content. Data were reported for compacted samples of a fire clay known commercially as Goose Lake clay (plastic limit 19 percent, liquid limit 26 percent) composed of 19 percent sand, 62 percent silt, and 19 percent clay. The standard maximum dry density and optimum water content were 122 lb/ft^3 and 10.5 percent, respectively. The test cell is shown in Figure 11. Moisture moving into the clay produced changes in soil suction which were measured by the sensors (thermocouple psychrometers).

In Figure 12 measured values of suction are contrasted with values computed by the Galerkin finite element model. Agreement is excellent for all but the first sensor probe. This same computer model could be used to predict clay soil liner lifetimes based on pF values corresponding to breakthrough at a clay/sand interface. Input data required for the model are shown in Figures 13 and 14.

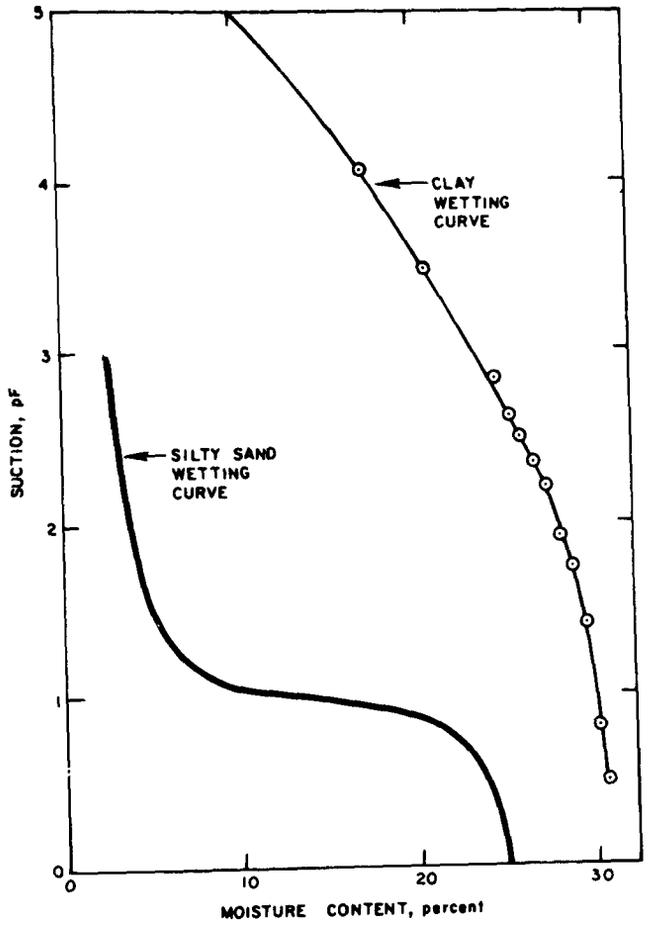

Figure 9. Response of a clay/sand interface to wetting (after Croney and Coleman).

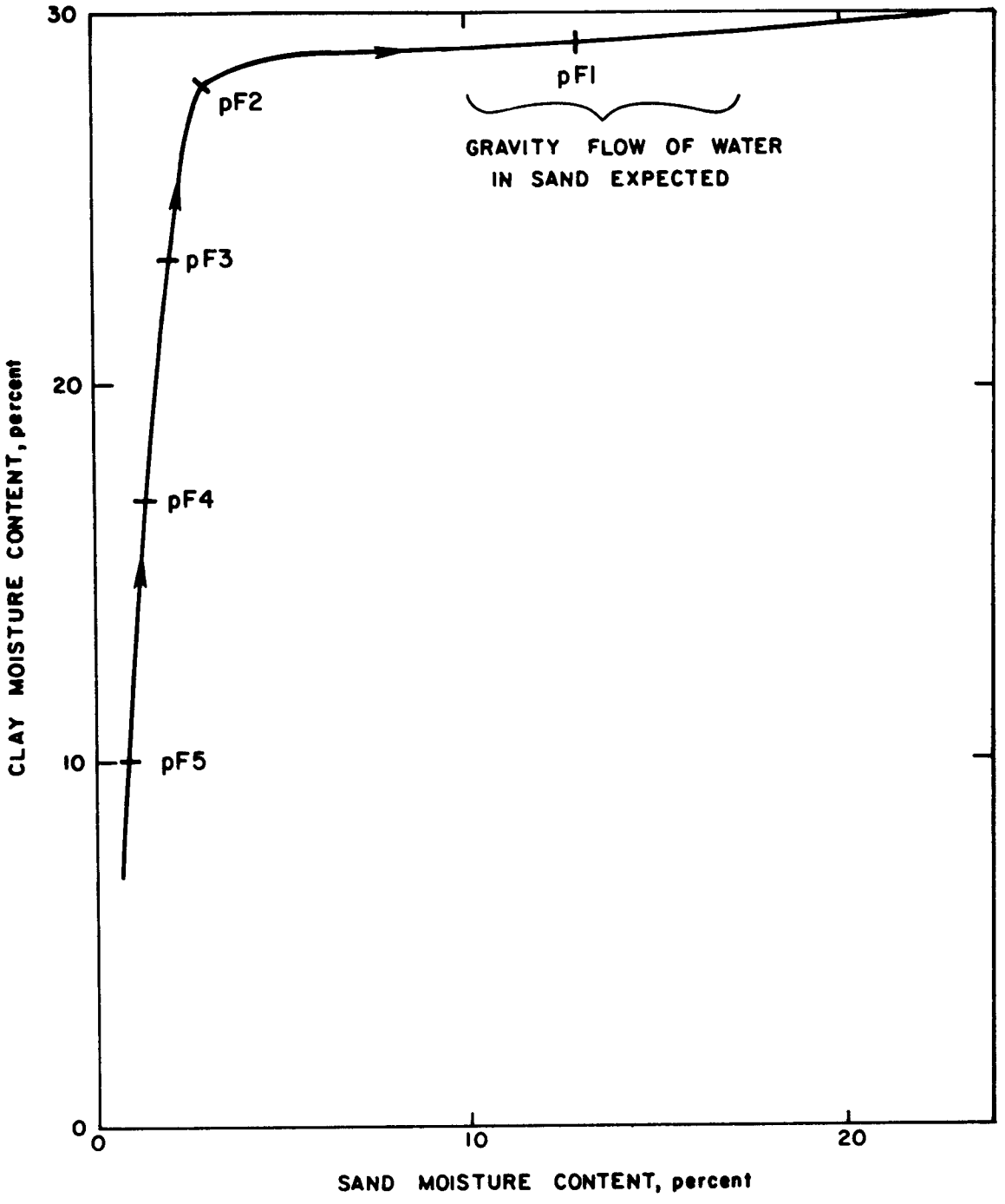

Figure 10. Wetting behavior at clay/sand interface.

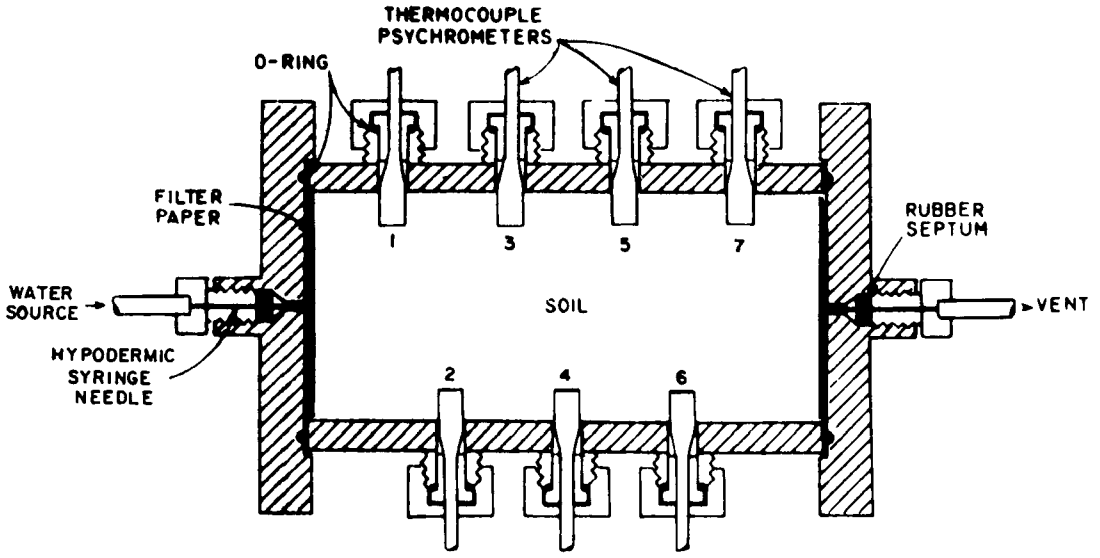

Figure 11. Schematic cross section through a permeameter (Hamilton, et al.).

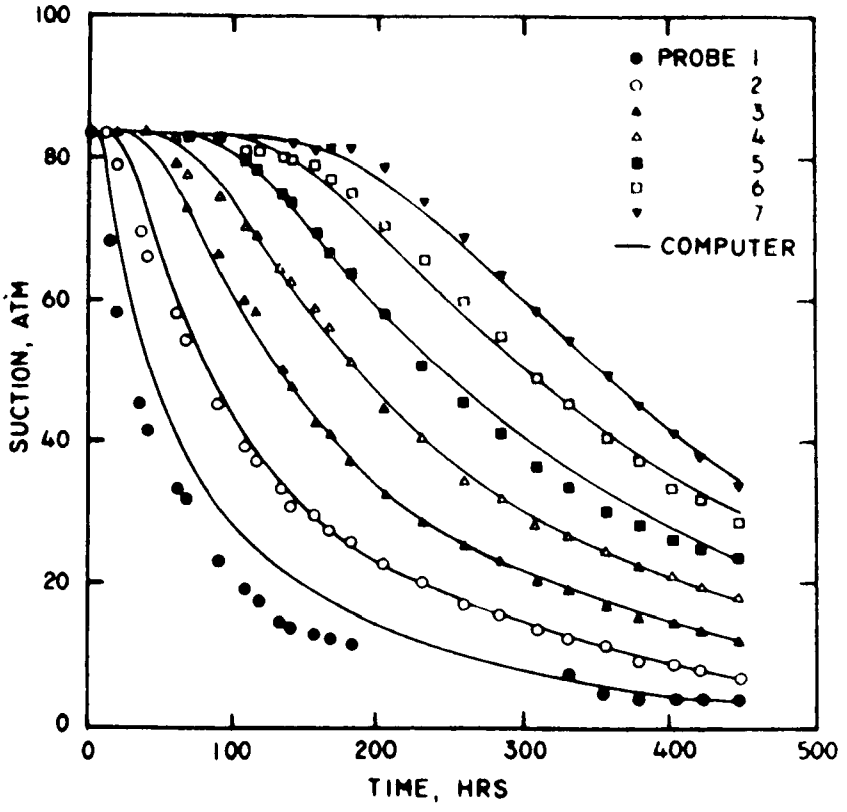

Figure 12. Comparison of measured suctions with values calculated using measured properties and a finite-element computer program (Hamilton, et al.).

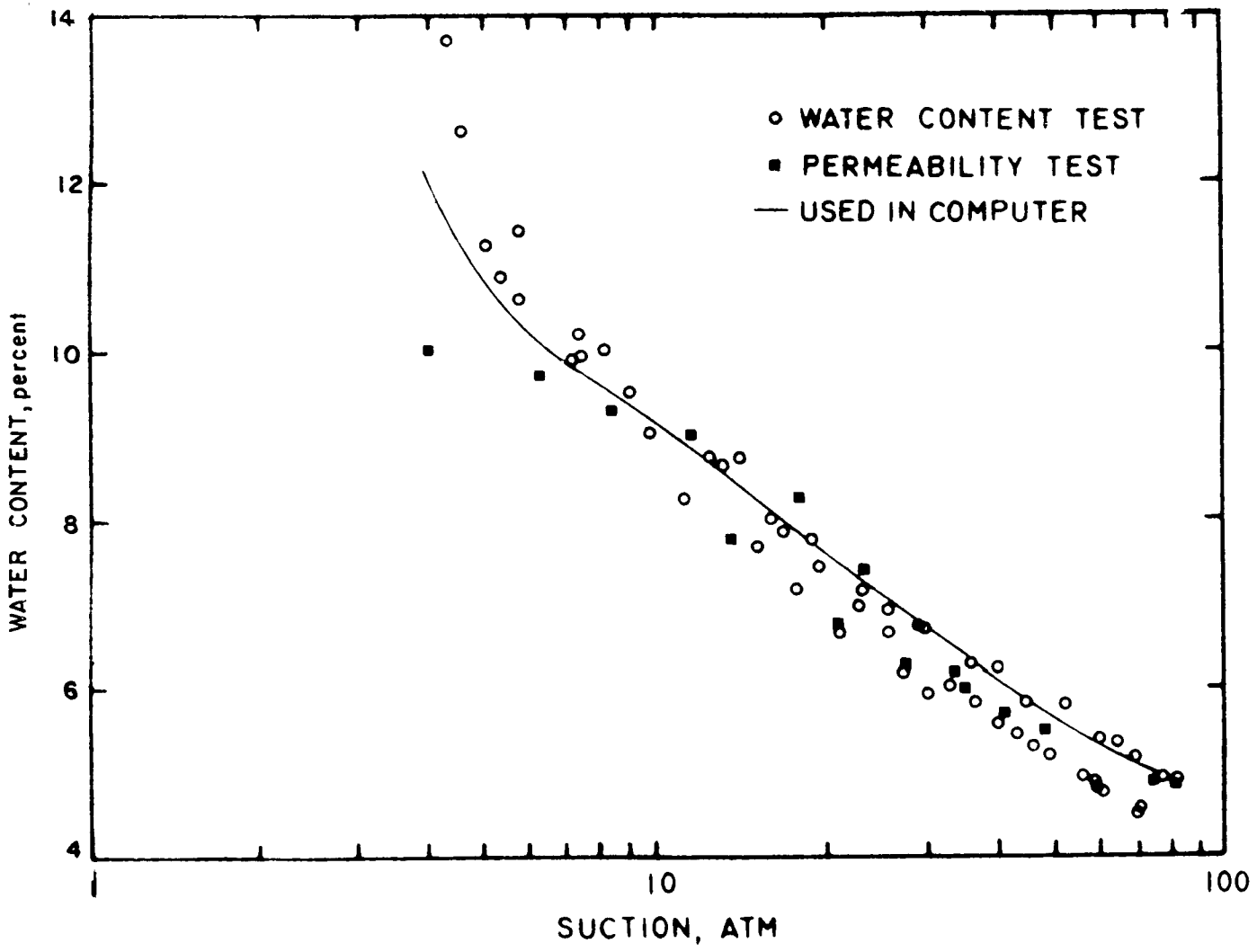

Figure 13. Relationship between water content and suction for Goose Lake clay, (Hamilton et al).

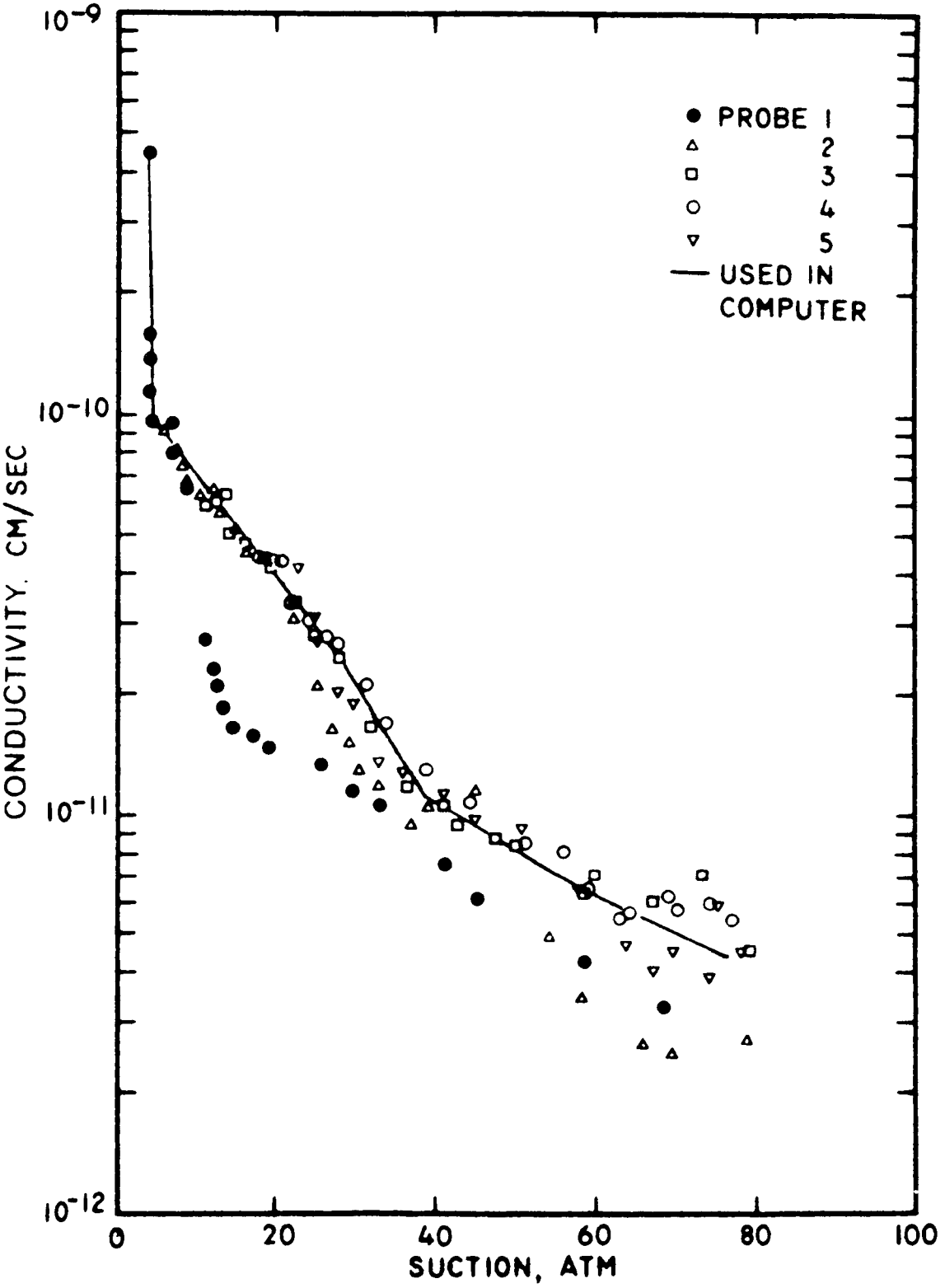

Figure 14. Calculated coefficients of hydraulic conductivity for Goose Lake clay.(Hamilton et al.)

For a waste impoundment, a clay liner would be placed just wet of the optimum moisture content which for Goose Lake clay is 10.5 percent. The expected suction value is under five atmospheres (pF 3.7). Thus, far less experimental data would be required than Figures 13 and 14 might otherwise indicate. For the purposes of predicting liner lifetimes, it is not yet clear whether one should gather basic data such as that shown in Figures 13 and 14, or whether one should employ a curve fitting procedure to data of the type shown in Figure 12.

NUMERICAL SOLUTION OF UNSATURATED FLOW

Due to the nonlinearities of the unsaturated flow equation, exact analytical solutions have not been obtained. Thus, the approximate treatments have been discussed above. Numerical techniques are available to solve the unsaturated flow equations. These techniques, namely finite difference and finite elements, retain the nonlinearity of the liner column matrix with piece-wise continuous approximate representations and are thus most faithful to the original governing equation. Available programs range from basic flow (Bruch, 1975, Johnson, et al., 1982) to coupled heat and moisture transport with vapor transport and hysteresis (Milly, 1982). Using these programs, it is possible to evaluate specific liner designs, with parameters from field and laboratory tests, as well as develop generic "empirical" relations between field and lab parameters and flow characteristics. Not the least important of these characteristics is breakthrough time for a wetting front.

The finite element method is an advanced numerical technique related to finite difference techniques. We start with the governing one-dimensional flow equation on our domain, the liner:

$$\frac{\partial \psi}{\partial t}\frac{d\theta}{d\psi} + \frac{\partial}{\partial z} K \frac{\partial \psi}{\partial z} - \frac{dK}{d\psi}\frac{\partial \psi}{\partial z} = 0 \qquad (1)$$

where ψ [L] is the suction head; θ [L^3/L^3] is moisture content; $K = K(\psi)$ [L/T] is vertical hydraulic conductivity; t [T] is time; and z [L] is the vertical cartesian coordinate positive upward.

Instead of solving for the continuous function ψ, we replace it by an approximation

$$\psi \simeq \sum_{i=1}^{n} N_i \hat{\psi}_i$$

where N_i is an interpolation function which is a function of space, z, and $\hat{\psi}_i$ are values of approximate pressure head at node i. A common type of interpolation function is the linear or chapeau (hat) function. On any element, defined by the nodes, the pressure head at any point is a linear interpolation of the pressure head at these two nodes. Thus, when all the $\hat{\psi}_i$'s are known, the pressure distribution is a piece-wise continuous function made up of linear (straight) segments. Quadratic interpolation uses three nodes per element and results in curved segments.

The terms $d\theta/d\psi$ and $K(\psi)$, which depend on ψ, can also be approximated in this way:

$$\frac{d\theta}{d\psi} \simeq \sum_{i=1}^{n} N_i \left(\frac{d\theta}{d\psi}\right)_i$$

$$K \simeq \sum_{i=1}^{n} N_i K_i$$

Since, during infiltration, the $\hat{\psi}_i$'s vary in time and space, the moisture retention and hydraulic conductivities vary accordingly. Substituting the approximations into (1), the right hand side will no longer equal exactly zero, but will equal some residual error. The best approximation is obtained by forcing this error to zero.

The Galerkin finite element technique is a subset of the family of weighted residual methods. In this procedure the error of the approximation to (1) is multiplied by weighing functions which are then integrated over the domain. These weighing functions are the interpolation functions discussed above. The solution is obtained by solving a system of algebraic equations for the unknown values of $\hat{\psi}_i$, pressure head at each node.

The reader is referred to Pinder and Gray (1977) for a thorough introduction to finite elements, as well as their relation to finite difference techniques. Finite elements have been applied to unsaturated flow problems by many authors, including, for example, Bruch (1975), Milly (1982), Johnson (1982), Hamilton, et al. (1981), Maslia and Johnston (1982) and Trautwein, et al. (1982). It is stressed that this tool is proven and currently available through universities and research groups to which ground water consulting engineers have access.

Maslia and Johnston (1982) used a two-dimensional saturated-unsaturated finite element model to investigate ground water flow beneath a failed landfill. Trautwein, et al. (1982) investigated leakage from a waste pond using a one-dimensional finite element model of unsaturated vertical flow.

In order to develop empirical relations between liner breakthrough and field and lab test results, a finite element model could be used. An almost infinite range of soil types could be simulated, for both the short term (field and lab tests) and the long term (liner performance). By analyzing the results of these simulations, dimensionless relationships could be developed which would relate test data, such as Proctor density or pore size distribution, to breakthrough time. These empirical relations would be based on solution of the complete nonlinear unsaturated flow equations and the results of real lab and field tests. This combination of field tests and numerical simulation would then remove much of the lack of confidence in scaling data to predict long term reliability.

In addition to basic soil data (porosity, density, etc.) the numerical model requires definition of the hydraulic conductivity and moisture retention curves. Moisture retention is easily measured by equilibrating a soil sample with a controlled suction and measuring water content by weight. The hydraulic conductivity relationship is more ellusive, but can be effectively determined (see Hamilton, et al., 1981; Daniel, 1982).

There are many methods available for generating hydraulic conductivity curves (Miller and Bresler, 1977; Brutsaert, 1979; Clapp and Hornberger, 1978; Elzeftawy and Cartwright, 1981; Gruber, 1982; Brooks and Corey, 1966). The method of Elzeftawy and Cartwright (1981) involves computing the hydraulic conductivity curve incrementally using the measured moisture retention at a given suction. These methods have been successful with granular soils but their applicability to clays is tenuous.

Although it is beyond the scope of this work to recommend laboratory procedures, the evaluation of a liner can be outlined. Laboratory tests on the liner material generate preliminary soil data, including hydraulic properties. As the liner is installed, undisturbed samples from each lift are analyzed to verify anticipated properties (moisture content, Proctor density, etc.). Finally, the entire liner column is monitored and simulated using in-place properties as determined from undisturbed samples. The model can also be used to estimate sensitivity of the thickness to errors in parameters.

SECTION 4

SUMMARY

CONCLUSIONS

Based on GCA's review of mathematical expressions or models applicable to estimate the thickness of storage impoundment bottom liners, we conclude that the transit time equation is inappropriate for predicting the time to breakthrough. Under unsaturated conditions, capillary tension controls the movement of the wetting front whereas the influence of liquid head above the liner and gravitational forces are negligible. Comparison of modeling results using the transit time equation, models for unsteady state flow, and unsaturated flow suggest that the transit time equation underestimates required liner thickness as a function of design life.

The proposed EPA transit time equation is based on steady state fully saturated flow in the liner. GCA has modified this equation to include the effects of reduced effective porosity, and negative pressure head (suction) on the liner bottom. This modified equation still fails to capture the major dynamics of the infiltration event of a wetting front moving into an unsaturated soil. Primarily, this error is a result of ignoring capillary forces during the transient infiltration period. This equation underestimates design liner thickness required for containment.

The Green-Ampt (1911) model of infiltration has been suggested as a liner design equation (see Pope-Reid Associates, 1982). This model approximates the infiltration wetting front as a square wave to which saturated Darcy flow analysis is applied. The resulting liner thickness equation captures more of the dynamics of the infiltration event, but is difficult to apply because unknown parameters must be specified, to which the solution is very sensitive. In the presented comparison, this model led to both over-conservative and insufficient design thickness.

The unsaturated flow governing equation can be linearized. Analytical solutions are available for this linearized form, and liner thickness can be iteratively determined. Although capturing much of the dynamics of the wetting front movement, this technique is not recommended because liner conductivity and moisture retention are assumed to be independent of moisture content, and the constant parameters K* and D* must be determined by some sort of fitting procedure, which cannot be performed <u>a priori</u>.

RECOMMENDATIONS

Numerical simulation is recommended as a method for determining liner behavior during infiltration. The nonlinear unsaturated flow governing equation can be approximately solved, retaining the system nonlinearity, as well as simulating both gravity and capillary forces. The finite element method is particularly well suited to this application because it is more accurate at representing the nonlinearities in hydraulic conductivity and moisture retention across the discretized domain. The numerical model can then be applied to particular liner simulations, and can simulate an endless variety of soil types and moisture conditions. The numerical code is verified (programming errors) by solving simple idealized problems for which solutions are available. By changing input soil characteristics and boundary conditions, the model is used to investigate and expose patterns of liner behavior which can be incorporated into empirical relations of field test data and long-term liner performance.

The recommended alternative liner thickness determination method requires a combination of laboratory and field tests, and the use of an empirical method for scaling test behavior to long-term liner reliability. Specific tests should be conducted in the field and the lab on the undisturbed liner, and its underlying layer. The results of these tests can be extrapolated to facility scale behavior using relationships determined by physical and numerical experimentation.

Numerical simulation techniques, such as finite difference and finite elements, can be applied to the unsteady, unsaturated flow equation. These solutions are not limited by the exclusion of complicated flow and porous medium properties and can include a rigorous, albeit approximate, representation of the system nonlinearity. Simulation of a wide range of liner types and moisture conditions will lead to generic expressions, fitted to numerical results, which will allow results of lab and field tests to be scaled to the facility size and design life.

The approach demonstrated by Hamilton et al. (1981) provides an accurate estimate of liner life, neither overestimating nor underestimating required clay thickness. Laboratory tests of the type shown in Figure 12 of Section 3 or of the type shown in Figures 13 and 14 of Section 3 are appropriate. The numerical model provides a means to scale up from the laboratory scale to field conditions. Due care will be required in specifying details of laboratory testing to duplicate essential features of field conditions such as kneading action and permeant composition.

LINER SPECIFICATIONS

Guidance should be available to the prospective owner of storage impoundment to specify practical aspects of selecting, and testing soils, and installing and compacting liners. Based on our review we recommend use of the following criteria as a minimum:

- Soil selection
  - minimum plasticity index = 10 for clayey till, clayey fine sand, or clay
  - sand lenses in borrow area to be less than 1 inch in thickness
- Liner placement
  - place liner in the presence of a qualified soils engineer
  - place and compact soil slightly wet of optimum (for heavy clays optimum water content is slightly lower than the plastic limit)
  - achieve suction pressure $\leq$10 atm at placement
  - minimum liner thickness = 1 meter
  - place liner in lifts of 8 to 12 inches and compact using a sheeps-foot roller
  - place liner on a working mat (minimum 12 inch thickness) of graded sand to provide a filter layer of low suction
- Soil testing
  - prior to installation test conductivity at three conditions (2 percent dry of optimum, optimum, and 2-4 percent wet of optimum) with planned permeant and with local ground water
  - during installation, conduct Atterberg limits testing at the rate of three tests per 500 cu yds of liner soil placed, subject to the approval of the inspecting soils engineer
  - during installation, test dry density of the liner soil using a nuclear densometer, at a frequency specified by the inspecting soils engineer.

SECTION 5

REFERENCES

Bear, J. Hydraulics of Groundwater. McGraw-Hill, New York, 1979.

Bruch, J. L., Jr. Finite Element Solutions for Unsteady and Unsaturated Flow in Porous Media. California Water Resources Center, Contribution No. 151. 1975.

Brutsaert, W. Universal Constants for Scaling the Exponential Soil Water Diffusivity, Water Resources Research, 1979, pp. 481-483.

Clapp, R. B., and G. M. Hornberger. Empirical Equations for Some Soil Hydraulic Properties, Water Resources Research 14(4), 1978, pp. 601-604.

Crank, J. The Mathematics of Diffusion. Clarendon Press, Oxford, 1975, p. 389.

Croney, D., and J. D. Coleman. Soil Structure in Relation to Soil Suction (pF). Road Research Laboratory, Department of Scientific and Industrial Research. Published in the Journal of Soil Science, Vol. 5, No. 1, 1954. pp. 75-84.

Daniel, D. E., personal communication, August 25, 1982.

Day, Arthur. Correspondence to GCA from U.S. Environmental Protection Agency Office of Solid Waste and Emergency Response. June 1982.

Elzeftawy, A., and K. Cartwright. Evaluating the Saturated and Unsaturated Hydraulic Conductivity of Soils, in Permeability and Groundwater Contaminant Transport ASTM STP 746, T. F. Zimmie and C. O. Riggs, eds., American Society for Testing and Materials, 1981, pp. 168-181.

Green, W. H. and G. A. Ampt. Studies in Soil Physics I: The Flow of Air and Water Through Soils, Journal of Agricultural Science 4, 1911, pp. 1-24.

Gruber, P. A. Simplified Method for the Calculation of Unsaturated Hydraulic Conductivity. Presented at AGU Spring Meeting, Philadelphia, PA, May 31-June 4, 1982.

Hamilton, J. M., D. E. Daniel, and R. E. Olson. "Measurement of Hydraulic Conductivity of Partially Saturated Soils," Permeability and Groundwater Contaminant Transport, ASTM STP 746. T. F. Zimmie and C. O. Riggs, Eds., American Society for Testing and Materials, 1981, pp. 182-196.

Johnson, T. M., S. A. Rojstaczer, and K. Cartwright. Modeling of Moisture Movement Through Layered Covers Designed to Limit Infiltration at Low-Level Radioactive Waste Disposal Sites, Presented at AGU Spring Meeting, Philadephia, PA. May 31-June 4, 1982.

Maslia, M. L., and R. H. Johnston. Simulation of Ground-Water Flow in the Vicinity of Hyde Park Landfill, Niagara Falls, New York, U.S.G.S. Open-file Report No. OF82-0159, April 1982.

McIntyre, D. S., R. B. Cunningham, V. Vatanakul, and G. A. Stewart. Measuring Hydraulic Conductivity in Clay Soils: Methods, Techniques, and Errors, Soil Science 128(3), pp. 171-183, 1979.

McWhorter, D. B., and J. D. Nelson. Unsaturated Flow Beneath Tailings Impoundments. J. Geotech. Eng. Div. ASCE GT(11), 1979, pp. 1317-1334.

Miller, R. D., and E. Bresler. A Quick Method for Estimating Soil Water Diffusivity Functions. Soil Science Soc. Am. J. 41, 1977, pp. 1020-1022.

Milly, P. C. D. Moisture and Heat Transport in Hysteretic, Inhomogeneous Porous Media: A Matrix Head-Based Formulation and a Numerical Model, Water Resources Research, 18(3), 1982, pp. 489-498.

Moore, Charles A. Landfill and Surface Impoundment Performance Evaluation Manual. Submitted to the U.S. Environmental Protection Agency, Office of Water and Waste Masnagement, by Geotechnics, Inc. SW-869, September 1980.

Ogata, A., and R. B. Banks. "A Solution of the Differential Equation of Longitudinal Dispersion in Porous Media," U.S. Geol. Survey Prof. Paper No. 411-A, 1961.

Pinder, G. F., and W. G. Gray. Finite Element Simulation in Surface and Subsurface Hydrology, Academic, New York, 1977.

Philip, J. R. The Theory of Infiltration, 6, Effect of Water Depth Over Soil. Soil Science, 85(5), 1958, pp. 278-286.

Pope-Reid Associates, Inc. Correspondence to Mr. Arthur Day, U.S. Environmental Protection Agency, February through April 1982. Incorporated into GCA Work Assignment 68-02-3168, Task 72-(3), as Attachment B.

Trautwein, S. J., D. E. Daniel, and M. W. Cooper. A Case History Study of Water Flow Through Unsaturated Soils. Presented at AGU Spring Meeting, Philadelphia, PA, May 31-June 4, 1982.

APPENDIX B

PARTIAL LIST OF AVAILABLE UNSATURATED FLOW MODELS

Brutsaert, W. F., A functional iteration technique for solving the Richards equation applied to two-dimensional infiltration problems, Water Resource Research 6(7), 1583-1596, 1971.

2-D INFILTRATION MODEL. Non-steady, vertical cross-section, up to 5 soil types, user-oriented, FDM. 1971.

Cooley, R. L., A finite difference method for unsteady flow in variably saturated porous media: application to a single pumping well, Water Resources Research, 7(6), 1607-1625, December 1971.

Finite difference on 2-D unsaturated equations and application to well hydraulics.

Cooley, Prediction of transient or steady state hydraulic head distribution in unsaturated, anisotropic, heterogeneous, two-dimensional, cross-sectional flow systems.

Corey, A. T.

AGDRG and WADSOR. Solves the two-dimensional, transient flow drainage problems in unsaturated/saturated soils.

Davis, L. A. Computer analysis of seepage and groundwater response beneath tailings impoundments, National Science Foundation, (available through NTIS: NSF/RA-800054) Washington, D. C., 1980.

SEEPV. A transient flow model to simulate vertical seepage from a tailings impoundment, including saturated/unsaturated modeling of impoundment with liner, and underlying aquifer, 1980.

Dutt, G. R., M. J. Shaffer, and W. J. Moore, Computer simulation model of dynamic bio-physicochemical processes in soils, Universtiy of Arizona Agricultural Experiment Station Technical Bulleten 196,1972.

SALT TRANSPORT IN IRRIGATED SOILS. A transient one-dimensional, vertical simulation of solute transport in the unsaturated zone, coupled with a chemistry model, 1976.

Freeze, R. A., The mechanism of natural ground-water recharge and discharge: 1. One-dimensional, vertical, unsteady, unsaturated flow above a recharging or discharging ground-water flow system, Water Resources Research, 5(1), 153-171, February 1969.

1-D finite difference model, over review of previous models.

Freeze, R. A., Three-dimensional, transient, saturated-unsaturated flow in a groundwater basin, Water Resources Research, 7, 347-366, April 1971.

3-D finite difference and application to several flow problems.

Giesel, W., M. Renger, and O. Strebel, Numerical treatment of the unsaturated water flow equation: comparison of experimental and computed results, Water Resources Research, 9, 174-177, February 1973.

Finite difference technique on pressure and experiment on sand column, one dimensional.

Gillham, R. W., A. Klute, and D. F. Heermann, Hydraulic properties of a porous medium: measurement and empirical representation, Soil Science Society of America Journal, 40, 203-207, March-April 1976.

Presents an emperical extension to King's [1965] hysteretic curve fitting model.

Haverkamp, R. and M. Vauchlin.

SIMTUS. 1-D, non-steady, unsaturated flow in isotropic soils, FDM. 1977.

Huyakorn, P.

SATURN2. Studies transient, two-dimensional variably saturated flow and solute transport in anisotropic, heterogeneous porous media, 1982.

INTERA Environmental Consultants, Inc.

HYDROLOGIC CONTAMINANT TRANSPORT MODEL. A three-dimensional model to simulate flow and solute transport in a saturated/unsaturated, anisotropic, heterogeneous aquifer system, 1975.

Kaszeta, F. E., C. S. Simmons, and C. R. Cole

MMT-1D. Simulates transient, one-dimensional movement of radionuclides and other contaminants in saturated/unsaturated aquifer systems.

Khaleel, R. and D. L. Redell, Simulation of pollutant movement in groundwater aquifers, Texas Water Resources Institute, Texas A&M University, Technical Report No. 81, 1977.

A two-dimensional vertical model for the simulation of unsteady two-phase flow and dispersion in saturated-unsaturated porous media.

Konikow, L. F. and J. D. Bredehoeft, Computer model of two-dimensional solute transport and dispersion in groundwater, in Techniques of Water Resource Investigation, Book 7, Chapter C2, 1974.

Kraeger-Rovey, C. E.

LINKFLO. Simulates three-dimensional steady and unsteady saturated and unsaturated flow in a stream-aquifer system.

Marino, M. A.

INFILTRATION FEM. Simulates transient movement and distribution of a solute (introduced as a constituent or artificial recharge) in a saturated-unsaturated porous medium.

McCracken, G.

MULTIPURPOSE. Solves any of the equations generally encountered in subsurface flow and transport.

Milly, P. C. D., and P. S. Eagleson, The coupled transport of water and heat in a vertical soil column under atmospheric excitation, R. M. Parsons Laboratory for Water Resources and Hydrodynamics, M.I.T., Technical Report No. 258, July 1980.

Develops 1-D vertical finite element model and verifies by comparison to infiltration solutions. Good review of current soil moisture research.

Molz, F. J.

2-D horizontal-saturated zone, 1-D vertical unsaturated zone, non-steady, phreatic, finite-difference model, lumped, unsaturated zone. Auburn University, 1974.

Narasimhan, T. N. and S. P. Neuman

FLUMP. 2-D in vertical or horizontal plane, phrestic, confined and leaky, specific storativity, versatile, flexible, tested, finite-element model, U. Berkeley, 1975.

National Energy Software Center (NESC)

ODMOD. Prediction of coupled one-dimensional, vertical movement of water and trace contaminants through layered, unsaturated soils.

Neuman, S. P., Saturated-unsaturated seepage by finite elements, Journal of the Hydraulics Division, ASCE, 99(HY12), 2233-2250, December 1973.

UNSAT II. Computes hydraulic heads, pressure heads, water content, boundary fluxes and internal sinks and sources in a saturated/unsaturated, nonuniform, anisotropic, porous medium under nonsteady state conditions.

Pickens, J. F.

UNFLOW. Simulation of two-dimensional (cross-sectional) transient movement of water in saturated-unsaturated nonuniform porous media, 1977.

Pikul, M. F., R. L. Street, and I. Remson, A numerical model based on coupled one-dimensional Richards and Boussinesq equations, Water Resources Research, 295-302, April 1974.

Quasi 2-D finite difference model: horizontal flow in saturated zone, vertical flow in unsaturated zone.

Reed, J. E.

2-D horizontal-saturated zone, 1-D vertical-unsaturated one, non-steady phreatic, confined and leaky, specific storativity, roots, river, aquitard, user oriented, mass storage, finite-difference model. USGS, 1974.

Reeves, M. and J. O. Duguid, Water movement through saturated-unsaturated porous media: a finite-element galerkin model, Oak Ridge National Laboratories, Report No. ORNL-4927, February 1975.

User's manual and development of 2-D vertical flow model, comparison to Freeze's (1971) simulations.

MOISTURE TRANSPORT CODE. A two-dimensional transient model for flow through saturated/unsaturated porous media.

Reisenauer, A. E.

TRUST. Computes steady and nonsteady pressure head distributions in multidimensional, heterogeneous, variably saturated, deformable porous media with complex geometry.

Robertson, J. B.

TRA POND MODEL. Simulates subsurface transport of radionuclide solutes from seepage pond through perched water zones to regional aquifer.

Selim, H. M., R. S. Mansell, and A. Elzeftawy, Distributions of 2,4-D and water in soil during infiltration and redistribution, Soil Science, 121(3), 176-183, 1976.

NMODEL. Predicts water and nitrogen transport and transformations under transient and steady unsaturated water flow in homogeneous or multilayered soils.

Simmons, C. S., see: User's Manual Unsaturated groundwater flow model - UNSAT1D, EPRI Report CS-2434-CCM.

UNSAT1D. One dimensional simulation of unsteady vertical unsaturated flow, 1978.

Skaggs, R. W., Combinationsurface-subsurface drainage systems for humid regions, J. of the Irrigation and Drainage Div., ASCE, 106(IR4), 265-283, 1980.

DRAINMOD. An unsteady, one-dimensional, horizontal/vertical, saturated/unsaturated model to simulate watertable position and soil water regime above water table for artificially drained soils.

Terry, J. E.

SUPERMOCK. Simulates transient stress and response in a saturated-unsaturated ground water flow system including a water-table aquifer overlying a confined aquifer.

Washburn, J. F.

MMI-DPRW. Predicts the transient three-dimensional movement of radionuclides and other contaminants in unsaturated/saturated aquifer systems.

Wierenga, P. J., Solute distribution profiles computed with steady-state and transient water movement models, Soil Science Society of America Journal, 41, 1050-1055, 1977.

Compare predicted solute concentrations using steady vs transient unsaturated flow. Under pulsed boundary conditions, both flow models produced very similar concentration histograms. Silty clay loam. Exponential moisture characteristic and relative permeability.

Wind, G. P. and W. Van Doorne, A numerical model for the simulation of unsaturated vertical flow of moisture in soils, Journal of Hydrology, 24, 1-20, 1975.

Yeh, G. T. and D. S. Ward, FEMWATER: a finite-element model of water flow through saturated-unsaturated porous media, Oak Ridge National Laboratories, Report No. ORNL-5567, October 1980.

User's manual and modifications to 2-D vertical flow model of Reeves and Duguid (1975). Based on pressure head.

APPENDIX C

LISTING OF EXAMPLE COMPUTER PROGRAM SOILINER

```
 09/26/83   08:39:59   GCAGD.SOILINER.FORT.DATA

00000010 C*****************************************************************
00000020 C
00000030 C     SOILINER.FORTRAN  FINITE DIFFERENCE OF VERTICAL UNSATURATED
00000040 C                              INFILTRATION
00000050 C
00000060 C      DAN GOODE          JUNE 1983
00000070 C
00000080 C      COPYRIGHT 1983     GCA/TECHNOLOGY DIVISION
00000090 C                         213 BURLINGTON ROAD
00000100 C                         BEDFORD, MA  01730
00000110 C                         (617) 275-5444
00000120 C
00000130 C*****************************************************************
00000140 C
00000150       COMMON/MASSB/STOR,TOTV1,TOTV2,FLUX10,FLUX20
00000160       COMMON/DEVICE/IRD,IPRT,IFILE
00000170       COMMON/FILES/IFGRD,IFSOIL,IFINIT,IFPOUT,IFMOUT,IFSOUT,IFLUX,IFZOUT
00000180       COMMON/INFO/NUMNP,NUMEL,NPM1,NPM2,NUMEL2,AM1,ISPACE,ITOL,
00000190      *            DEPTH,ENDTIM,DT,DTMAX,ALPHA,PSIBOT,H,NZOUT,
00000200      *            PSINIT,NCPTS,ERRMAX,MAXIT,CHPARM,MAXNT,ISTEDY
00000210       COMMON/TIMES/TIME,TIME1,NT,ERR,NOUT,TOUT(10),NOUT1,TOUT1
00000220       COMMON/ERRORS/IERR,IWARN
00000230       DIMENSION PSI(200),PSIOLD(200),DZ(200),C(200),
00000240      *          RK(200),WORK(200),RMCURV(10),
00000250      *          RKCURV(10),PSICRV(10),RMOIST(200),
00000260      *          STIFF(3,200),DPSI(200),F(200),
00000270      *          Z(200),SATK(200),PSICRT(200),POR(200)
00000280       DIMENSION VNEW(200),VOLD(200),OLDC(200),DZN(200),STARK(200),
00000290      *          IZOUT(10),ISOIL(200),BETA(200)
00000291       DIMENSION RKL(400),CL(400),RMSTL(400),OLDML(400)
00000300 C
00000310       DATA NMAX/200/
00000320       IWARN=0
00000330       IRD=5
00000340       IPRT=7
00000350 C
00000360 C     READ AND WRITE PROBLEM PARAMETERS AND INITIALIZE
00000370 C
00000380       CALL INPUT(PSI,RMCURV,RKCURV,PSICRV,SATK,POR,ISOIL,DZ,BETA,DZN,Z,
00000390      *           PSICRT,IZOUT)
00000400 CBUG  CALL OUTPUT(PSI,RMOIST,RK,Z,RKL,CL,RMSTL,STARK,POR,DZ,ITER)
00000410 C
00000420 C
00000430 C      SAVE ALPHA, SET ALPHA=1 FOR STEADY STATE SOLUTION
00000440       ALPHAS=ALPHA
00000450       IF(ISTEDY.NE.1) GOTO 140
00000460 C
00000470 C     ============================
00000480 C      STEADY STATE SOLUTION
00000490 C     ============================
00000500       ITER=0
00000510       ALPHA=1.D0
00000520       AM1=0.D0
00000530 C
00000540       CALL CLEAR(OLDC,NUMNP)
00000550       CALL CLEAR(VOLD,NPM2)
00000560 C
00000570 C     ******************
00000580 C     MAIN ITERATION LOOP
00000590 C     ******************
```

```
00000600 C
00000610 C
00000620   120 ITER=ITER+1
00000630 C
00000640 C       COMPUTE MOISTURE CONTENT AND CONDUCTIVITY
00000650        CALL SPROP1(PSI,PSICRV,RMCURV,RKCURV,RMOIST,C,
00000660       *             RK,RMSTL,CL,RKL,STARK,SATK,POR,ISOIL,PSICRT,0)
00000670 C
00000680 C       ZERO STORAGE VECTOR
00000690        CALL CLEAR(C,NUMNP)
00000700 C
00000710 C       BUILD VELOCITY VECTOR
00000720        CALL BUILDV(VNEW,PSI,STARK,DZN,DZ,BETA,RK)
00000730 C
00000740 C       BUILD STIFFNESS MATRIX
00000750        CALL BUILDS(STIFF,RK,STARK,C,OLDC,DZN,DZ,BETA)
00000760 C
00000770 C       BUILD FORCING VECTOR   BOUNDARY CONDITION TERMS
00000780        CALL BUILDF(F,C,OLDC,PSI,PSIOLD,VNEW,VOLD)
00000790 C
00000800 C       SOLVE MATRIX EQUATION USING THOMAS ALGORITHM
00000810 C       RESULT IS INCREMENTAL CHANGE IN PSI, DPSI
00000820        CALL THOMAS(STIFF,F,DPSI,WORK,NPM2,0)
00000830 C
00000840 C       UPDATE PSI
00000850        DO 125 I=1,NPM2
00000860        N=I+1
00000870        PSI(N)=PSI(N)+DPSI(I)
00000880   125 CONTINUE
00000890 C
00000900 CBUG   CALL OUTPUT(PSI,RMOIST,RK,Z,RKL,CL,RMSTL,STARK,POR,DZ,ITER)
00000910 C
00000920 C      CHECK SOLUTION FOR CONVERGENCE
00000930 C
00000940        CALL ERROR(DPSI,NPM2,ERR,ITOL)
00000950        IF(ERR.LT.ERRMAX) GOTO 140
00000960        IF(ITER.LE.MAXIT) GOTO 120
00000970 C
00000980 C       **************************
00000990 C       END OF MAIN ITERATION LOOP
00001000 C       **************************
00001010 C
00001020        WRITE(IPRT,2000) NT
00001030        IWARN=IWARN+1
00001040 C
00001050 C      WRITE REQUESTED OUTPUT TO PRINT AND PLOT FILES
00001060 C
00001070   140 CALL SPROP1(PSI,PSICRV,RMCURV,RKCURV,RMOIST,C,
00001080       *             RK,RMSTL,CL,RKL,STARK,SATK,POR,ISOIL,PSICRT,1)
00001090 C
00001100        ALPHA=ALPHAS
00001110        AM1=1.D0-ALPHA
00001120 C
00001130 C      ============================
00001140 C       END OF STEADY STATE SOLUTION
00001150 C      ============================
00001160 C
00001170 C       OUTPUT INITIAL CONDITIONS AND/OR STEADY STATE SOLUTION
00001180        CALL OUTPUT(PSI,RMOIST,RK,Z,RKL,CL,RMSTL,STARK,POR,DZ,ITER)
00001190        IF(NZOUT.GT.0) CALL ZOUT(IZOUT,PSI,RMOIST)
00001200 C
00001210        IF(MAXNT.LE.0) GOTO 50
```

```
00001220 C
00001230 C      BUILD VELOCITY VECTOR IF NOT ALREADY COMPUTED FROM STEADY STATE
00001240        IF(ISTEDY.NE.1) CALL BUILDV(VNEW,PSI,STARK,DZN,DZ,BETA,RK)
00001250 C
00001260 C      READ IN NEW BOUNDARY CONDITIONS IF INITIAL CONDITION IS SS
00001270        IF(ISTEDY.EQ.1) CALL NEWBC(PSI)
00001280 C
00001290 C
00001300 C      ========================
00001310 C      START TRANSIENT SOLUTION
00001320 C      ========================
00001330 C
00001340        CALL MASBAL(PSI,RMSTL,OLDML,STARK,DZ,-1)
00001350     10 ITER=0
00001360        NT=NT+1
00001370 C
00001380 C      SAVE OLD VECTORS AND PREDICT NEW PSI FROM V
00001390        CALL PREDCT(PSI,PSIOLD,VNEW,VOLD,C,OLDC,
00001400       *            OLDML,RMSTL)
00001410 C
00001420 CBUG   CALL OUTPUT(PSI,RMOIST,RK,Z,RKL,CL,RMSTL,STARK,POR,DZ,ITER)
00001430 C
00001440 C      ********************
00001450 C      MAIN ITERATION LOOP
00001460 C      ********************
00001470 C
00001480        TIME=TIME1+DT
00001490 C
00001500     20 ITER=ITER+1
00001510 C
00001520 C        COMPUTE MOISTURE CONTENT AND CONDUCTIVITY
00001530        CALL SPROP1(PSI,PSICRV,RMCURV,RKCURV,RMOIST,C,
00001540       *              RK,RMSTL,CL,RKL,STARK,SATK,POR,ISOIL,PSICRT,0)
00001550 C
00001560 C      BUILD VELOCITY VECTOR
00001570        CALL BUILDV(VNEW,PSI,STARK,DZN,DZ,BETA,RK)
00001580 C
00001590 C      BUILD STIFFNESS MATRIX
00001592 CBUG   WRITE(6,6663) NT,DT,DTMAX,TIME,ENDTIM
00001593  6663 FORMAT(I5,1P4E15.4)
00001600        CALL BUILDS(STIFF,RK,STARK,C,OLDC,DZN,DZ,BETA)
00001610 C
00001620 C      BUILD FORCING VECTOR   TRANSIENT AND BOUNDARY CONDITION TERMS
00001630        CALL BUILDF(F,C,OLDC,PSI,PSIOLD,VNEW,VOLD)
00001640 C
00001650 C      SOLVE MATRIX EQUATION USING THOMAS ALGORITHM
00001660 C      RESULT IS INCREMENTAL CHANGE IN PSI, DPSI
00001670        CALL THOMAS(STIFF,F,DPSI,WORK,NPM2,0)
00001680 C
00001690 C      UPDATE PSI
00001700        DO 25 I=1,NPM2
00001710        N=I+1
00001720        PSI(N)=PSI(N)+DPSI(I)
00001730     25 CONTINUE
00001740 C
00001750 CBUG   CALL OUTPUT(PSI,RMOIST,RK,Z,RKL,CL,RMSTL,STARK,POR,DZ,ITER)
00001760 C
00001770 C      CHECK SOLUTION FOR CONVERGENCE
00001780 C
00001790        CALL ERROR(DPSI,NPM2,ERR,ITOL)
00001800        IF(ERR.LT.ERRMAX) GOTO 30
00001810        IF(ITER.LE.MAXIT) GOTO 20
```

```
00001820 C
00001830 C      *************************
00001840 C      END OF MAIN ITERATION LOOP
00001850 C      *************************
00001860 C
00001870       WRITE(IPRT,2000) NT
00001880       IWARN=IWARN+1
00001890 C
00001900 C     WRITE REQUESTED OUTPUT TO PRINT AND PLOT FILES
00001910 C
00001920    30 CALL SPROP1(PSI,PSICRV,RMCURV,RKCURV,RMOIST,C,
00001930      *              RK,RMSTL,CL,RKL,STARK,SATK,POR,ISOIL,PSICRT,1)
00001940       IF(NZOUT.GT.0) CALL ZOUT(IZOUT,PSI,RMOIST)
00001950       IF(IOUT.NE.1.OR.NOUT.EQ.-1) GOTO 35
00001960       NOUT1=NOUT1+1
00001970       TOUT1=TOUT(NOUT1)
00001980       IF(NOUT1.GT.NOUT.OR.TOUT1.LE.0.D0) NOUT=0
00001990    35 CONTINUE
00002000       IF(NOUT.EQ.-1.OR.TIME.GE.ENDTIM.OR.NT.GE.MAXNT)
00002010      *    IOUT=1
00002020       IF(IOUT.EQ.1) CALL OUTPUT(PSI,RMOIST,RK,Z,RKL,CL,RMSTL,STARK,POR,
00002030      *                          DZ,ITER)
00002040       CALL MASBAL(PSI,RMSTL,OLDML,STARK,DZ,IOUT)
00002050 C
00002060       IF(TIME.GE.ENDTIM.OR.NT.GE.MAXNT) GOTO 50
00002070 C
00002080 C      NEW TIMES
00002090 C
00002100       TIME1=TIME
00002110       IOUT=0
00002120       CALL NEWTIM(PSI,PSIOLD,IOUT)
00002130       GOTO 10
00002140 C
00002150 C      ======================
00002160 C      END OF SOLUTION PERIOD
00002170 C      ======================
00002180 C
00002190    50 WRITE(IPRT,2010) IWARN
00002200       STOP
00002210 C
00002220  2000 FORMAT(/' **** WARNING **** MAXIMUM ITERATIONS EXCEEDED ',
00002230      *'TIME STEP ',I5)
00002240  2010 FORMAT(/' EXECUTION ENDED NORMALLY - ',I5,' - WARNINGS')
00002250 C
00002260       END
00002270 C*********************************************************************
00002280 C
00002290       SUBROUTINE SPROP1(PSI,PSICRV,RMCURV,RKCURV,RMOIST,C,RK,
00002300      *     RMSTL,CL,RKL,STARK,SATK,POR,ISOIL,PSICRT,KODE)
00002310 C
00002320 C*********************************************************************
00002330 C
00002340 C....  LOOP OVER ELEMENTS AND COMPUTE SOIL PROPERTIES AT NODES
00002350 C         AT EACH END OF ELEMENT.  SINCE ADJACENT ELEMENTS MAY HAVE
00002360 C         DIFFERENT SOIL TYPES, A NODE HAS TWO VALUES FOR EACH PROP.,
00002370 C         ONE FOR ELEMENT ON TOP, AND ONE FOR BOTTOM ELEMENT.
00002380 C
00002390       COMMON/MASSB/STOR,TOTV1,TOTV2,FLUX10,FLUX20
00002400       COMMON/DEVICE/IRD,IPRT,IFILE
00002410       COMMON/INFO/NUMNP,NUMEL,NPM1,NPM2,NUMEL2,AM1,ISPACE,ITOL,
00002420      *            DEPTH,ENDTIM,DT,DTMAX,ALPHA,PSIBOT,H,NZOUT,
00002430      *            PSINIT,NCPTS,ERRMAX,MAXIT,CHPARM,MAXNT,ISTEDY
```

```
00002440       COMMON/ERRORS/IERR,IWARN
00002450       COMMON/FILES/IFGRD,IFSOIL,IFINIT,IFPOUT,IFMOUT,IFSOUT,IFLUX,IFZOUT
00002460       DIMENSION PSI(1),PSICRV(1),RMCURV(1),
00002470      *          RMOIST(1),RKL(1),SATK(1),POR(1),C(1),
00002480      *        RKCURV(1),RK(1),STARK(1),CL(1),RMSTL(1),ISOIL(1),PSICRT(1)
00002490 C
00002500       IP=0
00002510       N=1
00002520 C
00002530 C      LOOP AND CALCULATE SOIL PROPERTIES
00002540       DO 10 L=1,NUMEL
00002550       JSOIL=ISOIL(L)
00002560 C      TOP NODE
00002570       IP=IP+1
00002580       K=1
00002590 CBUG  WRITE(6,6666) L,K,N,IP,JSOIL,PSI(N),PSICRT(L)
00002600  6666 FORMAT(5I5,2F10.2)
00002610       IF(PSI(N).GT.PSICRT(L)) GOTO 5
00002620       GOTO 22
00002630 C      BOTTOM NODE
00002640     8 IP=IP+1
00002650       K=2
00002660       N=N+1
00002670 CBUG  WRITE(6,6666) L,K,N,IP,JSOIL,PSI(N),PSICRT(L)
00002680       IF(PSI(N).GT.PSICRT(L)) GOTO 5
00002690 C
00002700 C      UNSATURATED NODE
00002710 C
00002720    22 PSINEG=-PSI(N)
00002730 CDP    CHANGE NEXT CARD FOR DOUBLE/SINGLE PRECISION
00002740       PSILN=ALOG(PSINEG)
00002750 C
00002760 C      CALCULATE RK
00002770 C
00002780       IF(JSOIL.EQ.1) RELK=
00002790      * 124.6D0/ (124.6D0 + PSINEG**1.77D0)
00002800       IF(JSOIL.EQ.2) RELK=
00002810      * 1.175D6/(1.175D6+PSINEG**4.74D0)
00002820       IF(JSOIL.EQ.3) RELK=
00002830      * 1.175D6/(1.175D6+PSINEG**4)
00002840       RKL(IP)=RELK*SATK(L)
00002850 C
00002860 C      CALCULATE MOIST = VOLUMETRIC MOISTURE CONTENT
00002870 C
00002880       IF(JSOIL.EQ.1) RMSTL(IP)=
00002890      * 739.D0*(POR(L)-0.124D0)/(739.D0+PSILN**4)+0.124D0
00002900       IF(JSOIL.EQ.2) RMSTL(IP) =
00002910      *   1.611D6*(POR(L)-0.075D0)/(1.611D6+PSINEG**3.96D0)+0.075D0
00002920       IF(JSOIL.EQ.3) RMSTL(IP)=
00002930      *   1.611D6*(POR(L)-0.075D0)/(1.611D6+PSINEG**3.96D0)+0.075D0
00002940 C
00002950 C      CALCULATE DMOIST/DPSI = C(PSI)
00002960 C
00002970       IF(JSOIL.EQ.1) CL(IP) =
00002980      * 2956.D0*(POR(L)-0.124D0)*PSILN**3/PSINEG/(739.D0+PSILN**4)**2
00002990       IF(JSOIL.EQ.2) CL(IP) =
00003000      * 6.3796D6*(POR(L)-0.075D0)*PSINEG**2.96D0/
00003010      *    ((1.611D6+PSINEG**3.96D0)**2)
00003020       IF(JSOIL.EQ.3) CL(IP) =
00003030      * 6.3796D6*(POR(L)-0.075D0)*PSINEG**2.96D0/
00003040      *    ((1.611D6+PSINEG**3.96D0)**2)
00003050 C
```

```
00003060 CBUG  WRITE(6,6667) PSINEG,PSILN,CL(IP),RKL(IP),RMSTL(IP)
00003070  6667 FORMAT(0P2F10.2,1P2E10.2,0PF10.4)
00003080       IF(K.EQ.1) GOTO 8
00003090       GOTO 10
00003100 C
00003110 C      SATURATED NODE
00003120 C
00003130     5 CONTINUE
00003140       RMSTL(IP)=POR(L)
00003150       CL(IP)=0.0D0
00003160       RKL(IP)=SATK(L)
00003170       IF(K.EQ.1) GOTO 8
00003180    10 CONTINUE
00003190 C      END OF LOOP
00003200 C
00003210 C      COMPUTE GEOMETRIC MEAN INTERBLOCK CONDUCTIVITY
00003220 C
00003230       I2=0
00003240       DO 20 L=1,NUMEL
00003250       I1=I2+1
00003260       I2=I1+1
00003270 CDP    CHANGE NEXT CARD FOR DOUBLE/SINGLE PRECISION
00003280       STARK(L)=SQRT(RKL(I1)*RKL(I2))
00003290    20 CONTINUE
00003300 C
00003310 C      COMPUTE MEAN MOIST, K, AND C AT NODES
00003320 C
00003330       L2=1
00003340       DO 30 I=2,NPM1
00003350       L1=L2+1
00003360       L2=L1+1
00003370       C(I)=(CL(L1)+CL(L2))/2.D0
00003380       RMOIST(I)=(RMSTL(L1)+RMSTL(L2))/2.D0
00003390 CDP    CHANGE NEXT CARD FOR DOUBLE/SINGLE PRECISION
00003400       RK(I)=SQRT(RKL(L1)*RKL(L2))
00003410    30 CONTINUE
00003420 C
00003430 C      USE ONE NODE VALUE AT TOP AND BOTTOM
00003440       C(1)=CL(1)
00003450       RMOIST(1)=RMSTL(1)
00003460       RK(1)=RKL(1)
00003470       C(NUMNP)=CL(NUMEL2)
00003480       RMOIST(NUMNP)=RMSTL(NUMEL2)
00003490       RK(NUMNP)=RKL(NUMEL2)
00003500 C
00003510 CBUG  CALL DUMP1('RKL SP1 ',RKL,NUMEL2)
00003520 CBUG  CALL DUMP1('RMSTLSP1',RMSTL,NUMEL2)
00003530 CBUG  CALL DUMP1('CL    SP1',CL,NUMEL2)
00003540 CBUG  CALL DUMP1('STARKSP1',STARK,NUMEL)
00003550 CBUG  CALL DUMP1('RK    SP1',RK,NUMNP)
00003560 CBUG  CALL DUMP1('RMOISTP1',RMOIST,NUMNP)
00003570 CBUG  CALL DUMP1('C     SP1',C,NUMNP)
00003580       RETURN
00003590       END
00003600 C
00003610 C*************************************************************************
00003620 C
00003630       SUBROUTINE BUILDV(V,PSI,STARK,DZN,DZ,BETA,RK)
00003640 C
00003650 C*************************************************************************
00003660 C
00003670 C.... COMPUTE C*D(PSI)/DT = V  USING CENTERED FINITE DIFFERENCE (CFDM)
```

```
00003680 C       THIS VERSION HAS SPECIAL ALGORITHM FOR VARIABLE SPACING
00003690 C
00003700       COMMON/MASSB/STOR,TOTV1,TOTV2,FLUX10,FLUX20
00003710       COMMON/TIMES/TIME,TIME1,NT,ERR,NOUT,TOUT(10),NOUT1,TOUT1
00003720       COMMON/DEVICE/IRD,IPRT,IFILE
00003730       COMMON/INFO/NUMNP,NUMEL,NPM1,NPM2,NUMEL2,AM1,ISPACE,ITOL,
00003740      *            DEPTH,ENDTIM,DT,DTMAX,ALPHA,PSIBOT,H,NZOUT,
00003750      *            PSINIT,NCPTS,ERRMAX,MAXIT,CHPARM,MAXNT,ISTEDY
00003760       COMMON/ERRORS/IERR,IWARN
00003770       DIMENSION V(1),PSI(1),STARK(1),DZN(1),DZ(1),RK(1),BETA(1)
00003780 C
00003790       IF(ISPACE.EQ.1) GOTO 20
00003800 C
00003810       DO 10 I=1,NPM2
00003820       L=I
00003830       LP1=L+1
00003840       N=I+1
00003850 C
00003860       V(I)=( STARK(LP1) * (PSI(N+1)-PSI(N))/ DZ(LP1) -
00003870      *      STARK(L) * (PSI(N)-PSI(N-1))/ DZ(L) +
00003880      *       STARK(LP1)-STARK(L)) /DZN(I)
00003890    10 CONTINUE
00003900       GOTO 50
00003910 C
00003920 C       VARIABLE SPACING ALGORITHM
00003930    20 DO 40 I=1,NPM2
00003940       L=I
00003950       LP1=L+1
00003960       N=I+1
00003970       NM1=N-1
00003980       NP1=N+1
00003990       B1=BETA(I)
00004000       IF(B1.EQ.1.D0) GOTO 30
00004010       B2=1.D0/B1
00004020       DZNI=DZN(I)
00004030       V(I)=(B2*STARK(LP1)*(PSI(NP1)-PSI(N))/DZ(LP1) -
00004040      *       B1*STARK(L)*(PSI(N)-PSI(NM1))/DZ(L) +
00004050      *      (B1-B2)*RK(N)*((PSI(NP1)-PSI(NM1))/(DZNI+DZNI) +1) -
00004060      *       B1*STARK(L)+B2*STARK(LP1)) /DZNI
00004070       GOTO 40
00004080    30 V(I)=( STARK(LP1) * (PSI(NP1)-PSI(N))/ DZ(LP1) -
00004090      *      STARK(L) * (PSI(N)-PSI(NM1))/ DZ(L) +
00004100      *       STARK(LP1)-STARK(L)) /DZN(I)
00004110    40 CONTINUE
00004120 C
00004130    50 CONTINUE
00004140 CBUG  CALL DUMP1('V BUILDV',V,NPM2)
00004150 C
00004160   999 RETURN
00004170       END
00004180 C*************************************************************
00004190 C
00004200       SUBROUTINE PREDCT(PSI,PSIOLD,VNEW,VOLD,C,OLDC,
00004210      *                  OLDML,RMSTL)
00004220 C
00004230 C*************************************************************
00004240 C
00004250 C.... STORE OLD VECTORS AND PREDICT NEW PSI
00004260 C
00004270       COMMON/MASSB/STOR,TOTV1,TOTV2,FLUX10,FLUX20
00004280       COMMON/DEVICE/IRD,IPRT,IFILE
00004290       COMMON/INFO/NUMNP,NUMEL,NPM1,NPM2,NUMEL2,AM1,ISPACE,ITOL,
```

```
00004300      *             DEPTH,ENDTIM,DT,DTMAX,ALPHA,PSIBOT,H,NZOUT,
00004310      *             PSINIT,NCPTS,ERRMAX,MAXIT,CHPARM,MAXNT,ISTEDY
00004320       COMMON/TIMES/TIME,TIME1,NT,ERR,NOUT,TOUT(10),NOUT1,TOUT1
00004330       COMMON/ERRORS/IERR,IWARN
00004340       DIMENSION PSI(1),PSIOLD(1),VNEW(1),VOLD(1),C(1),OLDC(1),
00004350      *          OLDML(1),RMSTL(1)
00004360 C
00004370       CALL COPY(PSI,NUMNP,PSIOLD)
00004380       CALL COPY(VNEW,NPM2,VOLD)
00004390       CALL COPY(C,NUMNP,OLDC)
00004400       CALL COPY(RMSTL,NUMEL2,OLDML)
00004410 C       PREDICT NEW PSI FROM V
00004420       DO 10 I=1,NPM2
00004430       N=I+1
00004440       IF(OLDC(N).LE.0.D0) GOTO 10
00004450       PSI(N)=PSI(N)+VOLD(I)/OLDC(N)*DT
00004460    10 CONTINUE
00004470 C
00004480 CBUG  CALL DUMP1('P PREDCT',PSI,NUMNP)
00004490       RETURN
00004500       END
00004510 C*************************************************
00004520 C
00004530       SUBROUTINE BUILDS(STIFF,RK,STARK,C,OLDC,DZN,DZ,BETA)
00004540 C
00004550 C*************************************************
00004560 C
00004570 C**** BUILD STIFFNESS MATRIX FOR ACTIVE NODES ONLY
00004580 C     THIS IS STANDARD FINITE DIFFERENCE
00004590 C
00004600       COMMON/MASSB/STOR,TOTV1,TOTV2,FLUX10,FLUX20
00004610       COMMON/DEVICE/IRD,IPRT,IFILE
00004620       COMMON/INFO/NUMNP,NUMEL,NPM1,NPM2,NUMEL2,AM1,ISPACE,ITOL,
00004630      *             DEPTH,ENDTIM,DT,DTMAX,ALPHA,PSIBOT,H,NZOUT,
00004640      *             PSINIT,NCPTS,ERRMAX,MAXIT,CHPARM,MAXNT,ISTEDY
00004650       COMMON/ERRORS/IERR,IWARN
00004660 C
00004670       DIMENSION STIFF(3,1),STARK(1),C(1),OLDC(1),DZN(1),DZ(1),BETA(1),
00004680      *     RK(1)
00004690 C
00004700       IF(ISPACE.EQ.1) GOTO 20
00004710 C
00004720 C     LOOP OVER MIDDLE NODES
00004730 C
00004740       IDZ=0
00004750       DO 10 I=1,NPM2
00004760       L=I
00004770       LP1=L+1
00004780       N=I+1
00004790       ADZINV=ALPHA/DZN(I)
00004800 C
00004810       STIFF(1,I)=-ADZINV*STARK(L)/DZ(L)
00004820       STIFF(2,I)=ADZINV*(STARK(L)/DZ(L)+STARK(LP1)/DZ(LP1))+
00004830      *           (ALPHA*C(N)+AM1*OLDC(N))/DT
00004840       STIFF(3,I)=-ADZINV*STARK(LP1)/DZ(LP1)
00004850    10 CONTINUE
00004860       GOTO 50
00004870 C
00004880 C      VARIABLE SPACING ALGORITHM
00004890 C
00004900    20 DO 40 I=1,NPM2
00004910       L=I
```

```
00004920       LP1=L+1
00004930       N=I+1
00004940       B1=BETA(I)
00004950       ADZINV=ALPHA/DZN(I)
00004960       IF(B1.EQ.1.D0) GOTO 30
00004970 C
00004980       B2=1.D0/B1
00004990       NM1=N-1
00005000       NP1=N+1
00005010       DZN2=DZ(L)+DZ(LP1)
00005020       STIFF(1,I)=-ADZINV*(B1*STARK(L)/DZ(L)+(B2-B1)*RK(N)/DZN2)
00005030       STIFF(2,I)=ADZINV*(B1*STARK(L)/DZ(L)+B2*STARK(LP1)/DZ(LP1))+
00005040      *              (ALPHA*C(N)+AM1*OLDC(N))/DT
00005050       STIFF(3,I)=-ADZINV*(B2*STARK(LP1)/DZ(LP1)+(B1-B2)*RK(N)/DZN2)
00005060       GOTO 40
00005070 C
00005080 C
00005090 C       CONSTANT SPACING FOR THIS NODE
00005100    30 STIFF(1,I)=-ADZINV*STARK(L)/DZ(L)
00005110       STIFF(2,I)=ADZINV*(STARK(L)/DZ(L)+STARK(LP1)/DZ(LP1))+
00005120      *              (ALPHA*C(N)+AM1*OLDC(N))/DT
00005130       STIFF(3,I)=-ADZINV*STARK(LP1)/DZ(LP1)
00005140    40 CONTINUE
00005150    50 CONTINUE
00005160 CBUG  CALL DUMP1('S BUILDS',STIFF,NPM2*3)
00005170   999 RETURN
00005180       END
00005190 C
00005200 C*****************************************************************
00005210 C
00005220       SUBROUTINE BUILDF(F,C,OLDC,PSI,PSIOLD,VNEW,VOLD)
00005230 C
00005240 C*****************************************************************
00005250 C
00005260 C.... BUILD FORCING VECTOR WITH BOUNDARY CONDITIONS AND TRANSIENTS
00005270 C
00005280       COMMON/MASSB/STOR,TOTV1,TOTV2,FLUX10,FLUX20
00005290       COMMON/DEVICE/IRD,IPRT,IFILE
00005300       COMMON/INFO/NUMNP,NUMEL,NPM1,NPM2,NUMEL2,AM1,ISPACE,ITOL,
00005310      *             DEPTH,ENDTIM,DT,DTMAX,ALPHA,PSIBOT,H,NZOUT,
00005320      *             PSINIT,NCPTS,ERRMAX,MAXIT,CHPARM,MAXNT,ISTEDY
00005330       COMMON/ERRORS/IERR,IWARN
00005340       DIMENSION F(1),C(1),PSI(1),PSIOLD(1)
00005350       DIMENSION VNEW(1),VOLD(1),OLDC(1)
00005360 C
00005370       DO 10 I=1,NPM2
00005380       N=I+1
00005390       F(I)=ALPHA*VNEW(I) + AM1*VOLD(I) -
00005400      *        (PSI(N)-PSIOLD(N))*(ALPHA*C(N)+
00005410      *         AM1*OLDC(N))/DT
00005420    10 CONTINUE
00005430 CBUG  CALL DUMP1('F BUILDF',F,NPM2)
00005440       RETURN
00005450       END
00005460 C
00005470 C*****************************************************************
00005480 C
00005490       SUBROUTINE NEWTIM(RNEW,OLD,KODE)
00005500 C
00005510 C*****************************************************************
00005520 C
00005530 C.... COMPUTE NEW TIME STEP BASED ON CHANGE DURING PREVIOUS STEP
```

```
00005540 C
00005550       COMMON/DEVICE/IRD,IPRT,IFILE
00005560       COMMON/TIMES/TIME,TIME1,NT,ERR,NOUT,TOUT(10),NOUT1,TOUT1
00005570       COMMON/INFO/NUMNP,NUMEL,NPM1,NPM2,NUMEL2,AM1,ISPACE,ITOL,
00005580      *             DEPTH,ENDTIM,DT,DTMAX,ALPHA,PSIBOT,H,NZOUT,
00005590      *             PSINIT,NCPTS,ERRMAX,MAXIT,CHPARM,MAXNT,ISTEDY
00005600       COMMON/ERRORS/IERR,IWARN
00005610       DIMENSION RNEW(1),OLD(1)
00005620 C
00005630 C      FIND LARGEST ABSOLUTE CHANGE
00005640 C
00005650       CHMAX=0.D0
00005660       DO 10 I=2,NUMEL
00005662 CDP    CHANGE NEXT CARD FOR DOUBLE/SINGLE PRECISION
00005670       CHANGE=ABS(RNEW(I)-OLD(I))
00005680       IF(CHANGE.GT.CHMAX) CHMAX=CHANGE
00005690    10 CONTINUE
00005700 C
00005710 C      COMPUTE NEW TIME STEP AS OLD TIME STEP TIMES RATIO OF
00005720 C       CHANGE ALLOWED TO CHANGE AT LAST STEP
00005730 C
00005740       DT=DT*CHPARM/CHMAX
00005750       IF(DT.GT.DTMAX) DT=DTMAX
00005760       IF(NOUT.LE.0) GOTO 20
00005770       TIM=TIME1+DT
00005780       IF(TIM.LT.TOUT1) GOTO 20
00005790       DT=TOUT1-TIME1
00005800       KODE=1
00005810    20 TIM=TIME1+DT
00005820       IF(TIM.GT.ENDTIM) DT=ENDTIM-TIME1
00005830 C
00005840       RETURN
00005850       END
00005860 C
00005870 C*******************************************************************************
00005880 C
00005890       SUBROUTINE INPUT(PSI,RMCURV,RKCURV,PSICRV,SATK,POR,ISOIL,
00005900      *                 DZ,BETA,DZN,Z,PSICRT,IZOUT)
00005910 C
00005920 C*******************************************************************************
00005930 C
00005940 C.... READ PROBLEM PARAMETERS, SOLUTION SPECIFICATION, GRID DATA, SOIL
00005950 C      PROPERTIES, AND INITIAL CONDITIONS, AS REQUIRED
00005960 C
00005970       DIMENSION TITLE(18)
00005980       DIMENSION PSI(1),RMCURV(1),RKCURV(1),PSICRV(1),SATK(1),
00005990      *          POR(1),ISOIL(1),DZ(1),BETA(1),DZN(1),Z(1),PSICRT(1),
00006000      *          IZOUT(1)
00006010       COMMON/MASSB/STOR,TOTV1,TOTV2,FLUX10,FLUX20
00006020       COMMON/TIMES/TIME,TIME1,NT,ERR,NOUT,TOUT(10),NOUT1,TOUT1
00006030       COMMON/DEVICE/IRD,IPRT,IFILE
00006040       COMMON/INFO/NUMNP,NUMEL,NPM1,NPM2,NUMEL2,AM1,ISPACE,ITOL,
00006050      *             DEPTH,ENDTIM,DT,DTMAX,ALPHA,PSIBOT,H,NZOUT,
00006060      *             PSINIT,NCPTS,ERRMAX,MAXIT,CHPARM,MAXNT,ISTEDY
00006070       COMMON/ERRORS/IERR,IWARN
00006080       COMMON/FILES/IFGRD,IFSOIL,IFINIT,IFPOUT,IFMOUT,IFSOUT,IFLUX,IFZOUT
00006090 C
00006100       TIME=0.D0
00006110       TIME1=0.D0
00006120       NT=0
00006130 CDAN    USE ITOL=0
00006140       ITOL=0
```

```
00006150 C
00006160       READ(IRD,1001) TITLE
00006170       WRITE(IPRT,2001) TITLE
00006180 C
00006190       READ(IRD,1002) IFGRD,IFSOIL,IFINIT,IFILE,IFPOUT,IFMOUT,IFSOUT,
00006200      *                IFLUX,IFZOUT
00006210       IF(IFGRD.LE.0) IFGRD=IRD
00006220       IF(IFSOIL.LE.0) IFSOIL=IRD
00006230       IF(IFINIT.LE.0) IFINIT=IRD
00006240       IF(IFILE.LE.0) IFILE=10
00006250       WRITE(IPRT,2002) IFGRD,IFSOIL,IFINIT,IFILE,IFPOUT,IFMOUT,IFSOUT,
00006260      *                IFLUX,IFZOUT
00006270 C
00006280 C      TEMPORAL CONTROL PARAMETERS
00006290 C
00006300       READ(IRD,1003) INITAL,ISTEDY,ENDTIM,DT,DTMAX,MAXNT,ALPHA,ERRMAX,
00006310      *     MAXIT,CHPARM
00006320       IF(DT.LE.0.D0) DT=1.D0
00006330       IF(ERRMAX.LE.0.D0) ERRMAX=0.05D0
00006340       IF(MAXIT.LE.0) MAXIT=3
00006350       AM1=1.D0-ALPHA
00006360       WRITE(IPRT,2000) INITAL,ISTEDY,ENDTIM,DT,DTMAX,MAXNT,ALPHA,
00006370      *                 ERRMAX,MAXIT,CHPARM
00006380 C
00006390 C      SPECIAL OUTPUT TIMES
00006400 C
00006410       READ(IRD,1010) NOUT
00006420       WRITE(IPRT,2010) NOUT
00006430       IF(NOUT.LE.0) GOTO 19
00006440 C
00006450 C      READ SPECIAL OUTPUT TIMES
00006460       IF(NOUT.GT.10) NOUT=10
00006470       READ(IRD,1050) (TOUT(IT),IT=1,NOUT)
00006480       WRITE(IPRT,2060) (TOUT(IT),IT=1,NOUT)
00006490       DO 18 IT=1,NOUT
00006500       NOUT1=IT
00006510       IF(TOUT(IT).GT.DT) GOTO 17
00006520    18 CONTINUE
00006530    17 TOUT1=TOUT(NOUT1)
00006540 C
00006550 C      SPATIAL CONTROL PARAMETERS
00006560    19 READ(IRD,1010) NUMNP,IREGLR,ISPACE
00006570       NPM2=NUMNP-2
00006580       NPM1=NUMNP-1
00006590       NUMEL=NUMNP-1
00006600       NUMEL2=2*NUMEL
00006610       WRITE(IPRT,2004) NUMNP,NUMEL,IREGLR,ISPACE
00006620 C
00006630 C      READ SPATIAL OUTPUT PARMS
00006640 C
00006650       READ(IRD,1030) NZOUT
00006660       WRITE(IPRT,2006) NZOUT
00006670       IF(NZOUT.LE.0) GOTO 96
00006680       READ(IRD,1006) (IZOUT(IZ),IZ=1,NZOUT)
00006690       WRITE(IPRT,2007) (IZOUT(IZ),IZ=1,NZOUT)
00006700    96 CONTINUE
00006710 C
00006720 C      READ GRID DATA
00006730 C
00006740       IF(IREGLR.EQ.1) GOTO 12
00006750 C      READ NODE POINT COORDINATES  Z
00006760       DO 10 I=1,NUMNP
```

```
00006770        READ(IFGRD,1061) IN,Z(I)
00006780     10 CONTINUE
00006790        GOTO 47
00006800 C       REGULAR SPACING
00006810     12 NL=0
00006820        IN2=1
00006822        ZZ=0.D0
00006830        Z(IN2)=ZZ
00006840 C
00006850     13 READ(IFGRD,1061) NLZ,THICK
00006860        NL=NL+NLZ
00006870        DZZ=THICK/FLOAT(NLZ)
00006880        IN1=IN2+1
00006890        IN2=IN1+NLZ-1
00006900        DO 14 IN=IN1,IN2
00006910        ZZ=ZZ-DZZ
00006920        Z(IN)=ZZ
00006930     14 CONTINUE
00006940        IF(IN2.LT.NUMNP) GOTO 13
00006950 C
00006960 C       COMPUTE SPATIAL DIFFERENCE TERMS
00006970 C       OVER ELEMENTS
00006980     47 DO 48 L=1,NUMEL
00006990        DZ(L)=Z(L+1)-Z(L)
00007000     48 CONTINUE
00007010 C       OVER INTERIOR NODES ONLY
00007020        DO 49 I=1,NPM2
00007030        N=I+1
00007040        NM1=N-1
00007050        NP1=N+1
00007060        DZN(I)=(Z(NP1)-Z(NM1))/2.D0
00007070        L=I
00007080        LP1=L+1
00007090        BETA(I)=DZ(LP1)/DZ(L)
00007100     49 CONTINUE
00007110 C
00007120 C
00007130 C       PRINT GRID DATA
00007140        WRITE(IPRT,2091)
00007150        I=1
00007160        WRITE(IPRT,2069) I,Z(1)
00007170        WRITE(IPRT,2071) I,DZ(1)
00007180 C
00007190        DO 69 I=2,NPM1
00007200        WRITE(IPRT,2069) I,Z(I),DZN(I-1),BETA(I-1)
00007210        WRITE(IPRT,2071) I,DZ(I)
00007220     69 CONTINUE
00007230        WRITE(IPRT,2069) NUMNP,Z(NUMNP)
00007240 C
00007250 C
00007260 C       READ SOIL SPECIFICATIONS
00007270 C         ELEMENT NUMBER, SOIL CURVE TYPE, AND REFERENCE VALUES
00007280        WRITE(IPRT,2092)
00007290        DO 68 I=1,NUMEL
00007300        READ(IFSOIL,1070) IN,ISOIL(I),SATK(I),POR(I),PSICRT(I)
00007310        WRITE(IPRT,2070) IN,ISOIL(I),SATK(I),POR(I),PSICRT(I)
00007320     68 CONTINUE
00007330 C
00007340 C       READ INITIAL CONDITION
00007350        IF(INITAL.EQ.1) GOTO 53
00007360 C       CONSTANT INITIAL CONDITION
00007370        READ(IFINIT,1081) PSINIT
```

```
00007380       WRITE(IPRT,2080) PSINIT
00007390       DO 52 I=1,NUMNP
00007400       PSI(I)=PSINIT
00007410    52 CONTINUE
00007420       GOTO 55
00007430 C      VARIABLE INITIAL CONDITION
00007440    53 DO 54 I=1,NUMNP
00007450       READ(IFINIT,1061) IN,PSI(I)
00007460    54 CONTINUE
00007470       WRITE(IPRT,2090) (PSI(I),I=1,NUMNP)
00007480 C
00007490 C      SET PRESSURE BOUNDARY CONDITIONS
00007500 C
00007510    55 CALL NEWBC(PSI)
00007520 C
00007530   999 RETURN
00007540 C
00007550  1001 FORMAT(18A4)
00007560  1002 FORMAT(9I5)
00007570  1003 FORMAT(2I5,3F10.0,I5,2F10.0,I5,F10.0)
00007580  1006 FORMAT(16I5)
00007590  1010 FORMAT(3I5)
00007600  1030 FORMAT(I5)
00007610  1040 FORMAT(3F10.0)
00007620  1050 FORMAT(8F10.0)
00007630  1061 FORMAT(I5,F10.0)
00007640  1070 FORMAT(2I5,3F10.0)
00007650  1080 FORMAT(I10,F10.0)
00007660  1081 FORMAT(F10.0)
00007670 C
00007680  2000 FORMAT(//' TEMPORAL DISCRETIZATION PARAMETERS'//
00007690      *' INITIAL CONDITION PARM',10(1H.),'INITAL=',I10/
00007700      *'   IF INITAL EQ 1, READ INITIAL PSI FOR EACH NODE'/
00007710      *'   OTHERWISE, READ CONSTANT INITIAL PSI'/
00007720      *' STEADY STATE PARM',12(1H.),'ISTEDY=',I10/
00007730      *'   IF ISTEDY EQ 1, COMPUTE STEADY STATE SOLUTION'/
00007740      *'   OTHERWISE, COMPUTE TRANSIENT ONLY'/
00007750      *' SIMULATION TIME',19(1H.),'ENDTIM=',F10.2/
00007760      *' TIME STEP',30(1H.),'DT=',F10.3/
00007770      *' MAXIMUM ALLOWABLE TIME STEP',10(1H.),'DTMAX=',F10.2/
00007780      *' MAXIMUM NUMBER OF TIME STEPS',12(1H.),'MAXNT=',I10/
00007790      *' TIME INTEGRATION PARAMETER',10(1H.),'ALPHA=',F10.2/
00007800      *' MAXIMUM ERROR FOR CONVERGENCE',7(1H.),'ERRMAX=',F10.4/
00007810      *' MAXIMUM ITERATIONS',20(1H.),'MAXIT=',I10/
00007820      *' TIME STEP CHANGE PARAMETER',15(1H.),'CHPARM=',F10.4)
00007830  2001 FORMAT(//1X,72(1H*)//' SOILINER OUTPUT'//
00007840      *1X,72(1H*)//1X,18A4//1X,72(1H*))
00007850  2002 FORMAT(' FILE NUMBERS'//
00007860      *' GRID INPUT',10(1H.),'IFGRD=',I10/
00007870      *' SOIL PROPERTIES',8(1H.),'IFSOIL=',I10/
00007880      *' INITIAL CONDITIONS',7(1H.),'IFINIT=',I10/
00007890      *' DUMP FILE',10(1H.),'IFILE=',I10/
00007900      *' PSI OUTPUT',9(1H.),'IFPOUT=',I10/
00007910      *' MOIST OUTPUT',7(1H.),'IFMOUT=',I10/
00007920      *' SOIL PROP OUTPUT',6(1H.),'IFSOUT=',I10/
00007930      *' FLUX OUTPUT',10(1H.),'IFLUX=',I10/
00007940      *' ZOJT OUTPUT',10(1H.),'IZOUT=',I10)
00007950  2004 FORMAT(//' SPATIAL DISCRETIZATION PARAMATERS'//
00007960      *' NUMBER OF NODE POINTS',10(1H.),'NUMNP=',I10/
00007970      *' NUMBER OF ELEMENTS (COMPUTED)',8(1H.),'NUMEL=',I10/
00007980      *' GRADATION PARAMETER',12(1H.),'IREGLR=',I10/
00007990      *'   IF IREGLR EQ 1, READ NO. ELEMENTS AND THICKNESS FOR LAYERS'/
```

```
00008000      *'   OTHERWISE, READ NODE POINT COORDINATES'/
00008010      *' WEIGHTED DIFFERENCE OPTION',12(1H.),'ISPACE=',I10/
00008020      *'   IF ISPACE EQ 1, USE SPECIAL DIFFERENCE ALGORITHM'/
00008030      *'   OTHERWISE, USE STANDARD FINITE DIFFERENCE')
00008040  2006 FORMAT(/' NUMBER OF SPECIAL OUTPUT NODES',10(1H.),'NZOUT=',I10)
00008050  2007 FORMAT(//' SPECIAL OUTPUT NODES'//
00008060     *1X,10I10)
00008070  2010 FORMAT(/' NUMBER OF SPECIAL OUTPUT TIMES',10(1H.),'NOUT=',I10)
00008080  2080 FORMAT(/' CONSTANT INITIAL PRESSURE',4(1H.),'PSINIT=',F10.3)
00008090  2025 FORMAT(//1X,10(1H=)/' SATURATED CONDUCTIVITY',10(1H.),'SATK=',
00008100     *1PE10.3/1X,20(1H=)//
00008110      *' CRITICAL POTENTIAL',10(1H.),'PSICRT=',1PE10.3/1X,18(1H=))
00008120  2030 FORMAT(//1X,30(1H=)/' MOISTURE RETENTION AND CONDUCTIVITY CURVES'/
00008130     *1X,30(1H=)//
00008140      *' NUMBER OF POINTS ON CURVE',15(1H.),'NCPTS=',I10//
00008150      *'      SUCTION       MOISTURE    RELATIVE CONDUCTIVITY'/
00008160      *'        (L)            (-)             (-)'/)
00008170  2040 FORMAT(3F13.3)
00008180  2050 FORMAT(//' DATA FROM INPUT CURVES'//
00008190      *' CRITICAL SUCTION PRESSURE',13(1H.),'PSICRT=',F10.3/
00008200      *' EFFECTIVE POROSITY',22(1H.),'POR=',F10.4)
00008210  2060 FORMAT(//' SPECIAL OUTPUT TIMES'//
00008220     *1X,1P10E12.3)
00008230  2069 FORMAT(I10,3F10.3)
00008240  2070 FORMAT(2I10,1PE10.3,0PF10.4,0PF10.3)
00008250  2071 FORMAT(I5,F10.3)
00008260  2090 FORMAT(//' VARIABLE INITIAL PSI'/30(8F10.0/))
00008270  2091 FORMAT(//' GRID DATA'//
00008280      *' ELMENT NODE    Z      DZ         DZN          BETA'/)
00008290  2092 FORMAT(//' SOIL PROPERTIES'//
00008300      *'   ELEMENT     SATK     POR      PSICRT'/)
00008310       END
00008320  C
00008330  C
00008340  C*****************************************************************
00008350  C
00008360       SUBROUTINE OUTPUT(PSI,RMOIST,RK,Z,RKL,CL,RMSTL,STARK,POR,DZ,ITER)
00008370  C
00008380  C*****************************************************************
00008390  C
00008400  C.... PRINT REQUESTED INFORMATION
00008410  C
00008420       COMMON/DEVICE/IRD,IPRT,IFILE
00008430       COMMON/TIMES/TIME,TIME1,NT,ERR,NOUT,TOUT(10),NOUT1,TOUT1
00008440       COMMON/INFO/NUMNP,NUMEL,NPM1,NPM2,NUMEL2,AM1,ISPACE,ITOL,
00008450      *            DEPTH,ENDTIM,DT,DTMAX,ALPHA,PSIBOT,H,NZOUT,
00008460      *            PSINIT,NCPTS,ERRMAX,MAXIT,CHPARM,MAXNT,ISTEDY
00008470       COMMON/ERRORS/IERR,IWARN
00008480       COMMON/FILES/IFGRD,IFSOIL,IFINIT,IFPOUT,IFMOUT,IFSOUT,IFLUX,IFZOUT
00008490       DIMENSION PSI(1),RMOIST(1),RK(1),Z(1),RKL(1),CL(1),RMSTL(1),
00008500      *          STARK(1),POR(1),DZ(1)
00008510  C
00008520       WRITE(IPRT,2000) TIME,NT,DT,ERR,ITER
00008530       WRITE(IPRT,2010) (I,PSI(I),RMOIST(I),RK(I),I=1,NUMNP)
00008540  C
00008550       IF(IFPOUT.LE.0) GOTO 5
00008560       DO 4 I=1,NUMNP
00008570       PF=0.D0
00008580  CDP   CHANGE NEXT CARD FOR DOUBLE/SINGLE PRECISION
00008590       IF(PSI(I).LT.0.D0) PF=ALOG10(-PSI(I))
00008600       WRITE(IFPOUT,2040) I,Z(I),PSI(I),PF
00008610     4 CONTINUE
```

```
00008620 C
00008630      5 IF(IFMOUT.LE.0) GOTO 20
00008640        IN=0
00008650        IP=1
00008660        DO 10 L=1,NUMEL
00008670        IN=IN+1
00008680        WRITE(IFMOUT,2030) L,Z(IP),RMSTL(IN)
00008690        IN=IN+1
00008700        IP=IP+1
00008710        WRITE(IFMOUT,2030) L,Z(IP),RMSTL(IN)
00008720     10 CONTINUE
00008730 C
00008740     20 IF(IFSOUT.LE.0) GOTO 35
00008750        IN=0
00008760        IP=1
00008770        DO 30 L=1,NUMEL
00008780        IN=IN+1
00008790        RKLOG=0.D0
00008800        CLOG=0.D0
00008810 CDP    CHANGE NEXT TWO CARDS FOR DOUBLE/SINGLE PRECISION
00008820        IF(RKL(IN).GT.0.D0) RKLOG=ALOG10(RKL(IN))
00008830        IF(CL(IN).GT.0.D0) CLOG=ALOG10(CL(IN))
00008840        WRITE(IFSOUT,2040) IN,Z(IP),RKL(IN),RKLOG,CL(IN),CLOG
00008850        IN=IN+1
00008860        IP=IP+1
00008870        RKLOG=0.D0
00008880        CLOG=0.DC
00008890 CDP    CHANGE NEXT TWO CARDS FOR DOUBLE/SINGLE PRECISION
00008900        IF(RKL(IN).GT.0.D0) RKLOG=ALOG10(RKL(IN))
00008910        IF(CL(IN).GT.0.D0) CLOG=ALOG10(CL(IN))
00008920        WRITE(IFSOUT,2040) IN,Z(IP),RKL(IN),RKLOG,CL(IN),CLOG
00008930     30 CONTINUE
00008940 C
00008950     35 IF(IFLUX.LE.0) GOTO 999
00008960        N1=0
00008970        N2=1
00008980        DO 40 L=1,NUMEL
00008990        N1=N1+1
00009000        N2=N2+1
00009010        FLUX=-STARK(L)*(1.D0+(PSI(N2)-PSI(N1))/DZ(L))
00009020        VEL=FLUX/POR(L)
00009030        ZZ=(Z(N1)+Z(N2))/2.D0
00009040        WRITE(IFLUX,2040) L,ZZ,FLUX,VEL
00009050     40 CONTINUE
00009060 C
00009070    999 RETURN
00009080 C
00009090   2000 FORMAT(//1X,71(1H*)//' TIME=',1PE12.3,'  TIME STEP=',I5,'  DT=',
00009100       *1PE12.3,'  ERR=',1PE12.3//' ITER=',I5,
00009110       *//1X,71(1H*)//
00009120       *'  NODE       POTENTIAL         MOISTURE                K'/)
00009130   2010 FORMAT(I6,4X,1PE13.4,4X,0PF12.4,4X,1PE13.4)
00009140   2020 FORMAT(I10,F10.3,F10.4)
00009150   2030 FORMAT(I10,F10.3,F10.7)
00009160   2040 FORMAT(I10,0PF10.2,2(1PE10.2,0PF10.3))
00009170        END
00009180 C
00009190 C*************************************************************************
00009200 C
00009210        SUBROUTINE ERROR(A,N,ERRM,ITOL)
00009220 C
00009230 C*************************************************************************
```

```
00009240 C
00009250 C.... COMPUTE ERROR  ITOL - 0  MAXIMUM ABSOLUTE
00009260 C                    ITOL - 1  RMS
00009270 C
00009280       DIMENSION A(1)
00009290       IF(ITOL.EQ.1) GOTO 20
00009300       ERRM=0.D0
00009310       DO 10 I=1,N
00009320       AERR=ABS(A(I))
00009330       IF(AERR.GT.ERRM) ERRM=AERR
00009340    10 CONTINUE
00009350       RETURN
00009360 C
00009370    20 SUM=0.D0
00009380       DO 30 I=1,N
00009390       SUM=SUM+A(I)*A(I)
00009400    30 CONTINUE
00009410       ERRM=SQRT(SUM/FLOAT(N))
00009420       RETURN
00009430       END
00009440 C
00009450 C*************************************************************************
00009460 C
00009470       SUBROUTINE THOMAS(A,B,C,W,N,IND)
00009480 C
00009490 C*************************************************************
00009500 C
00009510 C.... SOLVE TRIDIAGONAL MATRIX EQUATION,  SEE, FOR EXAMPLE,
00009520 C     PINDER AND GRAY 'FINITE ELEMENT SIMULATION IN
00009530 C     SURFACE AND SUBSURFACE HYDROLOGY', ACADEMIC PRESS 1977.
00009540 C
00009550       DIMENSION A(3,1),B(1),C(1),W(1)
00009560       IF(IND.EQ.2) GOTO 20
00009570 C
00009580 C     REDUCTION   REQUIRED IF STIFFNESS IS CHANGING
00009590 C
00009600       W(1)=A(2,1)
00009610       DO 10 I=2,N
00009620       IM1=I-1
00009630       W(I)=A(2,I)-A(1,I)*A(3,IM1)/W(IM1)
00009640    10 CONTINUE
00009650       IF(IND.EQ.1) RETURN
00009660 C
00009670 C     SUBSTITUTION
00009680 C
00009690    20 C(1)=B(1)
00009700       DO 30 I=2,N
00009710       IM1=I-1
00009720       C(I)=B(I)-A(1,I)*C(IM1)/W(IM1)
00009730    30 CONTINUE
00009740       C(N)=C(N)/W(N)
00009750       DO 40 I=2,N
00009760       M=N-I+1
00009770       MP1=M+1
00009780       C(M)=(C(M)-A(3,M)*C(MP1))/W(M)
00009790    40 CONTINUE
00009800 CBUG  CALL DUMP1(' STIFF T',A,N*3)
00009810 CBUG  CALL DUMP1(' F      T',B,N)
00009820 CBUG  CALL DUMP1(' DPSI   T',C,N)
00009830       RETURN
00009840       END
00009850 C
```

```
00009860 C*****************************************************************
00009870 C
00009880       SUBROUTINE MASBAL(PSI,RMSTL,OLDML,STARK,DZ,IOUT)
00009890 C
00009900 C*****************************************************************
00009910 C
00009920 C.... COMPUTE AND PRINT MASS BALANCE OF FLOW CALCULATIONS
00009930 C
00009940       COMMON/MASSB/STOR,TOTV1,TOTV2,FLUX10,FLUX20
00009950       COMMON/TIMES/TIME,TIME1,NT,ERR,NOUT,TOUT(10),NOUT1,TOUT1
00009960       COMMON/DEVICE/IRD,IPRT,IFILE
00009970       COMMON/INFO/NUMNP,NUMEL,NPM1,NPM2,NUMEL2,AM1,ISPACE,ITOL,
00009980      *            DEPTH,ENDTIM,DT,DTMAX,ALPHA,PSIBOT,H,NZOUT,
00009990      *            PSINIT,NCPTS,ERRMAX,MAXIT,CHPARM,MAXNT,ISTEDY
00010000       COMMON/ERRORS/IERR,IWARN
00010010       DIMENSION PSI(1),RMSTL(1),STARK(1),OLDML(1),DZ(1)
00010020 C
00010030       IF(IOUT.NE.-1) GOTO 5
00010040 C
00010050 C      INITIALIZE TERMS
00010060 C
00010070       TOTV1=0.D0
00010080       TOTV2=0.D0
00010090       STOR=0.D0
00010100       FLUX10=STARK(1)*(1.D0+(PSI(2)-PSI(1))/DZ(1))
00010110       IF(DZ(1).GT.0.D0) FLUX10=-FLUX10
00010120       FLUX20=STARK(NUMEL)*(1.D0+(PSI(NUMNP)-PSI(NUMEL))/DZ(NUMEL))
00010130       IF(DZ(NUMEL).LT.0.D0) FLUX20=-FLUX20
00010140       RETURN
00010150 C
00010160 C       TOP FLUX
00010170     5 FLUX1=STARK(1)*(1.D0+(PSI(2)-PSI(1))/DZ(1))
00010180       IF(DZ(1).GT.0.D0) FLUX1=-FLUX1
00010190       VOL1=(FLUX1*ALPHA+FLUX10*AM1)*DT
00010200       FLUX10=FLUX1
00010210       TOTV1=TOTV1+VOL1
00010220 C
00010230 C       BOTTOM FLUX
00010240       FLUX2=STARK(NUMEL)*(1.D0+(PSI(NUMNP)-PSI(NUMEL))/DZ(NUMEL))
00010250       IF(DZ(NUMEL).LT.0.D0) FLUX2=-FLUX2
00010260       VOL2=(FLUX2*ALPHA+AM1*FLUX20)*DT
00010270       FLUX20=FLUX2
00010280       TOTV2=TOTV2+VOL2
00010290 C
00010300 C       CHANGE IN STORAGE
00010310 C      COMPUTE STORAGE ON ELEMENTS ASSUMING LINEAR VARIATION
00010320 C
00010330       IN2=0
00010340       DSTOR=0.D0
00010350       DO 10 L=1,NUMEL
00010360 CDP    CHANGE NEXT CARD FOR DOUBLE/SINGLE PRECISION
00010370       DELZ=ABS(DZ(L))
00010380       IN1=IN2+1
00010390       IN2=IN1+1
00010400       DSTOR=DSTOR+(RMSTL(IN1)-OLDML(IN1)+RMSTL(IN2)-OLDML(IN2))*DELZ/
00010410      *      2.D0
00010420    10 CONTINUE
00010430       STOR=STOR+DSTOR
00010440       IF(IOUT.NE.1) RETURN
00010450       RATEST=DSTOR/DT
00010460 C
00010470 C       COMPUTE FLUX AND VOLUME ERRORS
```

```
00010480 C
00010490 CDP    CHANGE NEXT THREE CARDS FOR DOUBLE/SINGLE PRECISION
00010500       EFLUX=ABS(-FLUX1+FLUX2+RATEST)
00010510       EVOL=ABS(DSTOR-VOL1+VOL2)
00010520       ETOT=ABS(STOR-TOTV1+TOTV2)
00010530       EREL=ETOT/STOR
00010540 C
00010550       WRITE(IPRT,2020) FLUX1,FLUX2,RATEST,EFLUX,VOL1,VOL2,
00010560      *                 DSTOR,EVOL,TOTV1,TOTV2,STOR,ETOT,EREL
00010570 C
00010580       RETURN
00010590 C
00010600  2020 FORMAT(///' VOLUME BALANCE CALCULATIONS'//
00010610      *' TOP FLUX   ',1PE12.4/
00010620      *' BOTTOM FLUX',1PE12.4/
00010630      *' STORAGE RATE',1PE12.4/
00010640      *20X,12(1H-)/
00010650      *' ERROR             ',1PE12.4///
00010660      *' VOLUME IN         ',1PE12.4/
00010670      *' VOLUME OUT        ',1PE12.4/
00010680      *' STORAGE VOLUME    ',1PE12.4/
00010690      *20X,12(1H-)/
00010700      *' ERROR             ',1PE12.4///
00010710      *' CUMULATIVE CHANGES'//
00010720      *' VOLUME IN (-)     ',1PE12.4/
00010730      *' VOLUME OUT        ',1PE12.4/
00010740      *' STORAGE           ',1PE12.4/
00010750      *20X,12(1H-)/
00010760      *' ERROR             ',1PE12.4//
00010770      *' RELATIVE ERROR    ',0PF12.6)
00010780       END
00010790 C
00010800 C*********************************************************************
00010810       SUBROUTINE NEWBC(PSI)
00010820 C*********************************************************************
00010830 C
00010840 C....  READ AND CHANGE PRESSURE BOUNDARY CONDITIONS
00010850 C
00010860       DIMENSION PSI(1)
00010870       COMMON/INFO/NUMNP,NUMEL,NPM1,NPM2,NUMEL2,AM1,ISPACE,ITOL,
00010880      *            DEPTH,ENDTIM,DT,DTMAX,ALPHA,PSIBOT,H,NZOUT,
00010890      *            PSINIT,NCPTS,ERRMAX,MAXIT,CHPARM,MAXNT,ISTEDY
00010900       COMMON/DEVICE/IRD,IPRT,IFILE
00010910    19 READ(IRD,1020) H,PSIBOT
00010920       WRITE(IPRT,2020) H,PSIBOT
00010930 C      APPLY PRESSURE BOUNDARY CONDITIONS
00010940       PSI(1)=H
00010950       PSI(NUMNP)=PSIBOT
00010960       RETURN
00010970  1020 FORMAT(3F10.0)
00010980  2020 FORMAT(///1X,30(1H=)/' BOUNDARY AND INITIAL CONDITIONS'/1X,30(1H=)//
00010990      */' HEAD IN IMPOUNDMENT',20(1H.),'H=',F10.2/
00011000      *' UNDERLYING SOIL SUCTION PRESSURE',5(1H.),'PSIBOT=',F10.3)
00011010       END
00011020 C
00011030 C*********************************************************************
00011040       SUBROUTINE VSCALE(A,B,N,C)
00011050 C*********************************************************************
00011060 C.... MULTIPLY VECTOR A BY SCALAR B AND RETURN IN C
00011070       DIMENSION A(1),C(1)
00011080       IF(N.LE.0) RETURN
00011090       DO 10 I=1,N
```

```
00011100       C(I)=A(I)*B
00011110    10 CONTINUE
00011120       RETURN
00011130       END
00011140 C*************************************************************
00011150       SUBROUTINE CLEAR(A,N)
00011160 C*************************************************************
00011170 C.... FILL A WITH ZEROS
00011180       DIMENSION A(1)
00011190       IF(N.LE.0) RETURN
00011200       DO 10 I=1,N
00011210       A(I)=0.D0
00011220    10 CONTINUE
00011230       RETURN
00011240       END
00011250 C*****************************************************
00011260       SUBROUTINE MADD(VEC,RMATRX,ICOL,N,OUT)
00011270 C*****************************************************
00011280 C.... PROGRAM TO ADD A VECTOR TO A COLUMN OF A MATRIX
00011290       DIMENSION VEC(1),RMATRX(3,1),OUT(1)
00011300       IF(N.LE.0) RETURN
00011310       DO 10 I=1,N
00011320       RMATRX(ICOL,I)=RMATRX(ICOL,I)+VEC(I)
00011330    10 CONTINUE
00011340       RETURN
00011350       END
00011360 C*************************************************************
00011370       SUBROUTINE VECADD(A,B,N,C)
00011380 C*************************************************************
00011390 C.... PROGRAM TO RETURN THE SUM OF A AND B IN C
00011400       DIMENSION A(1),B(1),C(1)
00011410       IF(N.LE.0) RETURN
00011420       DO 10 I=1,N
00011430       C(I)=A(I)+B(I)
00011440    10 CONTINUE
00011450       RETURN
00011460       END
00011470 C*************************************************************
00011480       SUBROUTINE COPY(A,N,B)
00011490 C*************************************************************
00011500 C.... COPY VECTOR A INTO B
00011510       DIMENSION A(1), B(1)
00011520       IF(N.LE.0) RETURN
00011530       DO 10 I=1,N
00011540       B(I) = A(I)
00011550    10 CONTINUE
00011560       RETURN
00011570       END
00011580 C*************************************************************
00011590       SUBROUTINE DUMP1(NAME,ARRAY,N)
00011600 C*************************************************************
00011610 C.... PRINT ARRAY
00011620       COMMON/DEVICE/IRD,IPRT,IFILE
00011630       DIMENSION ARRAY(1),NAME(2)
00011640       WRITE(IFILE,2000) NAME
00011650       IF(N.LE.0) RETURN
00011660       WRITE(IFILE,2010) (ARRAY(I),I=1,N)
00011670       RETURN
00011680  2000 FORMAT(///' DUMPING ARRAY ',2A4,' . . .')
00011690  2010 FORMAT(1P8E10.3)
00011700       END
00011710 C
```

```
00011720 C*****************************************************************
00011730       SUBROUTINE ZOUT(IZOUT,PSI,RMOIST)
00011740 C*****************************************************************
00011750 C
00011760 C.... WRITE PSI AND RMOIST AT SPECIAL NODES EACH TIME STEP
00011770 C
00011780       COMMON/FILES/IFGRD,IFSOIL,IFINIT,IFPOUT,IFMOUT,IFSOUT,IFLUX,IFZOUT
00011790       COMMON/INFO/NUMNP,NUMEL,NPM1,NPM2,NUMEL2,AM1,ISPACE,ITOL,
00011800      *            DEPTH,ENDTIM,DT,DTMAX,ALPHA,PSIBOT,H,NZOUT,
00011810      *            PSINIT,NCPTS,ERRMAX,MAXIT,CHPARM,MAXNT,ISTEDY
00011820       COMMON/TIMES/TIME,TIME1,NT,ERR,NOUT,TOUT(10),NOUT1,TOUT1
00011830       COMMON/ERRORS/IERR,IWARN
00011840       DIMENSION IZOUT(1),PSI(1),RMOIST(1)
00011850       DO 10 I=1,NZOUT
00011860       N=IZOUT(I)
00011870       WRITE(IFZOUT,2000) N,TIME,PSI(N),RMOIST(N)
00011880    10 CONTINUE
00011890       RETURN
00011900  2000 FORMAT(I10,1PE10.3,0PF10.2,0PF10.4)
00011910       END
```

APPENDIX D

EXAMPLE INPUT AND OUTPUT FOR SOILINER MODEL

```
09/30/83   10:04:21   3CAGD.TEST3A.OUTPUT.DATA


*************************************************************************

SOILINER OUTPUT

*************************************************************************

TEST3A  50 1 CM ELEMENTS, 51 NUMNP   YOLO INFILTRATION H=25.

*************************************************************************
FILE NUMBERS

GRID INPUT..........IFGRD=         21
SOIL PROPERTIES.....IFSOIL=          22
INITIAL CONDITIONS..IFINIT=           23
DUMP FILE..........IFILE=        10
PSI OUTPUT.........IFPOUT=         31
MOIST OUTPUT.......IFMOUT=         32
SOIL PROP OUTPUT...IFSOUT=           33
FLUX OUTPUT........IFLUX=          34
ZOUT OUTPUT........IZOUT=           0


TEMPORAL DISCRETIZATION PARAMETERS

INITIAL CONDITION PARM.....INITAL=          0
  IF INITAL EQ 1, READ INITIAL PSI FOR EACH NODE
  OTHERWISE, READ CONSTANT INITIAL PSI
STEADY STATE PARM..........ISTEDY=          0
  IF ISTEDY EQ 1, COMPUTE STEADY STATE SOLUTION
  OTHERWISE, COMPUTE TRANSIENT ONLY
SIMULATION TIME.....................ENDTIM= 200000.00
TIME STEP...........................DT=      0.100
MAXIMUM ALLOWABLE TIME STEP.........DTMAX=   1000.00
MAXIMUM NUMBER OF TIME STEPS........MAXNT=       1000
TIME INTEGRATION PARAMETER..........ALPHA=       0.50
MAXIMUM ERROR FOR CONVERGENCE.......ERRMAX=     0.1000
MAXIMUM ITERATIONS..................MAXIT=         10
TIME STEP CHANGE PARAMETER..........CHPARM=    25.0000

NUMBER OF SPECIAL OUTPUT TIMES.....NOUT=          5


SPECIAL OUTPUT TIMES

   1.000E+03   1.000E+04   4.000E+04   1.000E+05   2.000E+05


SPATIAL DISCRETIZATION PARAMATERS

NUMBER OF NODE POINTS.....NUMNP=         51
NUMBER OF ELEMENTS (COMPUTED).....NUMEL=         50
GRADATION PARAMETER.......IREGLR=          1
  IF IREGLR EQ 1, READ NO. ELEMENTS AND THICKNESS FOR LAYERS
  OTHERWISE, READ NODE POINT COORDINATES
WEIGHTED DIFFERENCE OPTION.......ISPACE=          0
  IF ISPACE EQ 1, USE SPECIAL DIFFERENCE ALGORITHM
  OTHERWISE, USE STANDARD FINITE DIFFERENCE
```

NUMBER OF SPECIAL OUTPUT NODES.....NZOUT=

GRID DATA

ELMENT	NODE	Z	DZ	DZN	BETA
	1	0.0			
1		-1.000			
	2	-1.000	-1.000	1.000	
2		-1.000			
	3	-2.000	-1.000	1.000	
3		-1.000			
	4	-3.000	-1.000	1.000	
4		-1.000			
	5	-4.000	-1.000	1.000	
5		-1.000			
	6	-5.000	-1.000	1.000	
6		-1.000			
	7	-6.000	-1.000	1.000	
7		-1.000			
	8	-7.000	-1.000	1.000	
8		-1.000			
	9	-8.000	-1.000	1.000	
9		-1.000			
	10	-9.000	-1.000	1.000	
10		-1.000			
	11	-10.000	-1.000	1.000	
11		-1.000			
	12	-11.000	-1.000	1.000	
12		-1.000			
	13	-12.000	-1.000	1.000	
13		-1.000			
	14	-13.000	-1.000	1.000	
14		-1.000			
	15	-14.000	-1.000	1.000	
15		-1.000			
	16	-15.000	-1.000	1.000	
16		-1.000			
	17	-16.000	-1.000	1.000	
17		-1.000			
	18	-17.000	-1.000	1.000	
18		-1.000			
	19	-18.000	-1.000	1.000	
19		-1.000			
	20	-19.000	-1.000	1.000	
20		-1.000			
	21	-20.000	-1.000	1.000	
21		-1.000			
	22	-21.000	-1.000	1.000	
22		-1.000			
	23	-22.000	-1.000	1.000	
23		-1.000			
	24	-23.000	-1.000	1.000	
24		-1.000			
	25	-24.000	-1.000	1.000	
25		-1.000			
	26	-25.000	-1.000	1.000	
26		-1.000			
	27	-26.000	-1.000	1.000	
27		-1.000			
	28	-27.000	-1.000	1.000	

28	-1.000			
	29	-28.000	-1.000	1.000
29	-1.000			
	30	-29.000	-1.000	1.000
30	-1.000			
	31	-30.000	-1.000	1.000
31	-1.000			
	32	-31.000	-1.000	1.000
32	-1.000			
	33	-32.000	-1.000	1.000
33	-1.000			
	34	-33.000	-1.000	1.000
34	-1.000			
	35	-34.000	-1.000	1.000
35	-1.000			
	36	-35.000	-1.000	1.000
36	-1.000			
	37	-36.000	-1.000	1.000
37	-1.000			
	38	-37.000	-1.000	1.000
38	-1.000			
	39	-38.000	-1.000	1.000
39	-1.000			
	40	-39.000	-1.000	1.000
40	-1.000			
	41	-40.000	-1.000	1.000
41	-1.000			
	42	-41.000	-1.000	1.000
42	-1.000			
	43	-42.000	-1.000	1.000
43	-1.000			
	44	-43.000	-1.000	1.000
44	-1.000			
	45	-44.000	-1.000	1.000
45	-1.000			
	46	-45.000	-1.000	1.000
46	-1.000			
	47	-46.000	-1.000	1.000
47	-1.000			
	48	-47.000	-1.000	1.000
48	-1.000			
	49	-48.000	-1.000	1.000
49	-1.000			
	50	-49.000	-1.000	1.000
50	-1.000			
	51	-50.000		

SOIL PROPERTIES

ELEMENT	SATK	POR	PSICRT	
1	1	1.230E-05	0.4950	-1.000
2	1	1.230E-05	0.4950	-1.000
3	1	1.230E-05	0.4950	-1.000
4	1	1.230E-05	0.4950	-1.000
5	1	1.230E-05	0.4950	-1.000
6	1	1.230E-05	0.4950	-1.000
7	1	1.230E-05	0.4950	-1.000
8	1	1.230E-05	0.4950	-1.000
9	1	1.230E-05	0.4950	-1.000
10	1	1.230E-05	0.4950	-1.000

11	1	1.230E-05	0.4950	-1.000
12	1	1.230E-05	0.4950	-1.000
13	1	1.230E-05	0.4950	-1.000
14	1	1.230E-05	0.4950	-1.000
15	1	1.230E-05	0.4950	-1.000
16	1	1.230E-05	0.4950	-1.000
17	1	1.230E-05	0.4950	-1.000
18	1	1.230E-05	0.4950	-1.000
19	1	1.230E-05	0.4950	-1.000
20	1	1.230E-05	0.4950	-1.000
21	1	1.230E-05	0.4950	-1.000
22	1	1.230E-05	0.4950	-1.000
23	1	1.230E-05	0.4950	-1.000
24	1	1.230E-05	0.4950	-1.000
25	1	1.230E-05	0.4950	-1.000
26	1	1.230E-05	0.4950	-1.000
27	1	1.230E-05	0.4950	-1.000
28	1	1.230E-05	0.4950	-1.000
29	1	1.230E-05	0.4950	-1.000
30	1	1.230E-05	0.4950	-1.000
31	1	1.230E-05	0.4950	-1.000
32	1	1.230E-05	0.4950	-1.000
33	1	1.230E-05	0.4950	-1.000
34	1	1.230E-05	0.4950	-1.000
35	1	1.230E-05	0.4950	-1.000
36	1	1.230E-05	0.4950	-1.000
37	1	1.230E-05	0.4950	-1.000
38	1	1.230E-05	0.4950	-1.000
39	1	1.230E-05	0.4950	-1.000
40	1	1.230E-05	0.4950	-1.000
41	1	1.230E-05	0.4950	-1.000
42	1	1.230E-05	0.4950	-1.000
43	1	1.230E-05	0.4950	-1.000
44	1	1.230E-05	0.4950	-1.000
45	1	1.230E-05	0.4950	-1.000
46	1	1.230E-05	0.4950	-1.000
47	1	1.230E-05	0.4950	-1.000
48	1	1.230E-05	0.4950	-1.000
49	1	1.230E-05	0.4950	-1.000
50	1	1.230E-05	0.4950	-1.000

CONSTANT INITIAL PRESSURE....PSINIT= -600.000

==========
BOUNDARY AND INITIAL CONDITIONS
==========

HEAD IN IMPOUNDMENT.....H= 25.00
UNDERLYING SOIL SUCTION PRESSURE.....PSIBOT= -600.000

****

TIME= 0.0 TIME STEP= 0 DT= 1.000E-01 ERR= 0.0

ITER= 0

****

NODE POTENTIAL MOISTURE K

1	2.5000E+01	0.4950	1.2300E-05
2	-6.0000E+02	0.2376	1.8511E-08
3	-6.0000E+02	0.2376	1.8511E-08
4	-6.0000E+02	0.2376	1.8511E-08
5	-6.0000E+02	0.2376	1.8511E-08
6	-6.0000E+02	0.2376	1.8511E-08
7	-6.0000E+02	0.2376	1.8511E-08
8	-6.0000E+02	0.2376	1.8511E-08
9	-6.0000E+02	0.2376	1.8511E-08
10	-6.0000E+02	0.2376	1.8511E-08
11	-6.0000E+02	0.2376	1.8511E-08
12	-6.0000E+02	0.2376	1.8511E-08
13	-6.0000E+02	0.2376	1.8511E-08
14	-6.0000E+02	0.2376	1.8511E-08
15	-6.0000E+02	0.2376	1.8511E-08
16	-6.0000E+02	0.2376	1.8511E-08
17	-6.0000E+02	0.2376	1.8511E-08
18	-6.0000E+02	0.2376	1.8511E-08
19	-6.0000E+02	0.2376	1.8511E-08
20	-6.0000E+02	0.2376	1.8511E-08
21	-6.0000E+02	0.2376	1.8511E-08
22	-6.0000E+02	0.2376	1.8511E-08
23	-6.0000E+02	0.2376	1.8511E-08
24	-6.0000E+02	0.2376	1.8511E-08
25	-6.0000E+02	0.2376	1.8511E-08
26	-6.0000E+02	0.2376	1.8511E-08
27	-6.0000E+02	0.2376	1.8511E-08
28	-6.0000E+02	0.2376	1.8511E-08
29	-6.0000E+02	0.2376	1.8511E-08
30	-6.0000E+02	0.2376	1.8511E-08
31	-6.0000E+02	0.2376	1.8511E-08
32	-6.0000E+02	0.2376	1.8511E-08
33	-6.0000E+02	0.2376	1.8511E-08
34	-6.0000E+02	0.2376	1.8511E-08
35	-6.0000E+02	0.2376	1.8511E-08
36	-6.0000E+02	0.2376	1.8511E-08
37	-6.0000E+02	0.2376	1.8511E-08
38	-6.0000E+02	0.2376	1.8511E-08
39	-6.0000E+02	0.2376	1.8511E-08
40	-6.0000E+02	0.2376	1.8511E-08
41	-6.0000E+02	0.2376	1.8511E-08
42	-6.0000E+02	0.2376	1.8511E-08
43	-6.0000E+02	0.2376	1.8511E-08
44	-6.0000E+02	0.2376	1.8511E-08
45	-6.0000E+02	0.2376	1.8511E-08
46	-6.0000E+02	0.2376	1.8511E-08
47	-6.0000E+02	0.2376	1.8511E-08
48	-6.0000E+02	0.2376	1.8511E-08
49	-6.0000E+02	0.2376	1.8511E-08
50	-6.0000E+02	0.2376	1.8511E-08
51	-6.0000E+02	0.2376	1.8511E-08

****

TIME= 1.000E+03 TIME STEP= 35 DT= 3.462E+01 ERR= 1.724E-02

ITER= 2

****

NODE	POTENTIAL	MOISTURE	K

1	2.5000E+01	0.4950	1.2300E-05
2	-1.1466E+01	0.4780	7.6775E-05
3	-2.1312E+02	0.2991	1.1473E-07
4	-5.5319E+02	0.2417	2.1369E-08
5	-5.9774E+02	0.2378	1.8635E-08
6	-5.9991E+02	0.2376	1.8516E-08
7	-6.0000E+02	0.2376	1.8512E-08
8	-6.0000E+02	0.2376	1.8512E-08
9	-6.0000E+02	0.2376	1.8511E-08
10	-6.0000E+02	0.2376	1.8511E-08
11	-6.0000E+02	0.2376	1.8511E-08
12	-6.0000E+02	0.2376	1.8511E-08
13	-6.0000E+02	0.2376	1.8511E-08
14	-6.0000E+02	0.2376	1.8511E-08
15	-6.0000E+02	0.2376	1.8511E-08
16	-6.0000E+02	0.2376	1.8511E-08
17	-6.0000E+02	0.2376	1.8511E-08
18	-6.0000E+02	0.2376	1.8511E-08
19	-6.0000E+02	0.2376	1.8511E-08
20	-6.0000E+02	0.2376	1.8511E-08
21	-6.0000E+02	0.2376	1.8511E-08
22	-6.0000E+02	0.2376	1.8511E-08
23	-6.0000E+02	0.2376	1.8511E-08
24	-6.0000E+02	0.2376	1.8511E-08
25	-6.0000E+02	0.2376	1.8511E-08
26	-6.0000E+02	0.2376	1.8511E-08
27	-6.0000E+02	0.2376	1.8511E-08
28	-6.0000E+02	0.2376	1.8511E-08
29	-6.0000E+02	0.2376	1.8511E-08
30	-6.0000E+02	0.2376	1.8511E-08
31	-6.0000E+02	0.2376	1.8511E-08
32	-6.0000E+02	0.2376	1.8511E-08
33	-6.0000E+02	0.2376	1.8511E-08
34	-6.0000E+02	0.2376	1.8511E-08
35	-6.0000E+02	0.2376	1.8511E-08
36	-6.0000E+02	0.2376	1.8511E-08
37	-6.0000E+02	0.2376	1.8511E-08
38	-6.0000E+02	0.2376	1.8511E-08
39	-6.0000E+02	0.2376	1.8511E-08
40	-6.0000E+02	0.2376	1.8511E-08
41	-6.0000E+02	0.2376	1.8511E-08
42	-6.0000E+02	0.2376	1.8511E-08
43	-6.0000E+02	0.2376	1.8511E-08
44	-6.0000E+02	0.2376	1.8511E-08
45	-6.0000E+02	0.2376	1.8511E-08
46	-6.0000E+02	0.2376	1.8511E-08
47	-6.0000E+02	0.2376	1.8511E-08
48	-6.0000E+02	0.2376	1.8511E-08
49	-6.0000E+02	0.2376	1.8511E-08
50	-6.0000E+02	0.2376	1.8511E-08
51	-6.0000E+02	0.2376	1.8511E-08

VOLUME BALANCE CALCULATIONS

TOP FLUX 3.6408E-04
BOTTOM FLUX -1.8511E-08
STORAGE RATE 3.6251E-04

ERROR 1.4966E-06

```
VOLUME IN           1.2547E-02
VOLUME OUT         -6.4086E-07
STORAGE VOLUME      1.2553E-02
                    ----------
ERROR               5.0775E-06

CUMULATIVE CHANGES

VOLUME IN (-)       3.0680E-01
VOLUME OUT         -1.8511E-05
STORAGE             3.0623E-01
                    ----------
ERROR               5.8619E-04

RELATIVE ERROR        0.001914

********************************************************************************

TIME=   1.000E+04  TIME STEP=  109  DT=   1.284E+02  ERR=   1.969E-02

ITER=    2

********************************************************************************

 NODE       POTENTIAL          MOISTURE                K

    1        2.5000E+01           0.4950        1.2300E-05
    2        2.0385E+01           0.4950        1.2300E-05
    3        1.1389E+01           0.4950        1.2300E-05
    4        4.0702E+00           0.4950        1.2300E-05
    5       -3.1316E+00           0.4941        1.1598E-05
    6       -1.2718E+01           0.4751        7.1375E-06
    7       -3.2157E+01           0.4341        2.5973E-06
    8       -9.2790E+01           0.3603        4.8471E-07
    9       -2.7631E+02           0.2818        7.2709E-08
   10       -4.9493E+02           0.2475        2.6011E-08
   11       -5.7916E+02           0.2394        1.9705E-08
   12       -5.9658E+02           0.2379        1.8699E-08
   13       -5.9948E+02           0.2376        1.8540E-08
   14       -5.9992E+02           0.2376        1.8516E-08
   15       -5.9999E+02           0.2376        1.8512E-08
   16       -6.0000E+02           0.2376        1.8512E-08
   17       -6.0000E+02           0.2376        1.8512E-08
   18       -6.0000E+02           0.2376        1.8512E-08
   19       -6.0000E+02           0.2376        1.8512E-08
   20       -6.0000E+02           0.2376        1.8511E-08
   21       -6.0000E+02           0.2376        1.8511E-08
   22       -6.0000E+02           0.2376        1.8511E-08
   23       -6.0000E+02           0.2376        1.8511E-08
   24       -6.0000E+02           0.2376        1.8511E-08
   25       -6.0000E+02           0.2376        1.8511E-08
   26       -6.0000E+02           0.2376        1.8511E-08
   27       -6.0000E+02           0.2376        1.8511E-08
   28       -6.0000E+02           0.2376        1.8511E-08
   29       -6.0000E+02           0.2376        1.8511E-08
   30       -6.0000E+02           0.2376        1.8511E-08
   31       -6.0000E+02           0.2376        1.8511E-08
   32       -6.0000E+02           0.2376        1.8511E-08
   33       -6.0000E+02           0.2376        1.8511E-08
```

34	-6.0000E+02	0.2376	1.8511E-08
35	-6.0000E+02	0.2376	1.8511E-08
36	-6.0000E+02	0.2376	1.8511E-08
37	-6.0000E+02	0.2376	1.8511E-08
38	-6.0000E+02	0.2376	1.8511E-08
39	-6.0000E+02	0.2376	1.8511E-08
40	-6.0000E+02	0.2376	1.8511E-08
41	-6.0000E+02	0.2376	1.8511E-08
42	-6.0000E+02	0.2376	1.8511E-08
43	-6.0000E+02	0.2376	1.8511E-08
44	-6.0000E+02	0.2376	1.8511E-08
45	-6.0000E+02	0.2376	1.8511E-08
46	-6.0000E+02	0.2376	1.8511E-08
47	-6.0000E+02	0.2376	1.8511E-08
48	-6.0000E+02	0.2376	1.8511E-08
49	-6.0000E+02	0.2376	1.8511E-08
50	-6.0000E+02	0.2376	1.8511E-08
51	-6.0000E+02	0.2376	1.8511E-08

VOLUME BALANCE CALCULATIONS

TOP FLUX	6.9067E-05
BOTTOM FLUX	-1.8511E-08
STORAGE RATE	9.8334E-05
ERROR	2.9248E-05

VOLUME IN	1.2635E-02
VOLUME OUT	-2.3771E-06
STORAGE VOLUME	1.2627E-02
ERROR	9.6253E-06

CUMULATIVE CHANGES

VOLUME IN (-)	1.6463E+00
VOLUME OUT	-1.8512E-04
STORAGE	1.6415E+00
ERROR	4.8181E-03
RELATIVE ERROR	0.002935

****

TIME= 4.000E+04 TIME STEP= 175 DT= 5.115E+02 ERR= 3.534E-02

ITER= 2

****

NODE	POTENTIAL	MOISTURE	K
1	2.5000E+01	0.4950	1.2300E-05
2	2.4162E+01	0.4950	1.2300E-05
3	1.8944E+01	0.4950	1.2300E-05
4	1.5402E+01	0.4950	1.2300E-05
5	1.2220E+01	0.4950	1.2300E-05

6	9.0307E+00	0.4950	1.2300E-05
7	5.8390E+00	0.4950	1.2300E-05
8	2.6502E+00	0.4950	1.2300E-05
9	-5.5438E-01	0.4950	1.2300E-05
10	-3.9420E+00	0.4932	1.1274E-05
11	-7.9113E+00	0.4860	9.3738E-06
12	-1.3035E+01	0.4744	7.0066E-06
13	-2.0385E+01	0.4577	4.6117E-06
14	-3.2131E+01	0.4342	2.6003E-06
15	-5.3065E+01	0.4016	1.2220E-06
16	-9.3773E+01	0.3595	4.7610E-07
17	-1.7276E+02	0.3139	1.6568E-07
18	-2.9932E+02	0.2767	6.3158E-08
19	-4.3570E+02	0.2544	3.2577E-08
20	-5.2863E+02	0.2440	2.3154E-08
21	-5.7326E+02	0.2399	2.0065E-08
22	-5.9078E+02	0.2384	1.9025E-08
23	-5.9698E+02	0.2378	1.8678E-08
24	-5.9904E+02	0.2377	1.8564E-08
25	-5.9970E+02	0.2376	1.8528E-08
26	-5.9991E+02	0.2376	1.8517E-08
27	-5.9997E+02	0.2376	1.8513E-08
28	-5.9999E+02	0.2376	1.8512E-08
29	-5.9999E+02	0.2376	1.8512E-08
30	-5.9999E+02	0.2376	1.8512E-08
31	-5.9999E+02	0.2376	1.8512E-08
32	-5.9999E+02	0.2376	1.8512E-08
33	-6.0000E+02	0.2376	1.8512E-08
34	-6.0000E+02	0.2376	1.8512E-08
35	-6.0000E+02	0.2376	1.8512E-08
36	-6.0000E+02	0.2376	1.8512E-08
37	-6.0000E+02	0.2376	1.8512E-08
38	-6.0000E+02	0.2376	1.8512E-08
39	-6.0000E+02	0.2376	1.8512E-08
40	-6.0000E+02	0.2376	1.8512E-08
41	-6.0000E+02	0.2376	1.8512E-08
42	-6.0000E+02	0.2376	1.8512E-08
43	-6.0000E+02	0.2376	1.8512E-08
44	-6.0000E+02	0.2376	1.8512E-08
45	-6.0000E+02	0.2376	1.8512E-08
46	-6.0000E+02	0.2376	1.8512E-08
47	-6.0000E+02	0.2376	1.8512E-08
48	-6.0000E+02	0.2376	1.8512E-08
49	-6.0000E+02	0.2376	1.8512E-08
50	-6.0000E+02	0.2376	1.8511E-08
51	-6.0000E+02	0.2376	1.8511E-08

VOLUME BALANCE CALCULATIONS

TOP FLUX 2.2606E-05
BOTTOM FLUX -1.8516E-08
STORAGE RATE 5.1720E-05

ERROR 2.9095E-05

VOLUME IN 2.6478E-02
VOLUME OUT -9.4717E-06
STORAGE VOLUME 2.6457E-02

ERROR 3.0821E-05

CUMULATIVE CHANGES

VOLUME IN (-)	3.6517E+00
VOLUME OUT	-7.4053E-04
STORAGE	3.6446E+00
ERROR	7.8416E-03
RELATIVE ERROR	0.002152

****

TIME= 1.000E+05 TIME STEP= 238 DT= 2.031E+01 ERR= 7.258E-02

ITER= 2

****

NODE	POTENTIAL	MOISTURE	K
1	2.5000E+01	0.4950	1.2300E-05
2	2.0712E+01	0.4950	1.2300E-05
3	2.0804E+01	0.4950	1.2300E-05
4	1.9219E+01	0.4950	1.2300E-05
5	1.7275E+01	0.4950	1.2300E-05
6	1.5338E+01	0.4950	1.2300E-05
7	1.3403E+01	0.4950	1.2300E-05
8	1.1466E+01	0.4950	1.2300E-05
9	9.5441E+00	0.4950	1.2300E-05
10	7.6149E+00	0.4950	1.2300E-05
11	5.6794E+00	0.4950	1.2300E-05
12	3.7810E+00	0.4950	1.2300E-05
13	2.0092E+00	0.4950	1.2300E-05
14	3.7577E-01	0.4950	1.2300E-05
15	-1.2474E+00	0.4950	1.2156E-05
16	-3.0354E+00	0.4942	1.1634E-05
17	-5.2093E+00	0.4913	1.0705E-05
18	-7.6458E+00	0.4866	9.5064E-06
19	-1.0525E+01	0.4802	8.1061E-06
20	-1.4082E+01	0.4720	6.5910E-06
21	-1.8567E+01	0.4615	5.0689E-06
22	-2.4849E+01	0.4482	3.6531E-06
23	-3.3585E+01	0.4315	2.4433E-06
24	-4.6520E+01	0.4107	1.5034E-06
25	-6.6485E+01	0.3853	8.4761E-07
26	-9.8079E+01	0.3561	4.4104E-07
27	-1.4757E+02	0.3254	2.1804E-07
28	-2.1994E+02	0.2970	1.0857E-07
29	-3.1167E+02	0.2741	5.8815E-08
30	-4.0636E+02	0.2583	3.6842E-08
31	-4.8436E+02	0.2486	2.7022E-08
32	-5.3710E+02	0.2432	2.2513E-08
33	-5.6795E+02	0.2403	2.0397E-08
34	-5.8437E+02	0.2389	1.9395E-08
35	-5.9260E+02	0.2382	1.8922E-08
36	-5.9658E+02	0.2379	1.8700E-08
37	-5.9844E+02	0.2377	1.8597E-08
38	-5.9930E+02	0.2377	1.8550E-08
39	-5.9969E+02	0.2376	1.8529E-08

```
   40      -5.9986E+02          0.2376       1.8519E-08
   41      -5.9994E+02          0.2376       1.8515E-08
   42      -5.9997E+02          0.2376       1.8513E-08
   43      -5.9998E+02          0.2376       1.8512E-08
   44      -5.9999E+02          0.2376       1.8512E-08
   45      -5.9999E+02          0.2376       1.8512E-08
   46      -5.9999E+02          0.2376       1.8512E-08
   47      -6.0000E+02          0.2376       1.8512E-08
   48      -6.0000E+02          0.2376       1.8512E-08
   49      -6.0000E+02          0.2376       1.8512E-08
   50      -6.0000E+02          0.2376       1.8512E-08
   51      -6.0000E+02          0.2376       1.8511E-08

VOLUME BALANCE CALCULATIONS

TOP FLUX     6.5047E-05
BOTTOM FLUX -1.8534E-08
STORAGE RATE  3.5356E-05
                          -----------
ERROR                     2.9709E-05


VOLUME IN                 7.1503E-04
VOLUME OUT               -3.7647E-07
STORAGE VOLUME            7.1818E-04
                          -----------
ERROR                     2.7665E-06

CUMULATIVE CHANGES

VOLUME IN (-)             6.1434E+00
VOLUME OUT               -1.8519E-03
STORAGE                   6.1338E+00
                          -----------
ERROR                     1.1426E-02

RELATIVE ERROR              0.001863

*************************************************************************

TIME=   2.000E+05  TIME STEP=  340  DT=   3.567E+02  ERR=   9.142E-02

ITER=    2

*************************************************************************

 NODE       POTENTIAL          MOISTURE                K

    1        2.5000E+01           0.4950       1.2300E-05
    2        2.1246E+01           0.4950       1.2300E-05
    3        2.1872E+01           0.4950       1.2300E-05
    4        2.0821E+01           0.4950       1.2300E-05
    5        1.9411E+01           0.4950       1.2300E-05
    6        1.8008E+01           0.4950       1.2300E-05
    7        1.6607E+01           0.4950       1.2300E-05
    8        1.5204E+01           0.4950       1.2300E-05
    9        1.3816E+01           0.4950       1.2300E-05
   10        1.2421E+01           0.4950       1.2300E-05
   11        1.1019E+01           0.4950       1.2300E-05
```

12	9.6545E+00	0.4950	1.2300E-05
13	8.4164E+00	0.4950	1.2300E-05
14	7.3168E+00	0.4950	1.2300E-05
15	6.2892E+00	0.4950	1.2300E-05
16	5.3215E+00	0.4950	1.2300E-05
17	4.2836E+00	0.4950	1.2300E-05
18	3.2484E+00	0.4950	1.2300E-05
19	2.2666E+00	0.4950	1.2300E-05
20	1.2812E+00	0.4950	1.2300E-05
21	2.6801E-01	0.4950	1.2300E-05
22	-7.3933E-01	0.4950	1.2300E-05
23	-1.7568E+00	0.4949	1.2038E-05
24	-2.9237E+00	0.4943	1.1674E-05
25	-4.2899E+00	0.4928	1.1125E-05
26	-5.8026E+00	0.4903	1.0421E-05
27	-7.4741E+00	0.4870	9.5923E-06
28	-9.3685E+00	0.4828	8.6555E-06
29	-1.1567E+01	0.4778	7.6329E-06
30	-1.4173E+01	0.4717	6.5559E-06
31	-1.7336E+01	0.4645	5.4630E-06
32	-2.1269E+01	0.4558	4.3972E-06
33	-2.6285E+01	0.4453	3.4031E-06
34	-3.2851E+01	0.4329	2.5208E-06
35	-4.1672E+01	0.4180	1.7800E-06
36	-5.3815E+01	0.4006	1.1949E-06
37	-7.0856E+01	0.3806	7.6286E-07
38	-9.5014E+01	0.3585	4.6556E-07
39	-1.2905E+02	0.3354	2.7515E-07
40	-1.7557E+02	0.3128	1.6107E-07
41	-2.3538E+02	0.2924	9.6377E-08
42	-3.0535E+02	0.2754	6.0977E-08
43	-3.7793E+02	0.2625	4.1873E-08
44	-4.4393E+02	0.2533	3.1519E-08
45	-4.9694E+02	0.2472	2.5826E-08
46	-5.3534E+02	0.2433	2.2644E-08
47	-5.6109E+02	0.2409	2.0840E-08
48	-5.7754E+02	0.2395	1.9803E-08
49	-5.8790E+02	0.2386	1.9190E-08
50	-5.9474E+02	0.2380	1.8802E-08
51	-6.0000E+02	0.2376	1.8511E-08

VOLUME BALANCE CALCULATIONS

TOP FLUX	5.8478E-05
BOTTOM FLUX	-1.1682E-07
STORAGE RATE	2.7076E-05
ERROR	3.1518E-05

VOLUME IN	9.6963E-03
VOLUME OUT	-4.1219E-05
STORAGE VOLUME	9.6594E-03
ERROR	7.8096E-05

CUMULATIVE CHANGES

VOLUME IN (-)	9.1924E+00
VOLUME OUT	-4.9089E-03

```
STORAGE              9.1798E+00
                     ----------
ERROR                1.7465E-02

RELATIVE ERROR         0.001903

EXECUTION ENDED NORMALLY -      0 - WARNINGS



09/30/83    10:04:58    GCAGD.SOIL.LIB.DATA(GRID1)

  50       50.0
```

09/30/83 10:05:17 GCAGD.SOIL.LIB.DATA(PROP1)

1	1	1.230E-05	0.4950	-1.00
2	1	1.230E-05	0.4950	-1.00
3	1	1.230E-05	0.4950	-1.00
4	1	1.230E-05	0.4950	-1.00
5	1	1.230E-05	0.4950	-1.00
6	1	1.230E-05	0.4950	-1.00
7	1	1.230E-05	0.4950	-1.00
8	1	1.230E-05	0.4950	-1.00
9	1	1.230E-05	0.4950	-1.00
10	1	1.230E-05	0.4950	-1.00
11	1	1.230E-05	0.4950	-1.00
12	1	1.230E-05	0.4950	-1.00
13	1	1.230E-05	0.4950	-1.00
14	1	1.230E-05	0.4950	-1.00
15	1	1.230E-05	0.4950	-1.00
16	1	1.230E-05	0.4950	-1.00
17	1	1.230E-05	0.4950	-1.00
18	1	1.230E-05	0.4950	-1.00
19	1	1.230E-05	0.4950	-1.00
20	1	1.230E-05	0.4950	-1.00
21	1	1.230E-05	0.4950	-1.00
22	1	1.230E-05	0.4950	-1.00
23	1	1.230E-05	0.4950	-1.00
24	1	1.230E-05	0.4950	-1.00
25	1	1.230E-05	0.4950	-1.00
26	1	1.230E-05	0.4950	-1.00
27	1	1.230E-05	0.4950	-1.00
28	1	1.230E-05	0.4950	-1.00
29	1	1.230E-05	0.4950	-1.00
30	1	1.230E-05	0.4950	-1.00
31	1	1.230E-05	0.4950	-1.00
32	1	1.230E-05	0.4950	-1.00
33	1	1.230E-05	0.4950	-1.00
34	1	1.230E-05	0.4950	-1.00
35	1	1.230E-05	0.4950	-1.00
36	1	1.230E-05	0.4950	-1.00
37	1	1.230E-05	0.4950	-1.00
38	1	1.230E-05	0.4950	-1.00
39	1	1.230E-05	0.4950	-1.00
40	1	1.230E-05	0.4950	-1.00
41	1	1.230E-05	0.4950	-1.00
42	1	1.230E-05	0.4950	-1.00
43	1	1.230E-05	0.4950	-1.00
44	1	1.230E-05	0.4950	-1.00
45	1	1.230E-05	0.4950	-1.00
46	1	1.230E-05	0.4950	-1.00
47	1	1.230E-05	0.4950	-1.00
48	1	1.230E-05	0.4950	-1.00
49	1	1.230E-05	0.4950	-1.00
50	1	1.230E-05	0.4950	-1.00

```
09/30/83   10:05:21   GCAGD.SOIL.LIB.DATA(INITIAL3)

   -600.0
```

```
09/30/83   10:05:29   GCAGD.SOIL.LIB.DATA(INPUT3A)

TEST3A  50 1 CM ELEMENTS, 51 NUMNP   YOLO INFILTRATION H=25.
  21   22   23   10   31   32   33   34
   0    0      2.E5       0.1    1000.0 1000       0.5       0.1   10       25.
   5
     1.E3       1.E4       4.E4       1.E5       2.E5
  51    1    0
   0
     25.0    -600.0
```

APPENDIX E

COMPUTER PROGRAM FOR GARDNER'S ANALYTICAL SOLUTION

```
 09/26/83   08:40:42   GCAGD.GARDNER.FORT.DATA

00000010 C*******
00000020 C
00000030 C      GARDNER.FORT   STEADY STATE EVAPORATION IN UNSATURATED SOIL
00000040 C
00000050 C      SEE W.R. GARDNER, SOME STEADY-STATE SOLUTIONS OF THE UNSATURATED
00000060 C           MOISTURE FLOW EQUATION WITH APPLICATION TO EVAPORATION FROM
00000070 C           A WATER TABLE, SOIL SCIENCE, 85, 228-232, 1958.
00000080 C
00000090 C      STEADY STATE SOLUTION FOR SOIL WITH HYDRAULIC CONDUCTIVITY
00000100 C      FUNCTION AS FOLLOWS:
00000110 C
00000120 C     K =     A              S = - (PSI) SUCTION
00000130 C           ----------
00000140 C            4
00000150 C           S   + BETA
00000160 C
00000170 C      DAN GOODE       JUNE 1983
00000180 C
00000190 C****************
00000200 C
00000210       IRD=5
00000220       IPRT=6
00000230       IRSLT=9
00000240 C      READ SOIL FUNCTION PARAMETERS
00000250       READ(IRD,*) A,B,WT,FLUX
00000260       WRITE(IPRT,2001) A,B,WT,FLUX
00000270 C      COMPUTE SOLUTION PARAMETERS
00000280       SQR2=1.4142136
00000290       ALPHA=FLUX/A
00000300       BETA=ALPHA*B + 1.0
00000310       RO=(BETA/ALPHA)**0.25
00000320       RO2=RO*RO
00000330       RO3=RO2*RO
00000340       AINV=1.0/ALPHA
00000350       TERM1=1.0/(4.*RO3*SQR2)
00000360       TERM2=1./(2.*RO3*SQR2)
00000370       WRITE(IPRT,2004) ALPHA,BETA,RO,RO2,RO3,AINV,TERM1,TERM2
00000380 C
00000390 C      READ STEPPING FOR SOLUTION
00000400       READ(IRD,*) PF,DPF,PFEND,MAX
00000410       WRITE(IPRT,2002) PF,DPF,PFEND,MAX
00000420 C
00000430       PF=PF-DPF
00000440 C
00000450       DO 10 I=1,MAX
00000460       PF=PF+DPF
00000470       IF(PF.GT.PFEND) GOTO 999
00000480 C
00000490       S=10.0**PF
00000500       PSI=-S
00000510       S2=S*S
00000520       TERM3=RO*S*SQR2
00000530       ARG1=(S2+TERM3+RO2)/(S2-TERM3+RO2)
00000540       ARG2=TERM3/(RO2-S2)
00000550 C
00000560       PARM=ATAN(ARG2)
00000570       IF (ARG2.LT.0) PARM=PARM + 3.1415927
00000580       Z=(ALOG(ARG1)*TERM1+PARM*TERM2)*AINV-WT
00000590 C
00000600       WRITE(IPRT,2003) I,Z,PSI,PF,S,S2,TERM3,ARG1,ARG2
```

```
00000610       WRITE(IRSLT,2003) I,Z,PSI,PF
00000620    10 CONTINUE
00000630 C
00000640   999 STOP
00000650  2001 FORMAT(///' GARDNER OUTPUT'//
00000660      *' SOIL FUNCTION PARAMETERS'//
00000670      *' A',15(1H.),'A=',1PE10.2/
00000680      *' B',15(1H.),'B=',1PE10.2/
00000690      *' DEPTH TO WATER TABLE',5(1H.),'WT=',0PF10.2/
00000700      *' FLUX UPWARD',7(1H.),'FLUX=',1PE10.2)
00000710  2002 FORMAT(///' SOLUTION STEPPING PARAMETERS'//
00000720      *' BEGINNING SUCTION',10(1H.),'PF=',0PF10.2/
00000730      *' PF INCREMENT',10(1H.),'DPF=',0PF10.3/
00000740      *' FINAL PF',12(1H.),'PFEND=',0PF10.2/
00000750      *' MAXIMUM NUMBER OF POINTS',5(1H.),'MAX=',110///
00000760      *'          I         Z       PSI       PF          S          S2       TERM
00000770      *3        ARG1      ARG2',/)
00000780  2003 FORMAT(I10,0PF10.3,1PE10.2,0PF10.3,6(1PE10.2))
00000790  2004 FORMAT(///' INTERMEDIATE TERMS'//
00000800      *' ALPHA=',5(1H.),1PE10.4/
00000810      *' BETA=',5(1H.),1PE10.4/
00000820      *' RO=',5(1H.),1PE10.4/
00000830      *' RO2=',5(1H.),1PE10.4/
00000840      *' RO3=',5(1H.),1PE10.4/
00000850      *' AINV=',5(1H.),1PE10.4/
00000860      *' TERM1=',5(1H.),1PE10.4/
00000870      *' TERM2=',5(1H.),1PE10.4///)
00000880       END
```